November 2019

Reconstructing Geographic and Trophic Histories of Fish Using Bulk and Compound-Specific Stable Isotopes from Eye Lenses

Amy A. Wallace
University of South Florida

Reconstructing Geographic and Trophic Histories of Fish Using Bulk and Compound-Specific Stable Isotopes from Eye Lenses

by

Amy A. Wallace

A dissertation submitted in partial fulfillment
of the requirements for the degree of
Doctor of Philosophy in Marine Science
with a concentration in Marine Resource Assessments
College of Marine Science
University of South Florida

Major Professor: Ernst B. Peebles, Ph.D.
Jeffrey P. Chanton, Ph.D.
Greg S. Ellis, Ph.D.
David J. Hollander, Ph.D.
Steven A. Murawski, Ph.D.

Date of Approval:
20 November 2019

Keywords: migration, carbon, nitrogen, isoscape, amino acid

Dedication

This dissertation is dedicated to my amazing family: my parents, Earl and Ann Wallace, and my sister Mary Bock. You will never know how grateful I am for all the love and support throughout my life. You have always taught me that I can do and be anything I want if I work hard. I love y'all.

Acknowledgements

First and foremost, I would like to thank my committee for guiding me in my pursuit of this dissertation research. I am deeply indebted to you for all your support and guidance along the way…and the awesome fishing trips. You made this just as fun as you made it tough. I have learned a lot on this journey.

Thank you, Ethan Goddard and Greg Ellis, for your help generating my isotope data. You have taught me everything I know about mass spectrometry. I only wish I was able to learn everything you know. Thanks for answering all my late night and weekend phone calls and emails. I am sure I was a pest, but you never let it show.

To the crew of the R/V *Weatherbird II* and the various Mud and Blood crews (specifically 2013 and 2014), thank you for your hard work and dedication. Longline fishing is no easy task. I appreciate you gathering fish eyes although it seems rather barbaric at times. I will always treasure our conversations around the dissection table at sea.

I would like to thank Hubbard's Marina (John's Pass, Madeira Beach, FL) and Tom Herzhauser (the Tavern at Bayboro) for the continual supply of fish eyes. Chapter two, the basis of this research, would not have happened if you had not let me take your fish carcasses.

Finally, thank you to my friends and family. There is no difference between the two. You have celebrated during the successes and cursed during the failures with me. You have always seemed to know what I needed, even if I did not. I am only successful because of your love and support.

Table of Contents

List of Tables iii

List of Figures iv

Abstract vi

Chapter 1. Introduction 1
1.1 Tags used in fisheries management 2
1.1.1 Artificial tags 2
1.1.2 Natural tags 3
1.2 Stable isotopes 6
1.2.1 Bulk stable isotope analysis 7
1.2.2 Compound-specific stable-isotope analysis 9
1.2.3 Trophic discrimination factors 11
1.2.4 Isoscapes 13
1.3 Objectives and research overview 15

Chapter 2. Stable isotopes in fish eye lenses as potential recorders of trophic and geographic history 19
2.1 Introduction 19
2.2 Materials and Methods 23
2.2.1 Ethics Statement 23
2.2.2 Lens Collection and Dissection 24
2.2.3 Lens Sample Processing 25
2.2.4 Data Location and Analysis 26
2.3 Results 27
2.4 Discussion 29

Chapter 3. Nitrogen isotopic analysis of fish eye-lens amino acids 37
3.1 Introduction 37
3.2 Methods 39
3.2.1 Field Work/Sample Collection 39
3.2.2 AA-CSIA Processing 40
3.2.4 Ethics Statement 41
3.3 Results 41
3.4 Discussion 42

Chapter 4. Comparison of fish species using life-histories reconstructed from eye-lens amino acids 56

4.1 Introduction 56
4.2 Methods 59
4.2.1 Sample collection 59
4.2.2 Fish Length Estimation at Laminar Radial Midpoint 60
4.2.3 Bulk isotope analysis 60
4.2.4 Compound-specific isotope analysis 61
4.2.5 Trophic position calculation 62
4.2.6 Geographic variation and isoscape comparison 62
4.2.7 Ethics statement 64
4.3 Results 65
4.3.1 Isotopic assessment of reef species: Red Snapper 65
4.3.2 Isotopic assessment of highly migratory species: King Mackerel 66
4.3.3 Isotopic assessment of unknown teleost: Greater Amberjack 66
4.4 Discussion 67
4.4.1 Trophic growth comparison of reef and migratory species 67
4.4.2 Comparison of isotopic geography between reef and migratory species 69
4.4.3 Analysis of unknown: Greater Amberjack 73
4.4.5 Areas for future study 74

Chapter 5. Conclusions 94
5.1 Conclusions 94
5.2 Implications and future work 97

Chapter 6. References 100

Appendix A-Data analyzed 116

List of Tables

Table 3.1 Amino acid $\delta^{15}N$ values (δ, in ‰) for Red Snapper from station SL 4-40 48

Table 3.2 Amino acid $\delta^{15}N$ values (δ, in ‰) for Red Snapper from station SL 8-40 49

Table 3.3 $\delta^{15}N$ for King Mackerel muscle 50

Table 4.1 Red Snapper regression equations for the models presented in Figure 3 77

Table A.1 Catch data and metadata for Tables A.2, A.3, and A.4. 116

Table A.2 Red Snapper 117

Table A.3 King Mackerel 121

Table A.4 Greater Amberjack 123

List of Figures

Figure 1.1 Carbon isoscape of the Gulf of Mexico (Brianna Michaud, unpublished)..... 17

Figure 1.2 Nitrogen isoscape of the Gulf of Mexico (Brianna Michaud, unpublished) 18

Figure 2.1 Low-resolution screening..... 33

Figure 2.2 Low- and high-resolution comparison..... 34

Figure 2.3 High-resolution comparisons of left and right eyes of white grunt specimen 2..... 35

Figure 2.4 Intra- and inter-laminar comparison 36

Figure 3.1 Red Snapper sampling locations..... 51

Figure 3.2a Trophic amino acids in individual fish at laminar radial midpoints (LRMs)..... 52

Figure 3.2b Source and other (indicated by *) amino acids by laminar radial mipoints (LRMs). 53

Figure 3.3a Amino acid $\delta^{15}N$ measurements by fish at 4-40 54

Figure 3.3b Amino acid $\delta^{15}N$ measurements by fish at 8-40..... 55

Figure 4.1 Sample collection points..... 78

Figure 4.2 Red Snapper $\delta^{15}N_{Glu\text{-}Phe}$ and corresponding trophic position 79

Figure 4.3 Trophic growth models calculated by using best fit regression for the Red Snapper species compared to individuals..... 80

Figure 4.4 Bulk $\delta^{15}N$ for each individual, plotted against laminar radial midpoint (LRM) 81

Figure 4.5 Bulk $\delta^{13}C$ for each individual, plotted against laminar radial midpoint (LRM)..... 82

Figure 4.6 Red Snapper movements in isotopic space 83

Figure 4.7 Individual King Mackerel $\delta^{15}N_{Glu}$ and $\delta^{15}N_{Phe}$ 84

Figure 4.8 Trophic position at estimated standard length and laminar radial midpoint (LRM) for King Mackerel 85

Figure 4.9 King Mackerel movements in isotopic space..... 86

Figure 4.10 Individual Greater Amberjack $\delta^{15}N_{Glu}$ and $\delta^{15}N_{Phe}$ 87

Figure 4.11 Trophic position at estimated standard length and laminar radial midpoint (LRM) for Greater Amberjack 88

Figure 4.12. Greater Amberjack movements in isotopic space..... 89

Figure 4.13 Geographic variation using trophic corrected $\delta^{13}C$ and trophic corrected $\delta^{15}N$ for Red Snapper from 4-40 90

Figure 4.14 Geographic variation using trophic corrected $\delta^{13}C$ and trophic corrected $\delta^{15}N$ for Red Snapper from 8-40 91

Figure 4.15 Geographic variation using trophic corrected $\delta^{13}C$ and trophic corrected $\delta^{15}N$ for King Mackerel from Tampa Bay 92

Figure 4.16 Geographic variation using trophic corrected $\delta^{13}C$ and trophic corrected $\delta^{15}N$ for Greater Amberjack from 9-80 93

Abstract

The present research examined the viability and utility of eye lenses as a source of lifetime stable-isotope records in fish. It is presented in three sections. The first section compared bulk isotopic variation (bulk analysis) within fish eye-lenses at two temporal resolutions and compared patterns obtained from left and right eyes. The first temporal resolution was lower in an attempt to expose broad-scale isotopic changes during life while reducing effort and cost. This approach did reveal lifetime patterns, but tended to miss certain life events, particularly during early life. The second resolution was higher and provided detail that was missed at the lower resolution. Isotopic trends in left and right eyes from the same individual were nearly identical for both $\delta^{13}C$ and $\delta^{15}N$. It therefore appears unnecessary to process only the left or right eyes.

The second section tested the prospect of applying compound-specific isotope analysis (CSIA) to amino acids within individual eye-lens layers (laminae). CSIA of amino acids (CSIA-AA) allows trophic positions to be calculated at various life stages, thus enabling the reconstruction of trophic growth curves for individuals using the $\delta^{15}N$ differences between trophic and source amino acids. The methods used were successful at measuring $\delta^{15}N$ within ten intra-laminar amino acids. Of the ten amino acids, five were trophic, two were source, and three were neither trophic nor source. Lifetime variation was observed in all amino acids. While lifetime changes in trophic amino acids were expected because fish tend to increase their

trophic positions during life, lifetime variation in source amino acids was also observed, indicating change in the baseline $\delta^{15}N$ of primary producers at the base of the food web.

In the third section, bulk analysis and CSIA-AA were combined to isolate variation in geographic baseline from variation in trophic position; this approach was applied to 16 fish from three species: Red Snapper (*Lutjanus campechanus*), King Mackerel (*Scomberomorus cavalla*) and Greater Amberjack (*Seriola dumerili*). It was apparent that not all fish reached their trophic maximum in the same manner; lifetime trends in trophic position of individuals of the same species (Red Snapper) steadily increased along concave, convex, or linear pathways, whereas the lifetime trophic positions of King Mackerel fluctuated irregularly among multiple trophic positions instead of steadily increasing to similar trophic maxima, as in Red Snapper. These CSIA-AA-based trends in trophic position were subtracted from the bulk eye-lens trends for both $\delta^{15}N$ and $\delta^{13}C$, mathematically isolating the geographic component within the lifetime isotope records. Three geographic trends, or migration paths, were revealed: resident, lifetime (one-way) migrator, and seasonal migrator. This combined bulk and CSIA-AA method is likely to have widespread application to fishes in general and is particularly likely to provide new information on life stages that are poorly understood.

Chapter 1. Introduction

Fisheries managers are reliant on life-history data to conduct their work. Because diet and geography are principal components of the life-histories of individual fish, knowledge of both is relevant to understanding habitat use, food-web structures, habitat connectivity, and energy pathways through food webs (Hyslop 1980; Fisk et al 2001; Sheppard 2010; Hobson and Norris 2008; Ramos and Gonzalez-Solis 2012; McMahon and McCarthy 2016). Fish use multiple habitats in an effort to maximize survival, reproduction, and growth (Whitfield 1990; Gillanders and Kingsford 2003; Kurth et al 2018). However, there are knowledge gaps for particular life periods, including life periods that involve long migrations (Sutherland and Fable 1980; Bruger et al. 2018).

Migration occurs when animals redistribute from one area to another as they seek optimal combinations of prey availability and predation risk (Dingle and Drake 2007). Animal migrations are responsible for the movement of biomass, nutrients, and energy within and among ecosystems (Deegan 1993). Species-specific migration routes do not usually change over time and reflect selection for specific spawning and feeding locations (Hobson and Norris 2007; Schofield et al 2010).

One type of migration route is the “to-and-fro” migration (Dingle and Drake 2007). In this form of migration, the animal travels back and forth between two locations in a temporally

consistent manner. King Mackerel (*Scomberomorus cavalla*) undergo seasonal to-and-fro migrations when traveling from the northern Gulf of Mexico, which is used during summer, and the southern breeding grounds of South Florida, which are used during winter (Briggs 1958; Sutherland and Fable 1980). Another important migration classification is the "one-way" migration, where an animal travels to new locations and does not return to its point of origin (Dingle and Drake 2007). One cause of such migrations is too many animals competing for too few resources (intraspecific competition) that drives individuals toward other, more optimal habitats. As long as the animal does not return to the point of origin and settle again, this is considered a one-way migration. There are migrations when aquatic animals change depths (vertical migration), terrestrial animals move to higher ground (altitudinal migration), and fish move between fresh and saltwater habitats (diadromous migration) (Dingle and Drake 2007). No matter the type of migration, understanding changes in habitat use and associated migrations are important for both fisheries management and conservation (Hobson, 1999).

1.1 Tags used in fisheries management

Tags are used to help fill fish-movement data gaps in fisheries management. There are two types of tags used in fisheries management, artificial and natural tags.

1.1.1 Artificial tags

Most artificial tags require two captures, an initial capture to tag the animal and a second capture to retrieve the data and tag. There are various forms of artificial tags such as anchor tags, spaghetti tags, transmitters, satellite data loggers, and others. Tagging data are

useful, but there can be minimal return rates for the time and cost invested. For example, internal anchor tags were deployed on 1,968 King Mackerel between January 1983 and November 1985 (Fable et al. 1989). As of April 1986, only 55 tags (approximately 2.8%) had been returned or recaptured. This example illustrates the difficulty associated with finding the same fish twice.

Satellite tags are currently the only artificial tag that does not require an actual recapture (Hobson and Norris, 2008). Satellite tags are often used with many highly migratory species such as various species of sharks, tunas, marine mammals, and sea turtles. These artificial tags can be expensive but provide the most detailed data for individual animals over portions of life. In 2011, Tagging of Pacific Predators (TOPP) reported using a mixture of satellite-based tags and archival geolocation tags, which involved a total of 4,306 tags and yielded 1,701 animal tracks (Block et al. 2011). Tracking data, however, were acquired for periods of less than one year for each individual (Block et al. 2011).

1.1.2 Natural tags

In contrast to artificial tags, natural tags only require one capture to gather important information. Genetics, trace elements, contaminants, and stable isotopes are all examples of natural tags used in fisheries management that allow every capture to be a “recapture” (Hobson and Norris 2008). Otoliths, scales, fin spines, fin rays, and vertebrae are used to provide lifetime-scale records for microchemical and stable-isotope analyses in fish. Microchemical analysis is primarily used on inorganic material in calcified structures, whereas stable-isotope analysis is based on both inorganic and organic materials (Elsdon et al. 2010;

Tzadik et al. 2017). Campana (1999) and Tzadik et al. (2017) have reviewed these methods; a brief overview follows.

The most studied structure with respect to fish life-history records is the otolith. Otoliths consist of layers of calcium carbonate deposited within a proteinaceous matrix; otoliths grow for the entire life of the fish. Annual rings in sectioned otoliths (annuli) are used to determine fish age and to reconstruct habitat use (Jones 1986; Thorrold 1997). Otoliths provide one of the few lifelong records for fish, but lack enough organic nitrogen by weight (3-4%) for time-resolved stable-isotope analysis of nitrogen (Campana 1999).

Endoskeleton (e.g., vertebrae and cleithra), or bone, is vascularized and therefore metabolically active. When using endoskeleton for isotopic analysis, collagen (a structural protein) is often targeted for study if organic material within the bone is needed for analysis (Hobson and Clark 1992b). Bone collagen isotopically turns over in a matter of months to years, which is relatively slow, yet still makes the record incomplete with respect to entire lifetimes.

Fin rays and fin spines, much like endoskeletal bones, have both inorganic and organic material and used are used in microchemical and stable-isotope analyses (Smith 2010; Phelps 2012; Tzadik et al. 2015). Fin rays and fin spines are both natural records that can be sampled non-lethally. This is the major advantage to using rays and spines over other tissues; however, these provide incomplete records. Both tissues are vascularized and resorption occurs at the core of the structures, destroying the earliest part of life history, rendering the record incomplete (Hill et al 1989; Beamish and Chilton 1977; Drew et al. 2006). Fin spines are primarily used for microchemical analyses. Although stable-isotope analyses can be performed

on fin spines, this approach is rare and is primarily limited to the mineral matrix (Smith 2010; Tzadik 2017).

Scales have been used for more than a century as lifelong recorders of age and growth. Scales consist of two layers, the osseous upper layer and the proteinaceous base layer (Fouda 1979). Circuli are the concentric growth rings in the osseous layer, and these are comparable to otolith annuli (Fisher and Pearcy 1990). Microchemistry analyses have been conducted on scales since the 1970s, and stable-isotope-based analyses were initiated later (Bagenal et al 1973; Estep and Vigg 1985; Wainwright et al 1993). New scale growth overlaps older material during growth in the natural process of "overplating" (Hutchinson and Trueman 2006; Trueman and Moore 2007; Woodcock and Walther 2014). Overplating combines new and old isotopic material in a way that makes it very difficult to temporally isolate isotopic ratios (Hutchinson and Trueman 2006).

Eye lenses are composed of lens fiber cells that are synthesized in concentric layers like an onion. Lens-fiber cells begin as lens epithelial cells that become elongated as they synthesize new optical proteins (crystallins). Once elongation is complete, all organelles and DNA are removed from the fiber cells in a process known as "attenuated apoptosis," which renders these eye-lens layers ("laminae") metabolically inert (Nicol 1989; Berman 1991; Horwitz 2003; Dahm et al. 2007). Much like otoliths, eye lenses grow during the entire life of the fish. The lack of isotopic turnover and the large amount of protein make eye lenses an ideal structure for reconstructing lifetime carbon and nitrogen isotope records, which is the primary focus of this dissertation (Wallace et al. 2014).

1.2 Stable isotopes

Isotopes are atoms that have the same number of protons but a different number of neutrons, which increases the mass of the atom but leaves other elemental properties unchanged. Stable isotopes are used to determine basal-resource reliance, energy transfer through food webs, trophic omnivory, and migration (Peterson and Fry 1987; Vander Zanden and Rasmussen 1999; Post 2002; Hobson book). Unlike radioactive isotopes, stable isotopes do not decay over time. Whereas ^{14}C decays to ^{14}N over time, ^{12}C and ^{13}C are stable and remain unchanged. The increase in mass from the extra neutron lowers the zero-point energy of atomic bonds with the heavy isotopes, which requires more energy for dissociation (Sharp 2007). Thus, biogeochemical processes discriminate against the heavier atoms, and this results in isotopic fractionation (i.e., sorting of different isotopes into different pools). During diet assimilation (loss of waste nitrogen) and respiration (loss of waste CO_2), the tissues of the consumer thus become isotopically heavier than its diet.

By convention, stable isotope values are presented in the standard delta notation

$$\delta = \left[\left(\frac{R_X}{R_{Standard}}\right) - 1\right] \times 1000$$

where R is the isotopic ratio of heavy over light isotopes for the sample (X) and the standard. All values are reported as the measurement unit per mil (‰). The standards used for $\delta^{13}C$ or $\delta^{15}N$ are carbon from the PeeDee Belemnite formation (PDB) and atmospheric nitrogen, respectively (Sharp 2007).

1.2.1 Bulk stable isotope analysis

Bulk stable isotope analyses of carbon and nitrogen is a powerful and cost-effective tool that is widely used in studies of ecosystem energy pathways (Michener and Lajtha 2007). Isotopic values are influenced by an organism's physiology and the biochemical reactions that control the assimilation, synthesis, and degradation of macromolecules such as proteins, lipids, and carbohydrates (Paine 1988; Hairston and Hairston 1993; Post 2000). Carbon isotopes fractionate as carbon moves through food webs, but are primarily used to determine which primary producers form the base of the food web (basal resources). Common basal resources include benthic algae, phytoplankton, and C3 and C4 plants (DeNiro and Epstein 1978; Rounick and Winterbourn 1986; Peterson and Fry 1987; Post 2000). Isotope mixing models can be used to identify which isotopically distinct primary producers form the base of an organism's or biological community's food web, which is integral to understanding biological resiliency at these two organizational levels (Haines and Montague 1979; Rooney 2006; McMahon et al. 2016). Nitrogen isotopes fractionate more strongly than carbon isotopes between diet and consumer and are used to estimate trophic position (DeNiro and Epstein 1981; Minagawa and Wada 1984). Nitrogen can also be used to determine whether basal resources are marine or terrestrial and which types of nutrients support the dominant basal resources (i.e., nitrogen fixation versus primary production that depends on fixed nitrogen; Schoeninger et al 1983; Fry and Sherr 1984).

As an analytical method, analysis of bulk stable isotopes (i.e., whole biomass samples) is appealing due to the small amount of sample processing required, which primarily consists of

drying and weighing the biomass sample and placing a portion of it in tin capsules for subsequent combustion and analysis via an isotope-ratio mass spectrometer (IRMS). Bulk stable isotope analysis is also considerably less expensive than isolating compounds or classes of compounds prior to analysis via IRMS.

Traditionally, diet studies are based on the contents of a consumer's stomach (Deb 1997). However, there are difficulties associated with stomach-content analysis. For example, the size and type of prey can determine how long a given prey type remains in the stomach, biasing the results (Hyslop 1980; Stoner and Zimmerman 1988; Deb 1997). Diet analyses may only provide a biased snapshot of recent foraging, which can be problematic when analyzing the diet of species that switch prey types frequently. Stable-isotope analysis enables diet information to be integrated over longer time periods (Olson et al 2010) but does not yield the taxonomic information provided by traditional diet analyses. In stable-isotope analysis, each tissue represents a specific period that is associated with the time is takes for the tissue to assimilate the isotopic values of the diet (Hobson and Clark 1992b). Different tissues assimilate prey $\delta^{13}C$ and $\delta^{15}N$ at different rates. For example, blood isotopically incorporates prey on the scale of weeks, whereas bone takes months to years to turn over completely (Hobson and Clark 1992b). Therefore, $\delta^{13}C$ and $\delta^{15}N$ in the consumer represent a combination of the following information: (1) the $\delta^{13}C$ and $\delta^{15}N$ of the prey species, (2) the assimilated proportion of each prey, (3) the isotopic fractionation observed during tissue production, and (4) foraging location (Bearhop et al 2004).

Within a seascape that is dominated by a single basal resource (e.g., phytoplankton in the open ocean), isotopic analysis can be straightforward, whereas analysis of other study areas that have multiple basal resources can be complex (e.g., coastal ecosystems). In such cases, comparing one region to another requires a priori knowledge of landscape-level variations in baseline $\delta^{13}C$ and $\delta^{15}N$, both of which may vary across time in addition to space. Otherwise, there is no way to determine whether the observed isotopic variation reflects changes in food-web structure and energy flow or the geographic variation in underlying nutrient baselines (Post 2002). This is one of the most difficult problems with applying stable-isotope studies to food-web studies of complex ecosystems (Post 2002). However, pairing studies of $\delta^{13}C$ and $\delta^{15}N$ or adding other isotopes (e.g., oxygen, sulfur, or hydrogen isotopes) help resolve ambiguities in trophic position or geographic baseline variation (i.e., "trophic geography"; Fry and Sherr 1984).

1.2.2 Compound-specific stable-isotope analysis

Compound-specific stable-isotope analysis (CSIA) is an emerging technique that is used to more accurately identify geographic variation in basal-resource contribution to energy pathways, trophic position, and migration than bulk stable-isotope analysis can achieve. CSIA uses gas chromatography to separate individual compounds by mass, combusts each compound, and then measures the isotopic ratios of the resulting gases using an IRMS. Although CSIA can be used to measure isotopic ratios of many macromolecules, fatty acids and amino acids are mainly used to study trophic geography, with the most common application being amino-acid stable-isotope analysis (Whiteman et al. 2019). CSIA of amino acids has the potential to provide much more information than bulk stable-isotope analysis because many

compounds, and amino acids in particular, have unique biosynthetic pathways (Minagawa and Wada 1984). These pathways explicitly involve propagation of dietary nutrients and resolve ambiguities associated with different prey types that otherwise appear to be isotopically similar when only bulk isotopes are considered. Amino acids are classified in two ways: (1) essential versus non-essential for $\delta^{13}C$, and (2) trophic versus source for $\delta^{15}N$ (Braun et al 2014; Whiteman et al 2019). In regard to $\delta^{13}C$, the consumer has the ability to modify the carbon backbone of non-essential amino acids but not those of essential amino acids. Therefore, essential amino acids remain biochemically unchanged as they transfer through food webs, reflecting the $\delta^{13}C$ of the basal resources that support consumers or communities (Fantle et al. 1999; McClelland and Montoya 2002; Popp et al. 2007).

In contrast, amino-acid $\delta^{15}N$ is largely based on the amount of transamination (i.e., transfer of amino groups - or lack thereof) among amino acids (Braun et al. 2014; McMahon and McCarthy 2016). Trophic amino acids undergo frequent transamination and deamination reactions, resulting in nitrogen enrichment (more $\delta^{15}N$) as the lighter $\delta^{14}N$ is selectively excreted and the remaining $\delta^{15}N$ undergoes transamination from one pool of amino acids to another. Source amino acids, on the other hand, are structures that are far less likely to transaminate, and thus retain their isotopic resemblance to dominant basal resources as they are transferred within food webs.

Amino acids are difficult to separate using gas chromatography due their low volatility and large number of functional groups (Silfer et al. 1991). CSIA of amino acids via gas chromatography-combustion-isotope ratio mass spectrometry (GC-C-IRMS) requires amino

acids to be derivatized to more GC-suitable forms prior to analysis (Ellis 2002). Derivatization involves substitution reactions at the carboxyl and amino ends of the molecule, along with hydroxyl, amino, or thiol groups on side chains (Ellis 2002). These techniques are primarily based on existing techniques used in GC-MS analysis of these compounds (Kaiser et al. 1974; Adams 1974; Sobolevsky et al. 2003; Suresh Babu et al. 2005; Ellis 2002). While there are many methods that are used to derivatize amino acids, it is important to consider which amino acids and isotopes are being targeted. Some derivatization techniques are better at resolving certain amino acids than others, and the amount of carbon added during derivatization also varies among techniques (Silfer et al. 1991; O'Brien et al. 2002; Walsh et al. 2014). $\delta^{13}C$ can be corrected mathematically (i.e., stoichiometrically) to account for the addition of extrinsic C during derivatization (Silfer et al. 1991; O'Brien et al. 2002; Walsh et al. 2014). In contrast, nitrogen is not added during derivatization, and only requires standard IRMS corrections for linearity and instrument drift.

1.2.3 Trophic discrimination factors

Trophic discrimination factors (TDFs), also known as trophic enrichment factors, are defined as the quantity of isotopic enrichment that is associated with increasing trophic position (DeNiro and Epstein 1981; Minagawa and Wada 1984; Post 2002; Chikaraishi et al. 2007; Bradley et al 2017). TDFs are critical parameters for estimating isotopic assimilation and consumer trophic positions (Bastos et al 2017) because accurate trophic position estimates are dependent on accurate TDFs (McMahon and McCarthy 2016). The most widely used TDFs are 1.0‰ per trophic level for bulk $\delta^{13}C$ and 3.4‰ per trophic level for bulk $\delta^{15}N$, but these values

actually vary greatly among species, physiology types (i.e., poikilotherms vs. homeotherms), and the biochemical compositions of the dominant prey or forage types (Minagawa and Wada 1984; Vander Zanden and Rasmussen 2001; Post 2002; McCutchan et al. 2003; Martinez del Rio et al. 2009).

In contrast to bulk TDFs, TDFs used for analysis of CSIA $\delta^{15}N$ vary much more extensively among different types of predator-prey relationships (Germain et al. 2013; Chikaraishi et al. 2015; McMahon et al. 2015). An organism's waste-excretion method, diet quality, and type of diet (herbivory versus carnivory) all affect the $\delta^{13}C$ and $\delta^{15}N$ of the consumer (Vanderklift and Ponsard 2003; McMahon and McCarthy 2016). For example, Vanderklift and Ponsard (2003) studied the $\delta^{15}N$ of waste excreted from various taxa that belonged to five waste-excretion groups: ureotelic (excreting mainly urea), uricotelic (excreting uric acid), ammonotelic (excreting ammonia), guanicotelic (excreting guanine), and amino-acid excretors. Their results identified large, consistent differences in the $\delta^{15}N$ enrichment of these groups. It was hypothesized that the differences were due to different pathways involved in synthesis of the excreted products. Ammonia is produced as a byproduct of protein catabolism and cannot be stored because of toxicity (Rieutord 1999; Vanderklift and Ponsard 2003). Aquatic animals excrete ammonia continually, whereas terrestrial animals undergo successive steps to transform NH4 to NH3 that binds to uric acid or urea. Having more steps translates to more fractionation and, with other things being equal, organisms excreting urea and uric acid have a higher $\delta^{15}N$ difference between consumer and diet (Ponsard and Averbuch 1999). This suggests there should be differences among the TDFs of organisms according to differences in excretion type, diet quality, and type of diet, as all of these parameters may affect $\delta^{15}N$.

In another example, Chikaraishi et al. (2015) manipulated the diets of captive toads. The three controlled diets were commercial feed pellets, bloodworms, and boiled rice. CSIA results indicated TDF significantly changed depending on the amount of protein and amino acid in the diet. The amino-acid compositions of primary producers and consumers are very different (Roth and Hobson 2000; Clements et al. 2009). Low-protein diets may have a high amino-acid imbalance between diet and consumer, which leads to the consumer reworking amino acids that have already been enriched in $\delta^{15}N$ relative to the diet (McMahon and McCarthy 2016). This leads to a high $\delta^{15}N$ TDF. When diets are more similar to consumer needs, amino acids are more likely to be routed directly from the diet with much less transamination within the consumer, and this leads to a lower $\delta^{15}N$ TDF (Braun et al. 2014; McMahon and McCarthy 2016).

These effects of diet quality on TDFs are bringing about new perspectives on how TDFs are used in trophic position calculations. Most important among these new perspectives is the realization that TDF cannot always be considered to be constant throughout life (i.e., the "additive" model). Several studies have suggested—and some have demonstrated—that using a scaled TDF (i.e., one that changes with trophic position) better captures changes in trophic position during life (Caut et al. 2009; Germain et al. 2013; Hussey et al. 2014).

1.2.4 Isoscapes

Many spatial isotopic gradients have been identified on continental shelves (Fry 1988; Al-Epping et al. 2007; Nerot et al. 2012). Recently, marine scientists have begun plotting these spatial gradients to create higher-resolution, smaller-scale isoscapes (Barnes et al. 2009;

Radabaugh et al. 2013; Radabaugh and Peebles 2014); isoscapes are geographic maps of variation in background isotope ratios (Figures 1.1 and 1.2). Radabaugh et al. (2013) and Radabaugh and Peebles (2014) published the first $\delta^{13}C$ and $\delta^{15}N$ isoscapes for the West Florida Shelf (WFS), which is the study area for the present research. Two orthogonal isotopic patterns were repeatedly documented: (1) a north-south $\delta^{15}N$ gradient and (2) an offshore-inshore $\delta^{13}C$ gradient.

The WFS is located in the eastern Gulf of Mexico along the west coast of Florida. The Mississippi, Mobile, and Atchafalaya Rivers release relatively high-$\delta^{15}N$ water into in the Gulf of Mexico west and northwest of the WFS (Rabalais et al. 1996; Del Castillo et al. 2001). Although most of the Mississippi River discharge moves west, some discharged water is carried east and south along the WFS (Del Castillo et al. 2001; Radabaugh et al. 2013). Further south on the WFS, chlorophyll concentrations decrease and the water becomes more oligotrophic (Del Castillo et al. 2001; Radabaugh et al. 2013). Atmospheric nitrogen fixed by diazotrophs is more dominant as a nitrogen source there (Mulholland et al. 2006). Fixed nitrogen is isotopically lighter than the riverine input to the north, as it is based on atmospheric nitrogen, which is the reference standard for $\delta^{15}N$ (i.e., $\delta^{15}N = 0.0$). These two dominant processes result in a robust isotopic $\delta^{15}N$ gradient on the WFS that is present both seasonally and inter-annually (Radabaugh et al. 2013; Radabaugh and Peebles 2014).

In contrast to $\delta^{15}N$, the primary gradient for $\delta^{13}C$ is present in the offshore-inshore direction on the WFS, which is the direction of a gradient that has been observed in other parts of the world (Fry and Sherr 1984; Graham et al 2010; Radabaugh et al. 2013). Clear, shallow,

inshore waters tend to have basal resources that are dominated by benthic algae and seagrasses. Deeper waters offshore have less light reaching the bottom and are dominated by phytoplankton as a basal resource. On average, benthic algae and seagrasses are isotopically heavier than phytoplankton offshore (Fry and Sherr 1984; Finlay and Kendall 2007; Graham et al. 2010), and thus spatial variability in $\delta^{13}C$ can distinguish between inshore and offshore feeding in marine animals. On the WFS, variability in $\delta^{15}N$ relates to geographic differences in the isotopic baseline while also reflecting trophic position (Hobson 1999b; Vander Zanden and Rasmussen 2001; Hobson et al. 1994).

1.3 Objectives and research overview

This dissertation addresses the call for the development of more intrinsic lifetime-scale, natural-tag records, with a focus on lifetime records for δ^{13C} and $\delta^{15}N$. There are four primary objectives that serve as the framework of this dissertation:

- Examine eye lenses as a new stable-isotope record for bulk stable isotope analysis,
- Examine eye lenses as a new stable-isotope record for compound-specific stable-isotope analysis,
- Reconstruct trophic histories for individual lifetimes using compound-specific stable isotope analysis, and
- Subtract lifetime trophic-position trends from bulk-isotopic trends to isolate geographic effects (i.e., individual fish movement history).

In Chapter 2, which has already been published (Wallace et al. 2014), I tested the utility of eye-lens protein as a potential lifetime isotopic record. I used four species to test whether the bulk $\delta^{13}C$ and $\delta^{15}N$ information had trends and patterns over time. Bulk isotopic analyses are widely used in environmental studies; however, this chapter represents the first time fish eye lenses have been explored as stable-isotopic recorders.

In Chapter 3, I explored the possibility of using eye-lens proteins for compound-specific isotope analysis of amino acids (CSIA-AA). The study objective was to isolate isotopic variation within and between individuals, separating baseline (source) from trophic effects. Using muscle tissue, fractionation between source and trophic amino acids has been used to estimate trophic position in marine fishes (Popp et al. 2007). Using Red Snapper (*Lutjanus campechanus*) eye lenses, I was able to isolate isotopic changes in source and trophic amino acids on a lifetime temporal scale. I tested 60 laminae for isotopic variation and cross-referenced any trends with published data. This is the first record of its kind from individual fish.

In Chapter 4, I applied bulk and amino-acid isotope analyses to reconstruct individual trophic and geographic histories. Chapters 2 and 3 established the groundwork necessary for this process. In Chapter 4, I applied the methods and findings of the preceding chapters to isolate trophic-position effects from geographic baseline effects and used this method to compare individuals of a reef fish (Red Snapper, *Lutjanus campechanus*) with individuals of a highly migratory fish (King Mackerel, *Scomberomorus cavalla*). Finally, I compared these trends with those of two individuals of a species that has data gaps in its life history, the Greater Amberjack (*Seriola dumerili*), and inferred that either it or its prey is likely to be migratory.

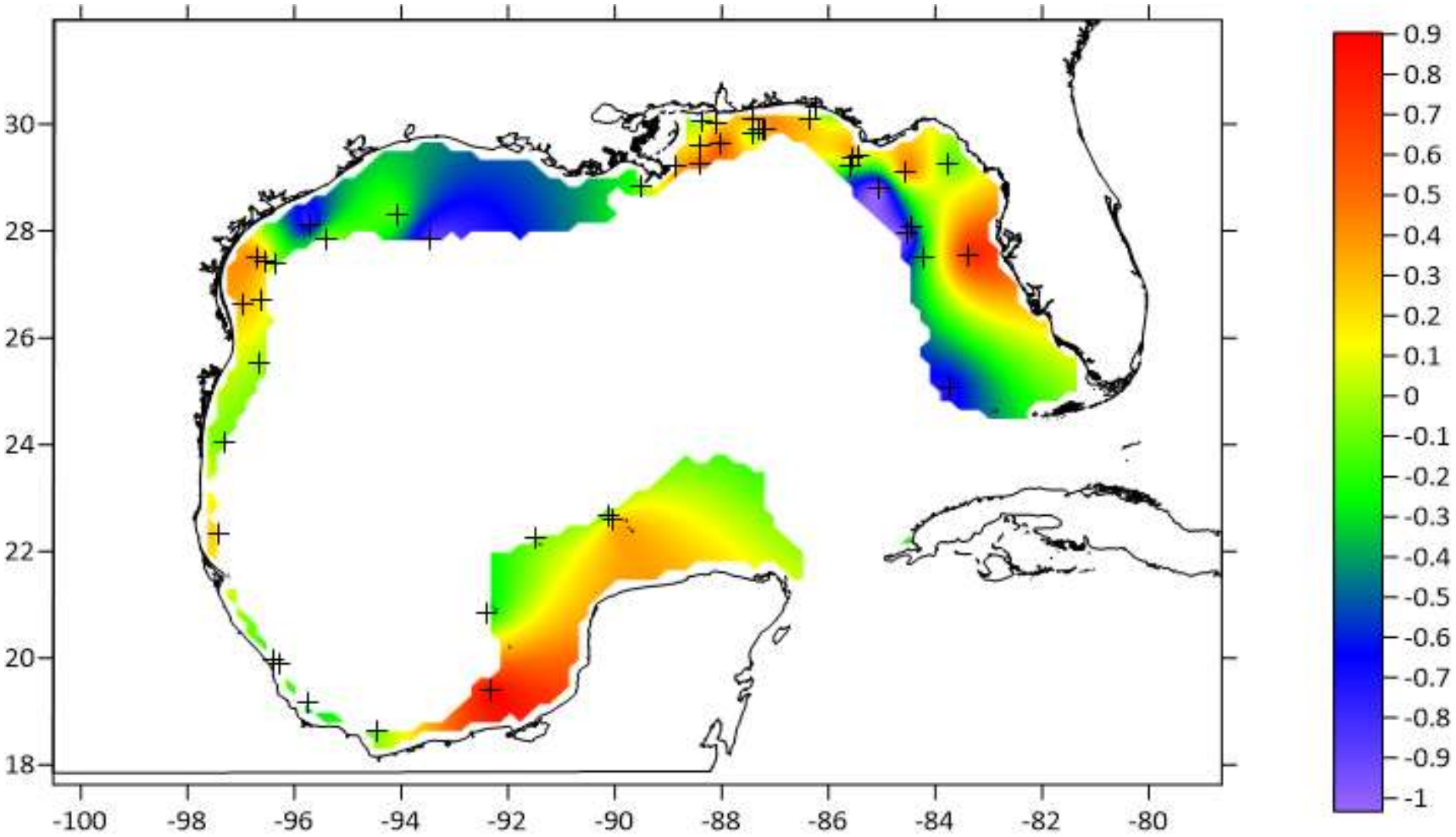

Figure 1.1 Carbon isoscape of the Gulf of Mexico (Brianna Michaud, USF, unpublished). The isoscape was created using fish muscle. The residuals from a regression between $\delta^{13}C$ and standard length of the fish are plotted to remove the effect of trophic level changing over space.

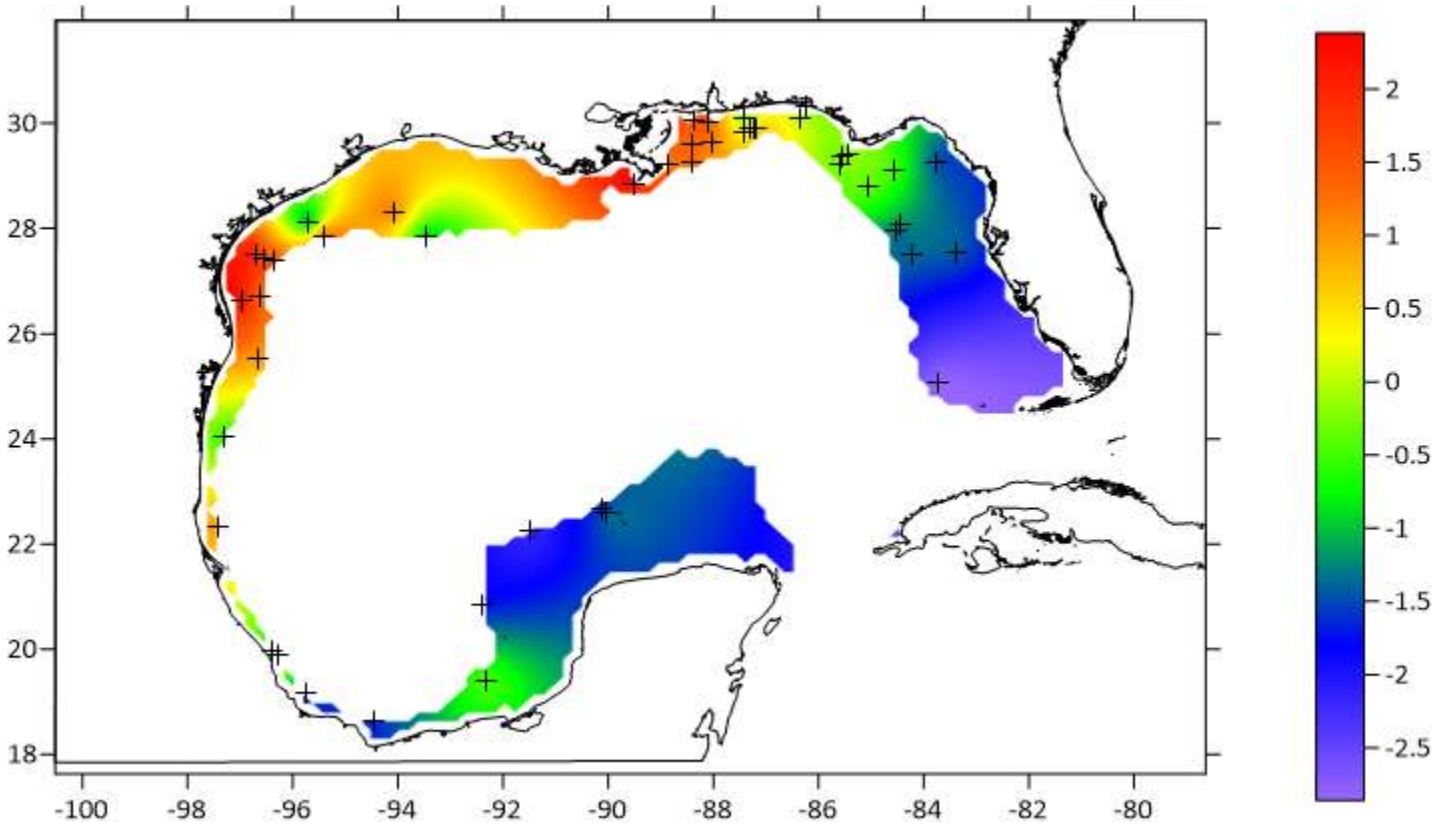

Figure 1.2 Nitrogen isoscape of the Gulf of Mexico (Brianna Michaud, USF, unpublished). The isoscape was created using fish muscle. The residuals from a regression between $\delta^{15}N$ and standard length of the fish are plotted to remove the effect of trophic level changing over space.

Chapter 2. Stable isotopes in fish eye lenses as potential recorders of trophic and geographic history

Note to Reader: The contents of this chapter have been published in the open access journal, PLoS ONE. Due to the open access nature of the journal, permission was granted to reprint the manuscript here as a chapter of this dissertation.

Citation: Wallace AA, Hollander DJ, Peebles EB (2014) Stable Isotopes in fish eye lenses as potential recorders of trophic and geographic history. PLoS ONE 9(10): e108935.

The online article can be accessed at https://doi.org/10.1371/journal.pone.0108935

2.1 Introduction

Internally recorded stable-isotope histories can be used to recreate lifelong trends in animal diets, trophic dependences, and movement within isotopically variable landscapes (Tiezen et al. 1983; Hobson and Clark 1992a; Hobson and Clark 1992b; Post 2002; Phillips and Eldridge 2006). Such lifelong records are difficult to obtain because most tissues undergo metabolic turnover, and this turnover places limits on the retrospective time period that can be investigated (Thompson and Ballou 1956; Fray and Arnold 1982; Hobson and Clark 1992a; Hobson and Clark 1992b; Phillips and Eldridge 2006).

Otoliths, fish scales, and vertebrae are tissues currently used to provide life-history records for fish. Otoliths are used to determine fish age and to reconstruct aquatic environments (Jones 1986; Thorrold et al. 1997). Otoliths grow during the entire life of the fish and consist of calcium carbonate deposited within a proteinaceous matrix. Otolith protein is generally not abundant enough (3-4% by weight) to allow retrospective $\delta^{15}N$ comparisons (Campana 1999). Fish scales grow during most of the life of the fish and provide a nonlethal way to measure isotopic ratios. Fish scales overlap old organic material with new material during growth in a phenomenon called "overplating" (Hutchinson and Truman 2006; Trueman and Moore 2007; Woodcock and Walther 2014). Overplating affects isotopic ratios by combining isotopic values from new and old material; scales may not provide a true representation of isotopic information on a temporal scale (Hutchinson and Trueman 2006). Some researchers have explored the use of vertebrae in sharks for stable-isotope analyses with encouraging results (Estrada et al. 2006; Kerr et al. 2006; Werry et al. 2001). The collagen extracted from cartilaginous vertebrae is preserved because cartilage has low metabolic activity (little or no turnover) and it deposits in sequential layers (Walker and Macko 1999). However, this approach cannot be applied to the vertebrae of bony fishes because bone collagen is reworked over time (Hobson and Clark 1992a; Hobson and Clark 1992b). Although this paper focuses on fish, it should be noted that there are a number of isotopic records for terrestrial animals as well. These include claws, hooves, hair, feathers, and teeth (Dalerum and Angerbjörn 2005; Ethier et al. 2010). Although these tissues are inert, the period of time represented by the record varies with tissue wear (e.g. claws, hooves) and replacement (e.g. feathers, hair) (Dalerum and Angerbjörn 2005; Ethier et al. 2010). Some tissues can be sampled non-invasively

on a regular basis to create a long-term isotopic record, but require recapture of the same animal on a regular basis (Dalerum and Angerbjörn 2005; Ethier et al. 2010).

In this paper, we evaluate fish eye lenses as potential recorders of the isotopic histories of individual fish; the eye lenses of squid (invertebrates) also appear to have this potential (Parry 2003; Hunsicker et al. 2010). Vertebrate eye lenses are composed of different forms of a structural protein, crystallin, that are deposited in layers (laminae) at the outer lens as the animal grows (Nicol 1989; Horwitz 2003). During the mid-to-late gastrula stage, lens cells derive from surface ectoderm and differentiate into two cell types, lens epithelial cells and fiber cells (Dahm et al. 2007; Wride 2011), although Bloemendal considered all lens cells to be epithelial (Bloemendal 1982). At the surface of the lens, epithelial cells form a one-cell-thick outer layer (lens epithelium) that encapsulates the fiber cells. Fiber cells remove their cytoplasmic organelles, including the cellular nucleus and its DNA, to establish and maintain optical transparency within the lens (Nicol 1989; Horwitz 2003; Dahm et al. 2007; Wride 2011; Vihtelic 2008). This process is a specialized form of apoptosis known as “attenuated” apoptosis, where the organelles are released from the cell over a period of days, leaving behind the nonliving, crystallin cytoskeleton (Wride 2011; Dahm 1999). Attenuated apoptosis is different from “classical” apoptosis in which everything, including the cell membrane, is degraded (Wride 2011).

Fish eye lenses are spherical, and crystallin protein fibers are laid down in concentric layers much like the layers of an onion (Nicol 1989; Horwitz 2003; Dahm et al. 2007). Fiber cells increase in length as the animal grows, but the increase in length is a step function of lens

radius rather than a continuous increase, and this step function creates the physical discontinuities that are visible between adjacent laminae. The oldest part of the lens is at the center (lens nucleus); the nuclear fiber cells are among the oldest cells in the body (Wride 2011). The outermost margin of the lens is the youngest material in the lens. Each successive lamina becomes metabolically inactive after deposition and attenuated apoptosis (Nicol 1989). As a structural protein, crystallin is rich in both carbon and nitrogen, and thus is suitable for $\delta^{13}C$ and $\delta^{15}N$ analysis; this contrasts with otoliths, which are nitrogen-poor. Eye lenses thus have the potential to allow reconstruction of lifetime $\delta^{13}C$ and $\delta^{15}N$ histories and their associated ecological interpretations.

To investigate variation in fish eye-lens stable isotopes, we selected fish species that occur in geographic locations that had already been the subject of isotopic mapping (isotope maps are known as “isoscapes”). This allowed comparison of any observed isotopic trends within the fish eye lenses with a known range and pattern of isotopic variation documented by Radabaugh et al. (2013). Four species (red snapper, red grouper, gag, white grunt) were selected that have life histories that are geographically bracketed between the polyhaline coastal zone and the outer continental shelf, a region that coincides with the Radabaugh et al. isoscapes (we avoided estuarine, strongly estuarine-dependent, and highly migratory species). We were otherwise limited to specimens that became available near the time of analysis, as no specimens were collected for the sole purpose of conducting the present study. We expected trophic positions to increase with age (as mouth gape increases), which generally causes $\delta^{13}C$ and $\delta^{15}N$ to increase with age (Karpouzi and Stergiou 2003; McMahon et al. 2013).

We conducted four tests to investigate variation in fish eye-lens isotopes ($\delta^{13}C$, $\delta^{15}N$). First, we conducted a low-resolution comparison of a small number (4-5) of eye-lens layers (groups of laminae) to determine if there was enough isotopic variation during life to warrant further study, with the specific objective being to compare lifetime isotopic variation with isoscapes recently produced by Radabaugh et al. (2013), therein possibly providing insight into changes in fish movement and trophic position during life. After discovering that substantial, measurable isotopic variation did exist within the lenses, we used the remaining, second lens to conduct high-resolution comparisons, dissecting (delaminating) the second lens into as many thin layers (hereafter referred to as "laminae") as was practical, and comparing the high-resolution results with the coarse patterns from the first test. We then compared high-resolution patterns in the left and right lenses of an additional specimen to investigate repeatability. Finally, we examined intra-laminar variation to identify the level of inherent variability (precision) in the method.

2.2 Materials and Methods

2.2.1 Ethics Statement

No fish were collected or killed for the purpose of this study. All tissues were collected post-mortem according to a protocol (IS00000504) approved by the University of South Florida Institutional Animal Care and Use Committee. None of the sampled species are protected except by recreational and commercial harvest regulations. Fish were obtained from surveys conducted by the Florida Fish and Wildlife Commission (FWC) and from a licensed

charter-fishing vessel operating within state and federal regulatory guidelines in waters no more than 80 km distant from John's Pass, Madeira Beach, Florida.

2.2.2 Lens Collection and Dissection

Four red grouper (*Epinephelus morio*) and three gag (*Mycteroperca microlepis*) were obtained from an FWC survey conducted 9-10 July, 2013. Eight red snapper (*Lutjanus campechanus*) were obtained from John's Pass charter vessels on 10 September, 2013 and one white grunt (*Haemulon plumierii*) was obtained from a charter vessel on 11 June, 2013. Whole eyes were removed by severing the sclera at its junction with the optic nerve and by severing the rectus (orbital) muscles near their junction with the sclera. Eyes were wrapped in aluminum foil, placed in plastic bags on ice, and frozen at -40 □C upon return to the laboratory.

Eyes were thawed individually before dissection. After thawing, an incision was made with a scalpel to create a flap in the cornea, which was folded back to allow removal of the lens using forceps. Exterior tissue and vitreous material were manually removed using a deionized water rinse. The rinsed lens, which contained the lens nucleus, cortex, and lens epithelium together as one cohesive unit (whole lens), was then placed on a glass petri dish where successive layers of cortical laminae were separated using two pairs of fine-tip forceps under a dissecting stereomicroscope, leaving the lens nucleus as the final tissue in the analyzed series. The lens nucleus did not visibly delaminate further when crushed. Because the total number of cortical laminae varied with lens diameter (age), the convention for numbering laminae started with the lens nucleus as 1, with assigned numbers increasing toward the outer lens margin. Lamina removal (delamination) started near one lens pole and proceeded to the

other, always starting the removal process at the same pole (note that the "anterior-posterior" polar axis referred to in studies of the human eye applies to forward-oriented eyes; most fish have laterally oriented eyes, and thus the homolog of the human anterior-posterior polar axis is usually mediolateral in fish, with the anterior pole and associated primary sutures being oriented laterally). Some forms of crystallin are water-soluble (Bloemendal 1982; Sharma and Santhoshkumar 2009); deionized water was used sparingly to assist delamination.

After each delamination, an ocular micrometer was used to measure the diameter at the equator (to nearest 0.1 mm); the equator was identified as the largest diametric measurement that could be made perpendicular to the (mediolateral) polar axis. Lamina position is the radial midpoint of the lamina (in mm) on the equator, where the midpoint is the lens radius after lamina removal plus half the thickness of the removed lamina.

2.2.3 Lens Sample Processing

Four types of isotopic variation were plotted: 1) low-resolution screening plots, 2) high-resolution plots for selected, screened individuals, 3) plots of left vs. right eyes, and 4) plots of variation within individual laminae (intra-laminar variation). For low-resolution screening, eye lenses were separated into 4-5 sections using fine-tip forceps, with multiple laminae intentionally included within each section; the number of true laminae constituting each section was not known. For all other tests, an effort was made to subdivide the lenses into the smallest thicknesses that were manually practical ("laminae"). Individual sections and laminae were stored separately in 1-dram glass vials. Laminae became desiccated in <1 hr. at 25 °C, after which most samples were homogenized using a mortar and pestle; exceptions were

laminae that were haphazardly selected for intra-laminar variation analysis, which were subdivided first and then homogenized.

Dried laminae were weighed to the nearest µg on an analytical balance. A dry weight of 300-600 µg of material was placed in tin capsules for combustion and isotopic analysis. $^{13}C/^{12}C$ and $^{15}N/^{14}N$ and C:N were measured in replicate using a Carlo-Erba NA2500 Series II elemental analyzer coupled to a continuous-flow ThermoFinnigan Delta+XL isotope ratio mass spectrometer at the University of South Florida College of Marine Science in St. Petersburg, Florida. The lower limit of quantification was 12 µg C or N. Calibration standards were NIST 8573 and NIST 8574 L-glutamic acid standard reference materials. Analytical precision, obtained by replicate measurements of NIST 1577b bovine liver, was ±0.11 ‰ for $\delta^{13}C$ and ±0.19 ‰ for $\delta^{15}N$ (average standard deviations of n = 30 replicates). Results are presented in standard notation (δ, in ‰) relative to international standards Pee Dee Belemnite (PDB) and air:

$$\delta^{j}/_{i}X = \frac{\left({}^{j}X/{}_{i}X\right)_{sample}}{\left({}^{j}X/{}_{i}X\right)_{standard}} - 1$$

where, X is the element and *j* and *i* are each an isotope of X.

2.2.4 Data Location and Analysis

All data are published at the Gulf of Mexico Research Initiative Information and Data Cooperative (https://data.gulfresearchinitiative.org/data/R1.x135.120:0006). In all comparisons except for the intra-laminar comparison, replicate isotope measurements were averaged and

plotted for descriptive purposes. In the intra-laminar comparison, the objective was to determine if inter-laminar variation was greater than intra-laminar variation; individual replicate isotope measurements were compared among laminae using one-way ANOVA. Individual laminae were compared using 95% Tukey HSD intervals as a multiple range test (Statgraphic Centurion, v. 16.2.04). In all comparisons, means and replicates were plotted without any exclusion.

2.3 Results

Low-resolution screening analyses were conducted for eight red snapper, four red grouper, and three gag. All individuals had variable isotopic values among lens layers (Figure 1). The majority of values were centered within ranges reported by Radabaugh et al. (2013) for trawl-caught demersal fishes on the West Florida Shelf (-19– -14 ‰ $\delta^{13}C$; 7–13.5‰ $\delta^{15}N$). Red snapper appeared to form two groups based on their $\delta^{15}N$ values; fish 45 and 47 (Figure 1) had consistently high $\delta^{15}N$ values. There were no clear groupings in red grouper. Gag 2 had higher $\delta^{13}C$ values for its innermost layer than the other two gag, and all three gag had isotopic values that converged in the outermost layers. $\delta^{15}N$ increased during life in all fish except red snapper 45.

Gag 2 and 38 were analyzed using high-resolution analysis to further evaluate the difference recorded in the innermost layers. The lens from gag 2 (3.1 mm radius) was dissected into 14 laminae plus a lens nucleus of 0.65 mm radius, indicating an average laminar thickness of 175 µm. The lens from gag 38 (3.2 mm radius) was dissected into 16 laminae plus a lens nucleus of 0.60 mm radius, indicating an average laminar thickness of 163 µm. When data from

the two lenses were combined, dry weight (DW, in mg) increased as DW = 3.24r3 (n = 32, R2 = 0.99, p <0.0001), where r is lens radius in mm. The mean dry density of these two gag lenses was 0.89 mg mm-3. Laminar thickness varied at a sub-annual scale in these two specimens, but did not have a strong positive or negative overall relationship with lens radius (slope p >0.05).

The exponential (cubic) increase in average laminar weight that accompanies increasing lens size translates into a mass-balanced bias toward outer laminae when groups of laminae are processed together as a collective layer (e.g., during low-resolution screening analysis). The innermost layer from the screening analysis was most likely to be misrepresentative of patterns observed in the high-resolution analysis (Figure 2). Nevertheless, the screening method indicated different incipient $\delta^{15}N$ values for gag 2 and 38, and this difference was borne out by the high-resolution analysis, albeit at a nominally lower difference (2.5 vs. 3.0 ‰).

The left lens of white grunt 2 was dissected into 12 laminae plus the lens nucleus. The radius of the left lens nucleus was 0.50 mm and the radius of the whole left lens was 2.85 mm, indicating a mean laminar thickness of 196 µm. The right lens was dissected into 13 laminae plus the lens nucleus. The radius of the right lens nucleus was 0.60 mm and the radius of the whole right lens was 2.88 mm, indicating a mean laminar thickness of 175 µm. Isotopes in both eyes were centered within ranges reported by Radabaugh et al. (2013), and $\delta^{15}N$ increased during life; this latter trend was observed in 15 of the 16 fish examined (94%). Isotopic patterns were very similar between left and right eyes (Figure 3), yet plotted pairings of radial midpoints in Figure 3, average laminar thicknesses (196 vs. 175 µm), and the difference in

total lamina count (12 vs. 13) were not in perfect agreement. One-way ANOVA indicated inter-laminar variation (Figure 4) was much larger than intra-laminar variation for both $\delta^{13}C$ [$F(6,16) = 40.6$, $p < 0.0001$] and $\delta^{15}N$ [$F(6,16) = 232.4$, $p < 0.0001$].

A total of 197 samples were analyzed (72 sections, 125 lamina). The range of mass C:N was 2.72-3.37. The mass C:N mean value was 2.97±0.12 (molar C:N range = 3.17-3.39; mean = 3.46±0.14). The C:N ratio was consistently < 3.5; therefore, no lipid correction or normalization was needed because the lipid concentrations were uniformly low [33].

2.4 Discussion

The results indicate low-resolution isotopic screening has strong potential as an index of broad-scale changes in the isotopic history of individual fish. Broad-scale changes were evident in all species, yet red snapper and gag appeared to originate from distinct groups that converged later in life (all fish were collected from the same geographic region). The magnitude of isotopic variation observed in both the low- and high-resolution tests (Figures 1-3) matches the scale of variation in isoscapes produced by Radabaugh et al. (2013) for the West Florida Shelf, the region from which the fish in our tests were collected. The low-resolution screening tests were rapid and cost-effective, but sometimes missed important life events. In the case of the gag (Figure 2), the missed detail involved early life history; the low-resolution analysis had a starting value of -13.8 ‰ for $\delta^{13}C$ while the high-resolution analysis was variable, ranging -16.4 to -12.9 ‰. The high-resolution approach contains the most information that can be obtained practically using the manual delamination method.

The white grunt's left and right eyes identified very similar lifelong trends (Figure 3), suggesting the temporal trends observed in the other comparisons (e.g., Figure 1) were repeatable and were not artifacts. The scale of variability between left and right eyes was similar to that of intra-laminar variation. Most intra-laminar variation was less than the instrument error calculated using bovine liver (±0.11 ‰ for $\delta^{13}C$; ±0.19 ‰ for $\delta^{15}N$,). Small, intra-laminar variation likely imparts a limit to the precision of the overall method.

All of the values and trends in the eye-lens isotopes are consistent with expected life-history patterns and trophic positions, as interpreted using published $\delta^{13}C$ and $\delta^{15}N$ isoscapes for demersal fish muscle (Radabaugh et al. 2013). Isoscapes visually portray spatial isotopic variation within natural systems (West et al. 2010). While many terrestrial isoscapes exist, a need exists for developing more marine isoscapes (Hobson et al. 2010). When eye-lens isotopes are compared to observed and modeled isoscapes for demersal fish muscle on the West Florida Shelf (Radabaugh et al. 2013; Radabaugh and Peebles 2014), it appears that the two red snapper with higher $\delta^{15}N$ (Figure 1) traveled from the northern end of a $\delta^{15}N$ latitudinal gradient, and those with lower $\delta^{15}N$ traveled from or remained within more southerly waters. Isoscape trends in $\delta^{13}C$ of demersal fishes are more depth-related (higher values in shallow water) than latitude-related (Radabaugh et al. 2013). Red snapper eye-lens $\delta^{13}C$ remained below -15.5‰ throughout life, which is consistent with the red snapper's known preference for deeper water on the middle and outer portions of West Florida Shelf. The three gag may have started life at different locations, but spent a lengthy period of time together before collection. Unlike the red snapper, the gag uses shallow inshore waters as nursery habitat (Fitzhugh et al. 2005). The elevated $\delta^{13}C$ in gag 2 (Fig. 2) is indicative of residence in shallow water. However,

because $\delta^{13}C$ for demersal fish in inshore waters varies along the coastline as a statistical function of water clarity/depth (photosynthetically active radiation at bottom), particulate organic carbon concentration, and sea-surface temperature (Radabaugh and Peebles 2014), not all gag can be expected to reside in high-$\delta^{13}C$ locations while in shallow nursery habitats.

All of the preceding geographic interpretations are subject to future corrections that accommodate shifts in trophic level and associated changes in total trophic fractionation. The increase in $\delta^{15}N$ that was observed in most (94%) specimens is consistent with increasing trophic level. The trend in the sole exception, red snapper 45, would be explained if the fish moved south later in life (Radabaugh et al. 2013; Radabaugh and Peebles 2014). Among the four species, the gag (a large, piscivorous grouper) had relatively high $\delta^{15}N$ values at capture; this is consistent with expected differences in trophic position among species.

Directions for future work include, but are not limited to, the following areas of study: 1) eye lens aging by synchronizing lamina radial position with otolith-based or known captive age; relationships between fish eye-lens diameter and age, lens wet-weight and age, and lens dry-weight and age have already been established (Burkett and Jackson 1971; Siezen 1989; Al-Hassan and Al-Sayab 1994; Al-Mamry et al. 2012), 2) validating diet relationships using compound specific stable isotope analysis of the both the trophic and source amino acids within different laminae (Popp et al. 2007; Chikaraishi et al 2009; Ellis 2012), 3) determination of long-term geographic histories for individual fish by combining isotope histories, knowledge of how trophic level changes with age (trophic growth rate), and output from isoscape models (Radabaugh and Peebles 2014); modeled isoscape outputs must be synchronized with time

periods within eye lenses for accuracy because spatial stationarity cannot be assumed (Radabaugh and Peebles 2014; Haché et al. 2014), 4) comparing isotopic fractionation of eye lens tissues with fractionation of other tissues (Caut et al. 2009; Martinez del Rio and Carleton 2012). Studying captive fish may be particularly definitive both for aging eye lenses and for validating diet relationships with eye-lens isotopes. However, the production and accurate interpretation of long-term geographic histories for individual fish require that eye-lens aging and trophic growth rate studies be completed first.

While our ability to rigorously interpret geographic histories from the eye-lens isotope data is limited by the present lack of the aforementioned studies, the patterns of variation within the eye lenses (Figs. 1-4) indicate that the overall approach is promising. There is no other known source of simultaneous $\delta^{13}C$ and $\delta^{15}N$ temporal records within bony fish. The approach presented here is not necessarily limited to bony fish and may also be applied to other vertebrates as long as the spatiotemporal distribution of apoptosis within the lens is taken into consideration. In fish, TUNEL assays (terminal deoxynucleotidyl transferase dUTP nick-end labeling) indicate that even recently formed laminae can be apoptotic and thus isotopically conservative (Dahm et al. 2007), whereas humans and other higher vertebrates may contain large proportions of pre-apoptotic (potentially non-conservative) cells in the outer cortical region of the lens.

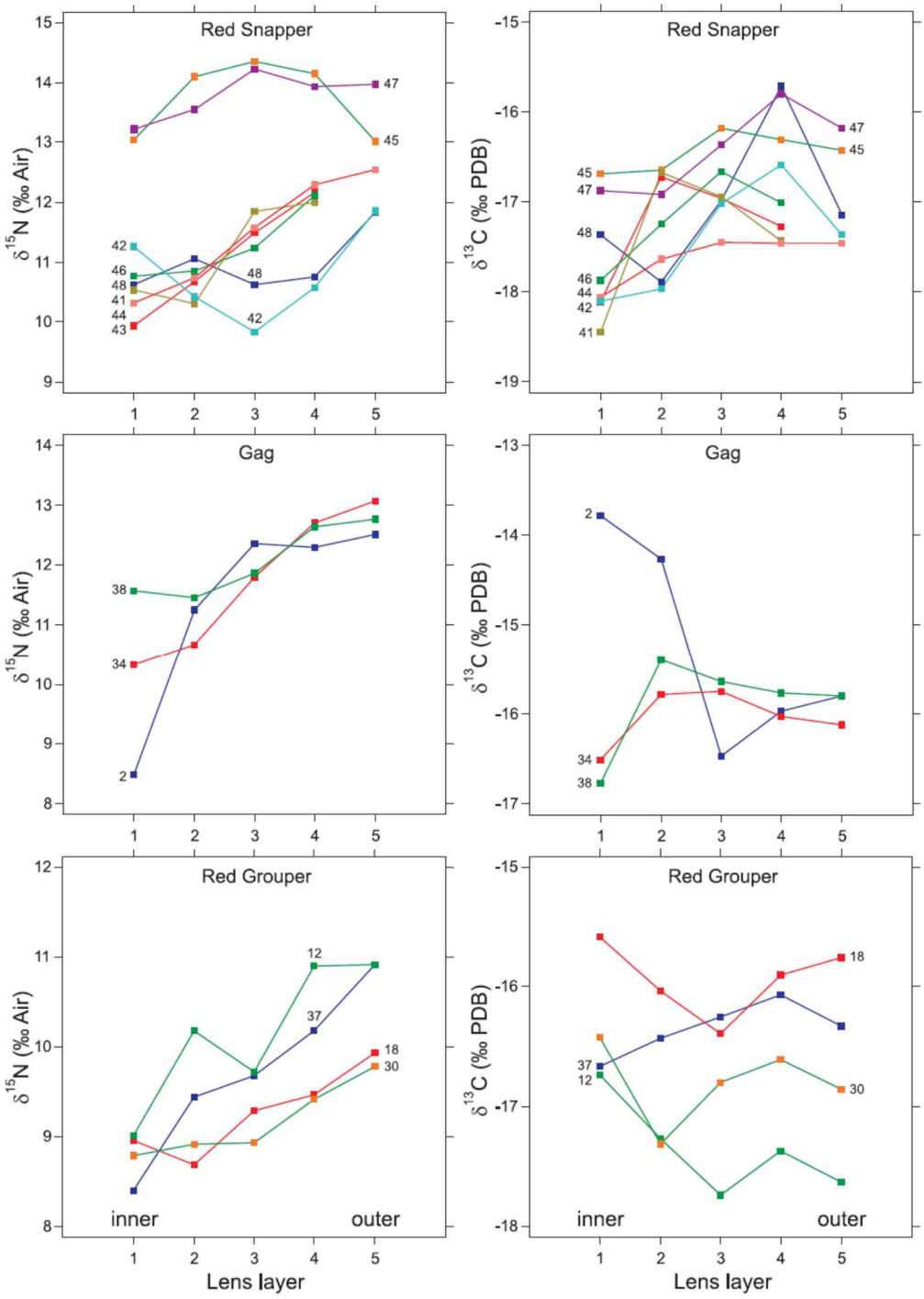

Figure 2.1 Low-resolution screening. Rapid screening of specimens to detect large-scale differences in isotopic history. Each plotted line is a different specimen; lines are labeled with specimen numbers.

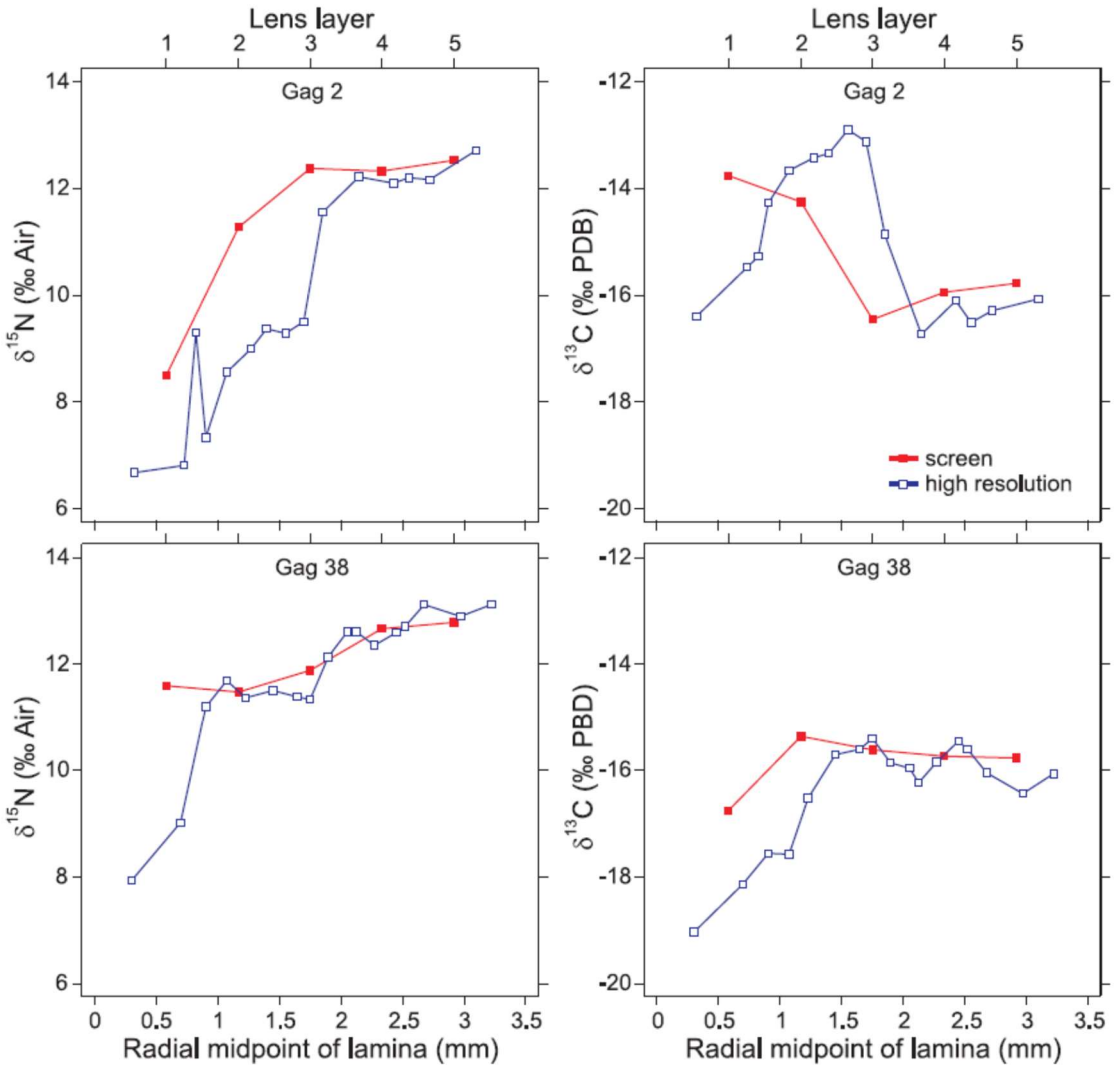

Figure 2.2 Low- and high-resolution comparison. The low-resolution screening method (analysis of coarse lens layers) is compared with the high-resolution method (analysis of individual laminae) for gag 2 (upper panels) and gag 38 (lower panels). The leftmost observation in the high-resolution method is for the lens nucleus; the remaining observations are for individual laminae. Gag 2 was 704 mm total length (TL); gag 38 was 832 mm TSL. Both were female.

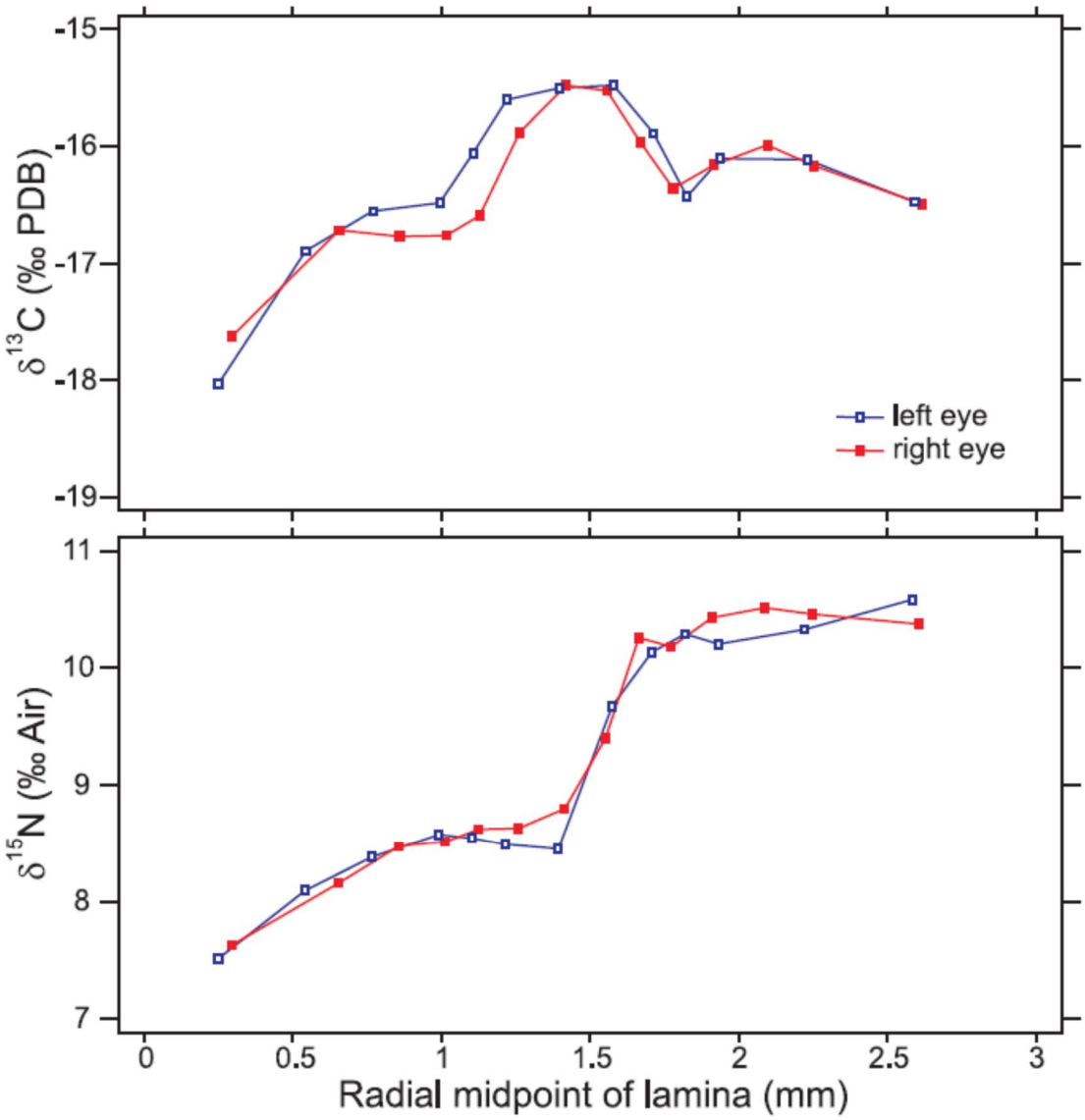

Figure 2.3 High-resolution comparisons of left and right eyes of white grunt specimen 2.

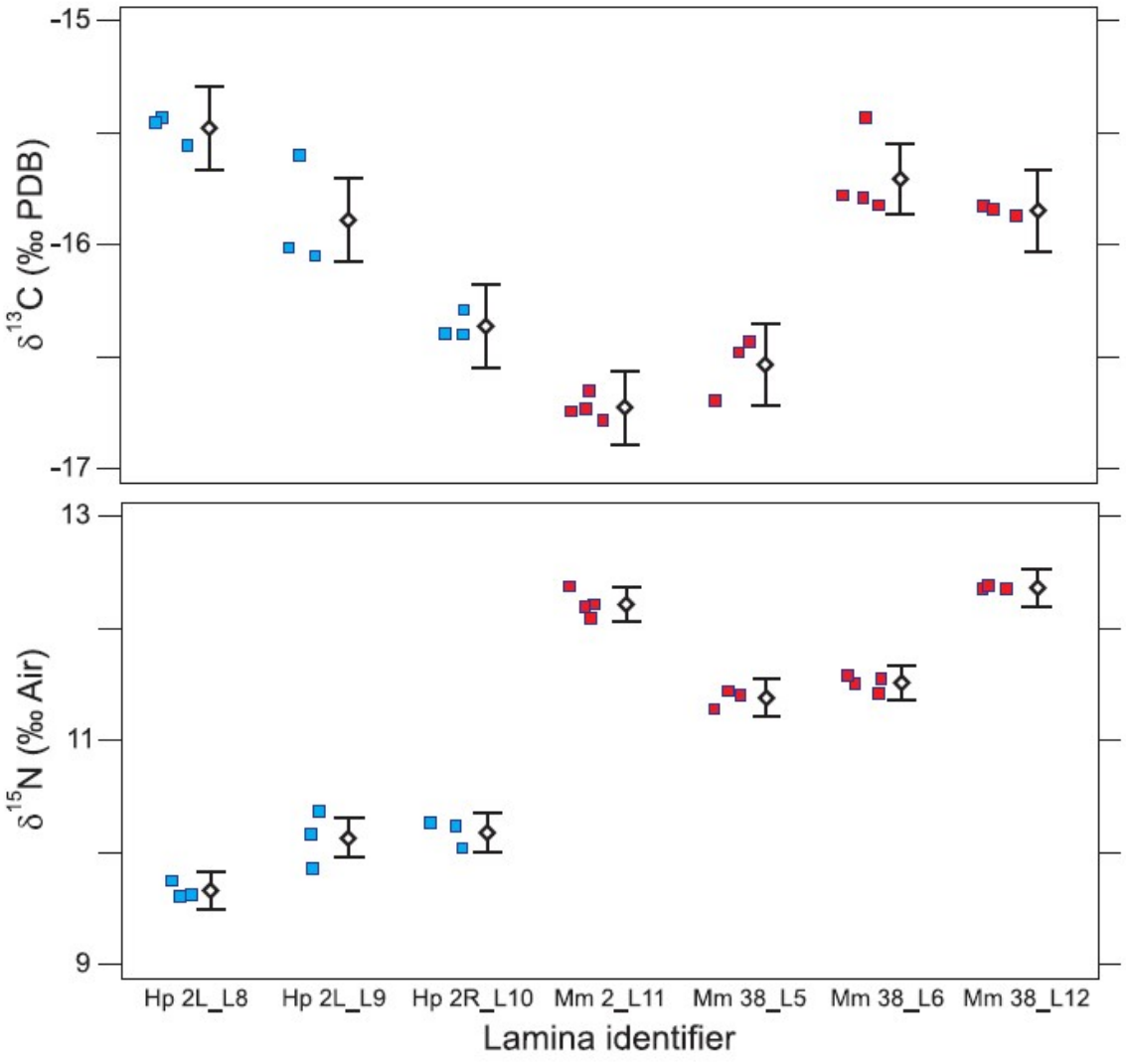

Figure 2.4 Intra- and inter-laminar comparison. Comparison of intra- and inter-laminar isotopic variation in white grunt specimen 2 (Hp 2) and gag specimens 2 and 38 (Mm 2 and Mm 38). Lamina number (e.g., L8 = lamina 8) is indicated within lamina identifiers. Data points have been horizontally jittered for clarity and are summarized by means (diamonds) with 95% Tukey HSD intervals.

Chapter 3. Nitrogen isotopic analysis of fish eye-lens amino acids

3.1 Introduction

The stable isotope analysis (SIA) approach to ecosystem studies has avoided many challenges prevalent in stomach-content and feeding-observation studies, but SIA presents its own complications, challenges, and opportunities. The first challenge is spatio-temporal variability in baseline nitrogen and the second challenge is that trophic fractionation variability is not always consistent with the previously published values (Post et al. 2002; McMahon and McCarthy 2016). This paper addresses the spatio-temporal variability problem by using compound-specific isotope analyses (CSIA) of amino acids (AAs) within fish eye lenses (Popp et al. 2007; Chikaraishi et al. 2010).

Compound-specific isotope analyses of amino acids (CSIA-AA) is a very useful method of analysis that requires fewer assumptions than bulk SIA and has become a powerful analytical tool for ecological interpretations (Boecklen et al. 2011; McMahon and McCarthy 2016). Based on patterns of nitrogen isotope fractionation, AAs can be categorized as “trophic”, “source”, and “others” (Whiteman et al. 2019). Trophic AAs show strong fractionation with increasing trophic position as a result of frequent involvement in transamination and deamination reactions. In contrast, source AAs are minimally fractionated with increasing trophic levels (Braun et al. 2014; McMahon and McCarthy 2016). Other AAs do not fractionate consistently

across organisms and so yield little useful information without further investigation (Whiteman et al. 2019). Analysis and comparison of trophic and source AAs has increased both the precision and accuracy of trophic position estimates (TP_{CSIA}; Chikaraishi et al. 2010; Bradley et al. 2015; McMahon and McCarthy 2016; Whiteman et al. 2019). Currently, CSIA-AA is commonly used on soft tissues of specimens, which gives an isotopic snapshot at the time of collection based on the tissue turnover rate. However, using CSIA-AA on fish eye lenses can potentially create a temporal history of amino-acid isotopes across an organism's lifetime.

Fish eye lenses consist of metabolically-inert, protein-rich layers (laminae) of lens fiber cells. Lens fibers cells are a product of the lens epithelium, a single layer of living cells surrounding most of the eye lens (Dahm 2007; Greiling and Clark 2012). During post-embryonic lens growth, lens epithelium cells at the lens equator transform into lens fiber cells by filling with crystallin (a structural protein), elongating towards the lens poles, and then removing their DNA and organelles through attenuated apoptosis. During typical apoptosis, the cell dies and the entire cell disintegrates. However, attenuated apoptosis is different than typical apoptosis in that the cell membrane and internal proteins remain. Attenuated apoptosis effectively stops further protein synthesis within the new lens fiber cells, rendering the cells metabolically inert in a manner analogous to hair, feathers, and hooves (Dahm 2007; Greiling and Clark 2012). As the cells elongate and meet at the poles, a layer, or lamina, is formed that contains multiple layers of lens fiber cells. Each new lamina is formed around the previous ones, creating concentric layers, with the oldest material in the center of the lens. Because eye lenses can form within a few days after fertilization (Dahm et al 2007), the nitrogen isotopes within the

lens laminae capture information throughout nearly the entire life of the fish (Wallace et al. 2014).

3.2 Methods

3.2.1 Field Work/Sample Collection

Fish samples were collected during August 2014 from the R/V *Weatherbird II* using longline fishing techniques. At each station (Figure 3.1), 8 km of 544 kg-test monofilament was deployed from the ship as the mainline, with approximately 500 baited hooks attached to the mainline via gangions. Gangions were 3.7 m long and used 91-kg-test and #13 circle hooks that were baited alternately with cut fish (Atlantic Mackerel*, Scomber scombrus*) and various species of squid.

Whole eyes were removed using a knife in the field and kept frozen between -20 and -40°C until time of lens dissection (delamination). Lenses were delaminated using forceps and a dissecting microscope according to a modification of the technique described in Wallace et al. (2014). In this modification, a water rinse was not used to remove the lens capsule; instead, it was cut away using forceps and a scalpel. This change to the processing method ensured there was no dissolution of the outmost lamina, which is highly water soluble. Before and after each lamina removal, lens diameter was measured to the nearest .005 mm using an ocular micrometer. Diameters were converted to radii, and the laminar radial midpoint (LRM, in mm) was calculated as the average of the two (before and after) radius measurements taken during eye lens delamination.

3.2.2 AA-CSIA Processing

AAs are difficult to separate using gas chromatography because they are insufficiently volatile and have a large number of functional groups. Therefore, AAs require derivatization prior to isotopic analysis (Silfer et al. 1991). All samples were derivatized using the methods outlined in Ellis (2012), described here in brief.

For each individual lamina, a dry weight of approximately 1 mg was placed in a 20 mL scintillation vial with 2 mL 6 M HCl and heated at 100°C for 24 hours to hydrolyze proteins. The acid solution was evaporated under a stream of N_2 at 70°C, after which samples were re-suspended in 0.05 N HCl. The digested sample was then transferred to a Dowex 50wx8, 200-400 mesh cation-exchange resin column assembled in a clean Pasteur pipette. Non-AA components were flushed from the column using deionized water. The AAs were then eluted from the Dowex resin column using 3 M NH_4OH. Next, the eluent was evaporated to dryness in a drying oven at 70°C. The dry amino-acid samples were then esterified using 2 mL of anhydrous isopropanol acidified with acetyl chloride (4:1) at 100°C for one hour. Next, the esterified AAs were evaporated to dryness under a N_2 stream, followed by acylation by adding a solution of acetone, trimethylamine, and acetic anhydride (5:2:1 by volume) and heating at 60°C for 10 minutes. The acylated AA samples were again evaporated to dryness under a N_2 stream. The acylated AA samples were then re-dissolved using 2 mL ethyl acetate. Approximately 1 mL of NaCl-saturated water was added to the solution and the organic phase was extracted and evaporated to dryness under a N_2 stream. All samples were refrigerated until injection into the gas chromatography-combustion-isotope ratio mass spectrometry (GC-C-IRMS). Prior to

injection into the GC-C-IRMS, the derivatized samples were re-dissolved in 1 mL ethyl acetate and 50 µL was transferred to a low-volume glass auto-sampler vial insert.

Six laminae per fish (10 fish) were selected for CSIA-AA. Each sample's (n = 60) $^{15}N/^{14}N$ ratio was measured in replicate using an Agilent 6890 GC and Thermo Finnigan GCC-III interface coupled with a continuous-flow Thermo Finnigan Delta+XL isotope ratio mass spectrometer at the University of South Florida College of Marine Science in St. Petersburg, Florida. For CSIA-AA, All results are presented in standard notation (δ, in ‰) relative to air

$$\delta^{15}N = [R_{sample}/R_{standard} -1]\times 1000,$$

where R is the ratio $^{15}N/^{14}N$. Replicate isotope measurements were averaged prior to data analysis.

3.2.4 Ethics Statement

Red snappers are not protected except by recreational and commercial harvest regulations. Fish were obtained from surveys conducted by the University of South Florida (Murawski et al. 2018) according to University of South Florida Institutional Animal Care and Use Committee (IACUC) protocol IS00000515. No fish were collected or killed for the purpose of this study. All tissues were collected post-mortem according to IUCUC protocol IS00000504.

3.3 Results

Isotopic values were obtained for 13 AAs, but only five trophic AAs, three source AAs, and two other AAs are reported in Figures 3.2, 3.3, and 3.4. Isoleucine and proline are not

reported because these AAs can coelute with leucine and serine, respectively, if chromatography is not optimal. Coelution causes these amino acids to be measured before background levels return to baseline values from the previous measurement. This causes the subsequent amino acid to be measured incorrectly and minimally affects the previous amino acid in most cases. Lysine is also not reported because it was not consistently resolved during analyses for these samples. In Figures 3.2 and 3.3, isotope values are plotted against LRM. Zero LRM represents the earliest time of life and the longest LRM is age of capture. All AA measurements had considerable variability within the eye lens. The standard deviation for each amino acid was based on CSIA-AA of King Mackerel (*Scomberomorus cavalla*) muscle from eight successive runs and are presented in Table 3.3.

The ranges of AA $\delta^{15}N$ are given in Tables 3.1 and 3.2. Threonine, which is an "other" type of AA, had the largest range, varying from -26.7 to -2.1. Threonine decreased across all laminae as LRM increased, which is consistent with previous literature (Whiteman et al. 2019; McMahon and McCarthy 2016). The smallest range was observed for phenylalanine ("source" AA), varying from -1.8 to 6.66. When comparing the two sample sites, 4-40, which is off of the West Florida Shelf, exhibited $\delta^{15}N$ maximum and minimum values for each AA were generally lower than 8-40 which is found south of Pensacola, Florida in the northern Gulf of Mexico.

3.4 Discussion

Fish eye lenses were established as likely lifetime geographic and trophic isotope recorders by Wallace et al (2014), and have since been used to study various teleosts and elasmobranchs (Curtis 2016; Quaeck-Davies 2018; Kurth et al. 2019; Simpson et al. 2019). To

the authors' knowledge, this is the first time that CSIA-AA has been conducted on eye-lens laminae to create lifetime records of AA $\delta^{15}N$ and to define the evolution of trophic behavior in a single organism. While $\delta^{15}N$ was measured for 13 AAs, only 10 are presented here; lysine, isoleucine, and proline were excluded. Lysine proved difficult to resolve across most laminae. Isoleucine and proline were measured but not presented because of their tendency to coelute with leucine and serine, as the peaks are approximately 10-20 seconds apart chromatographically. However, these AAs, and in fact all AAs, can be targeted and better resolved using derivatization and GC-C methods optimized specifically for them (Corr et al. 2007).

For visual representation, all AAs were placed into the three groups identified by Whiteman et al. (2019): trophic, source, and other. The trophic AAs are those that significantly fractionate with increasing trophic position. Source AAs fractionate much less, if they fractionate at all. The final group, other AAs, consists of AAs that do not behave consistently across organisms. Figures 3.2, 3.3, and 3.4 demonstrate isotopic variability within an individual eye lens as well as among eye lenses from multiple individuals. The trophic AA $\delta^{15}N$ values are considerably higher than the source AA $\delta^{15}N$ values and had a tendency towards having more enriched values with increasing fish size and age. However, variability was also present among the source AAs within individual lenses. As the study organisms here are reef fish with presumably high site fidelity, this was unexpected. The most probable explanation for source variability is changing baseline $\delta^{15}N$ values based on location or possibly water-mass movement. Fish can feed on different prey types according to availability, seasonality, location, etc., potentially shifting the baseline isotopic values of source AAs across an individual's lifetime

(Murdoch 1969; Newsome et al. 2007). While capture-recapture and tagging data suggest high site fidelity, the AA isotopes may suggest a different life history for Red Snapper.

Of the two locations, 8-40 is located farther north and west in the Gulf of Mexico, near the Florida-Alabama border (Figure 3.1). All AA $\delta^{15}N$ ranges (with the exception of leucine) started and ended at higher values for 8-40 fish than the fish further south on the West Florida Shelf at 4-40 (Table 3.1 and 3.2). This is consistent with observed and modeled isoscapes in the Gulf of Mexico. Radabaugh et al. (2013) identified a nitrogen isotopic gradient on the West Florida Shelf with lower $\delta^{15}N$ values to the south and higher $\delta^{15}N$ values to the north. This gradient exists because of the processes governing nitrogen inputs the different areas. The southern part of the WFS is has a greater extent of nitrogen fixation by diazotrophs (such as *Trichodesmium*), and the northern Gulf has stronger inputs of terrigenous nitrogen from the Mississippi, Atchafalaya, and Mobile Rivers. The two dominating forces create a latitudinal gradient along the West Florida Shelf that is seasonally and annually robust (Radabaugh et al. 2013; Radabaugh and Peebles 2014; Harper et al., 2018). Even though Radabaugh et al. (2013) used bulk isotope data to create their isoscapes, the documented gradient explains why the minimum and maximum $\delta^{15}N$ values for AA ranges are more enriched in ^{15}N at the more northern station, 8-40, than the southern station, 4-40.

Bulk isotope data has some limitations, the biggest one being that changing baseline $\delta^{15}N$ can confuse isotopic interpretation of predicting higher trophic levels. This is usually combated by conducting bulk $\delta^{15}N$ analysis on not only the consumer but its prey (Hyslop 1980; Dale et al. 2011). CSIA-AA eliminates the need to measures all trophic food web and has been

used to disentangle the effects of baseline changes that propagate through increasingly higher trophic positions (Dale et al. 2011, Seminoff et al. 2012, McMahon and McCarthy 2016). Eye-lens CSIA-AA directly documents lifetime baseline isotopic changes within individuals, lessening the need for grouping individuals for trophic position estimates. Trophic position can be derived using the following equation:

$$TP = \frac{\left(\delta^{15}N_{trophic} - \delta^{15}N_{source}\right) - \beta}{TDF} + 1$$

where $\delta^{15}N_{trophic}$ and $\delta^{15}N_{source}$ are the $\delta^{15}N$ of the representative trophic and source AAs, TDF is the calculated trophic discrimination factor, and β is the Δ $\delta^{15}N$ between the source and trophic AAs at the primary producer level (Bradley et al. 2015). Analyzing eye-lens AA nitrogen-isotope ratios for lifetime trophic positions can be used to recreate individual trophic histories, also known as trophic growth (Wallace et al. 2014, Bradley et al. 2015).

Bulk isotope data reflect a combination of trophic and geographic influences; if one can remove the trophic influence, then the geographic influence remains. Until now, there has not been a lifetime isotopic record with enough organic nitrogen to recreate geographic histories using CSIA-AA. In this regard, this study confirms that eye-lenses are a useful isotopic archive. However, there is one complication to re-creating geographic histories using CSIA-AA via eye-lens AAs. The geographic signal captured in the isotopes can result from the consumer or its prey, and because some prey types are highly mobile, there is currently no way to distinguish whether geographic influences originate from the consumer or mobile prey. For example, a high-site-fidelity predator might feed on migratory fishes traveling through its

territory (e.g., schooling clupeids, carangids, or scombrids). Another possibility is the predator is migratory but its prey has high site fidelity (e.g., benthic invertebrates). Either scenario can cause of geographic isotopic variability that cannot be definitively discerned.

Considering that this is the first case of creating individual CSIA-AA histories, further study of migratory patterns via CSIA-AA is necessary to parse more detailed information. It should also be kept in mind that, although isoscapes on the West Florida Shelf present robust gradients, these gradients are somewhat dynamic. Minor changes can affect baseline values, so one must be careful not to overinterpret data.

There are limitations to CSIA-AA interpretation. The first limitation is the parameter β in the equation above. Different values of β have been used for marine phytoplankton, C3, and C4 plants . However, the value of β for CAM plants and β variation within each of these primary producer types have not yet been investigated (Whiteman et al. 2019). Any changes to these values can change trophic position, although not as dramatically as the trophic discrimination factor (i.e., the second and most important limitation to CSIA-AA). The accuracy of calculated trophic positions are greatly dependent on the accuracy of the trophic discrimination factor, which has proven to be quite variable from one study to the next (McMahon and McCarthy 2016, Bradley et al. 2015, Nielsen et al. 2015, Chikaraishi et al. 2009). Although glutamic acid (trophic AA) and phenylalanine (source AA) are most commonly used for calculating trophic position, Bradley et al. (2015) demonstrated that estimated trophic position accuracy increases with a multi-amino acid analysis that combines more than one trophic and one source amino acid. Germain et al. (2013) have also called for the development of not only

multi-AA models, but also multi-trophic discrimination factor models, as a means of improving the accuracy of trophic position estimates.

Another, recent influence on trophic position calculations is the scaled framework approach to marine food webs presented by Hussey et al. (2014). Currently, the vast majority of TP_{CSIA} calculations assume a simple, additive framework, where the TDF remains constant as trophic position increases (e.g., 3.0 or 3.4‰ increase in bulk $\delta^{15}N$ per trophic step). However, Hussey et al. (2014) presented data indicating TDF decreases with increasing trophic position. A scaled framework approach based on narrowing TDF with increasing trophic position may more accurately represent organisms at higher trophic positions.

In summary, we have demonstrated that CSIA-AA can be successfully applied to individual eye-lens laminae to re-construct lifetime $\delta^{15}N$ trends, and that these trends can be used to account for variations in isotopic baselines (via source amino acids) and possibility to produce more accurate estimates of trophic (via the equation above) throughout life. While further work is still required to overcome certain limitations, there is great future potential for this method.

Table 3.1 Amino acid $\delta^{15}N$ values (δ, in ‰) for Red Snapper from station SL 4-40. Each amino acid is represented by the minimum, maximum, and (standard deviation), where Ala = alanine, Asp = aspartic acid, Glu = glutamic acid, Leu = leucine, Val = valine, Met = methionine, Phe = phenylalanine, Gly = glycine, Ser = serine, and Thr = threonine. The parentheses annotate what type of amino acid each is T = trophic, S = source, and O = other.

Sample ID	Ala (T)	Asp (T)	Glu (T)	Leu (T)	Val (T)	Met (S)	Phe (S)	Gly (O)	Ser (O)	Thr (O)
SL 4-40 (all fish)	11.8-21.8	11.8-19.9	14.7-25.5	15.6-24.6	13.5-27.0	5.65-18.7	-1.80-6.22	-3.90-8.16	2.03-19.9	-16.7--5.7
4-40-002	11.8-19.2	11.8-16.8	14.7-21.5	16.1-20.3	14.9-22.1	5.65-9.79	-1.80-2.37	-0.36-2.62	2.03-14.7	-19.8--10.3
4-40-003	16.2-21.8	15.5-18.4	18.7-23.2	19.3-23.1	20.0-24.2	8.85-18.7	4.09-6.22	0.33-8.16	11.7-16.4	-22.8--9.10
4-40-006	13.1-20.3	15.0-18.4	19.6-23.8	15.6-23.2	13.5-24.5	8.55-11.4	2.02-4.57	-3.17-5.68	9.35-18.5	-26.7--10.6
4-40-019	18.1-21.5	12.8-18.1	16.7-24.2	15.7-22.1	15.4-23.2	7.18-13.1	0.94-3.25	-3.9-5.19	7.98-14.4	-26.6--10.63
4-40-021	18.0-19.0	14.8-19.9	18.4-25.5	16.6-24.6	19.2-27.0	8.80-12.7	4.39-5.66	-0.39-7.80	9.27-17.63	-26.0--5.70

Table 3.2 Amino acid $\delta^{15}N$ values (δ, in ‰) for Red Snapper from station SL 8-40. Each amino acid is represented by the minimum, maximum, and (standard deviation), where Ala = alanine, Asp = aspartic acid, Glu = glutamic acid, Leu = leucine, Val = valine, Met = methionine, Phe = phenylalanine, Gly = glycine, Ser = serine, and Thr = threonine. The parentheses annotate what type of amino acid each is T = trophic, S = source, and O = other.

Sample ID	Ala (T)	Asp (T)	Glu (T)	Leu (T)	Val (T)	Met (S)	Phe (S)	Gly (O)	Ser (O)	Thr (O)
SL 8-40 (all fish)	14.2-26.1	14.1-22.0	17.2-27.1	16.0-27.4	18.3-28.7	7.85-13.3	1.41-6.66	1.42-8.20	12.5-21.2	-24.6--2.10
8-40-003	14.2-23.0	15.9-21.2	19.5-26.2	16.0-24.8	18.4-26.1	8.79-12.2	2.39-4.78	2.70-6.46	2.47-14.6	-21.6--11.6
8-40-008	15.6-25.0	14.2-20.7	17.4-26.2	16.4-25.0	18.3-27.0	7.85-11.5	2.00-4.69	1.42-7.57	8.71-17.4	-24.3--6.75
8-40-012	14.5-26.1	14.1-22.0	17.2-27.1	17.4-27.4	19.2-28.7	7.99-13.3	1.41-5.24	1.88-8.20	7.67-15.7	-24.6--5.60
8-40-019	18.0-22.6	17.0-20.2	20.0-24.8	18.9-24.0	20.5-24.5	11.1-13.2	3.49-6.66	4.30-8.07	10.7-17.1	-14.7--2.10
8-40-023	15.5-23.0	14.2-21.5	17.2-25.3	19.2-24.8	19.6-27.0	9.10-12.2	2.30-5.10	3.60-6.56	10.1-18.4	-20.2--5.6

Table 3.3 $\delta^{15}N$ for King Mackerel muscle. Muscle tissue was derivatized and run in succession to quantify machine error. The data below are individual measurements and not averaged replicates.

Injection	Alanine	Glycine	Valine	Leucine	Serine	Aspartic Acid	Glutamic Acid	Phenylalanine	Caffeine
Acq 62	24.0	-6.1	22.5	21.4	-4.9	23.8	23.2	0.9	-3.7
Acq 63	24.3	-4.8	23.2	22.9	-3.9	23.7	23.2	1.1	-3.7
Acq 64	23.4	-5.2	24.0	22.0	-3.8	24.2	23.5	1.0	-4.1
Acq 65	24.0	-5.5	22.8	22.5	-2.6	24.1	23.3	1.2	-3.9
Acq 66	24.2	-5.8	24.1	22.1	-4.1	23.9	23.4	2.1	-3.6
Acq 67	23.9	-4.8	23.5	22.2	-4.3	23.7	23.1	1.2	-4.3
Acq 68	24.3	-4.8	22.6	22.1	-4.4	23.9	23.1	0.7	-3.9
Acq 69	23.9	-4.9	22.6	21.8	-4.5	23.8	23.0	0.3	-4.0
Average	24.0	-5.2	23.2	22.1	-4.1	23.9	23.2	1.1	-3.9
Standard Deviation	0.29	0.51	0.64	0.45	0.69	0.18	0.17	0.52	0.23

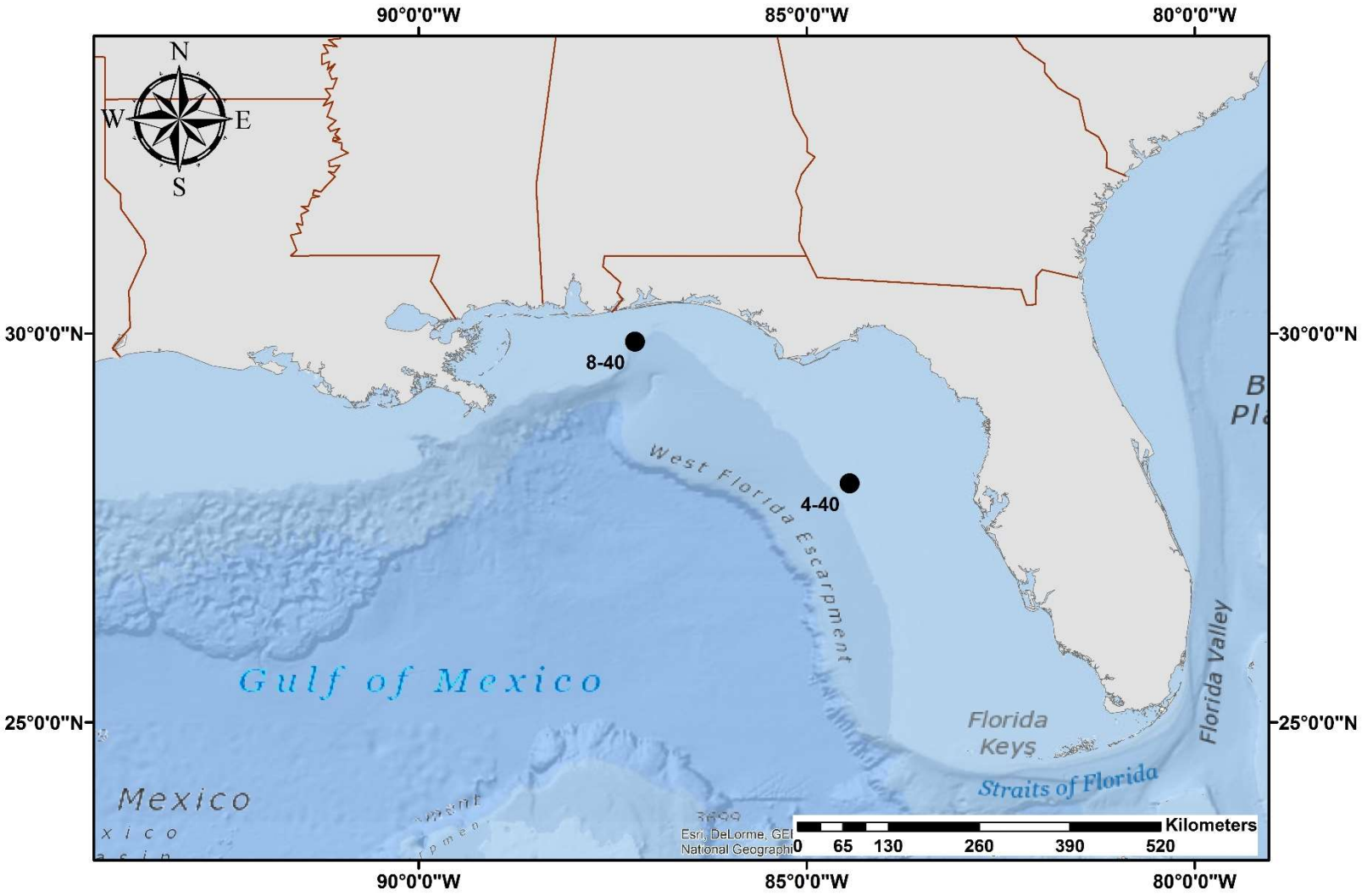

Figure 3.1 Red Snapper sampling locations.

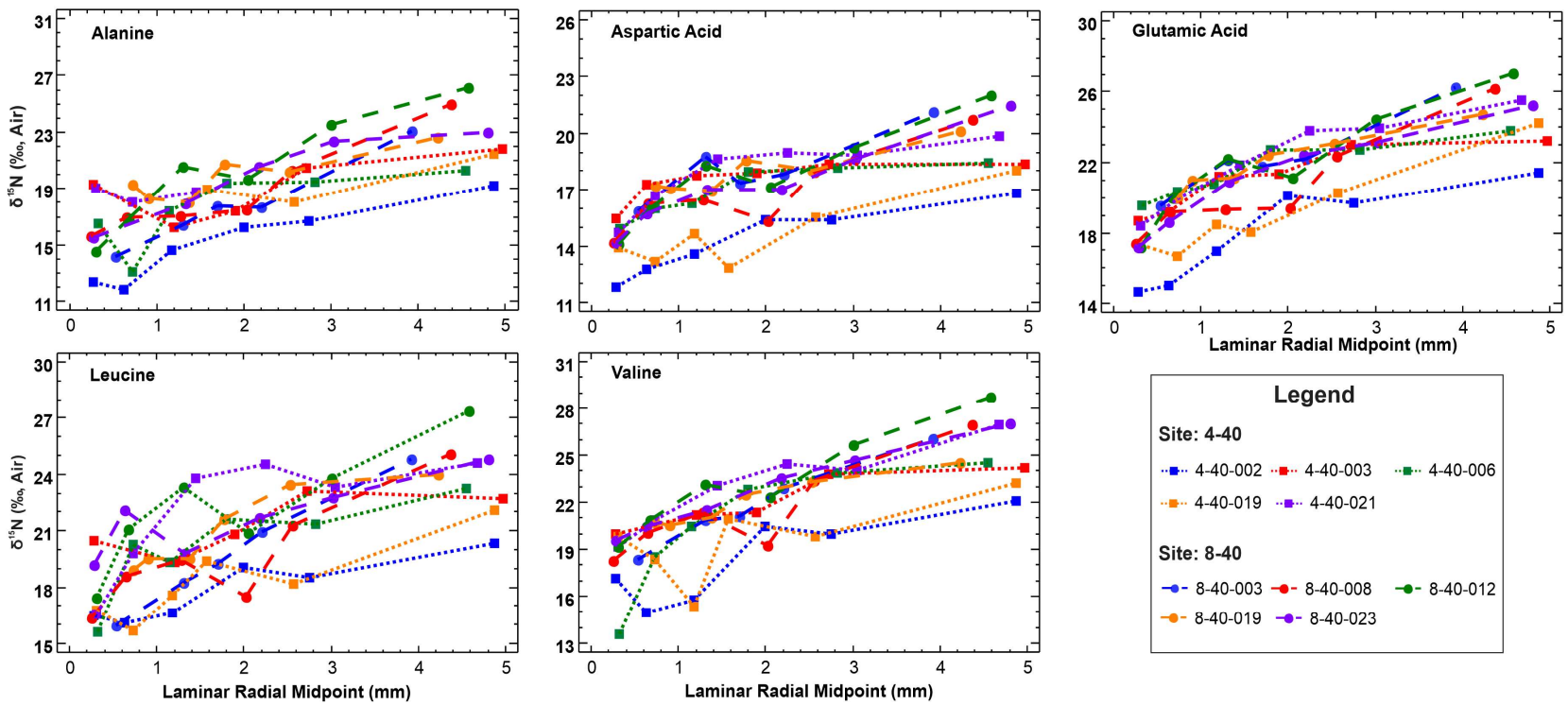

Figure 3.2a Trophic amino acids in individual fish at laminar radial midpoints (LRMs). Each line represents an individual fish. Squares are Red Snapper from 4-40 and circles are Red Snapper from 8-40.

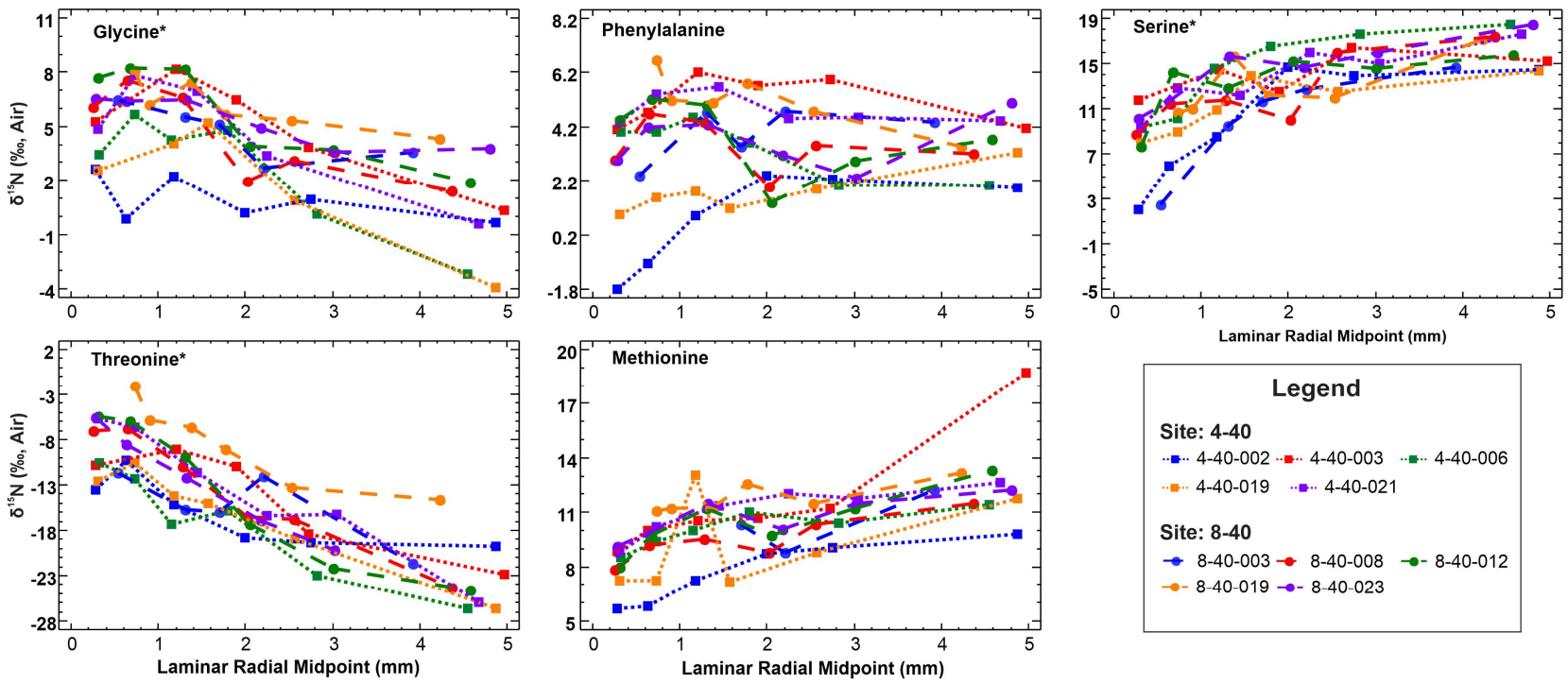

Figure 3.2b Source and other (indicated by *) amino acids by laminar radial mipoints (LRMs). Each line represents and individual.

Squares are Red Snapper from 4-40 and circles are Red Snapper from 8-40.

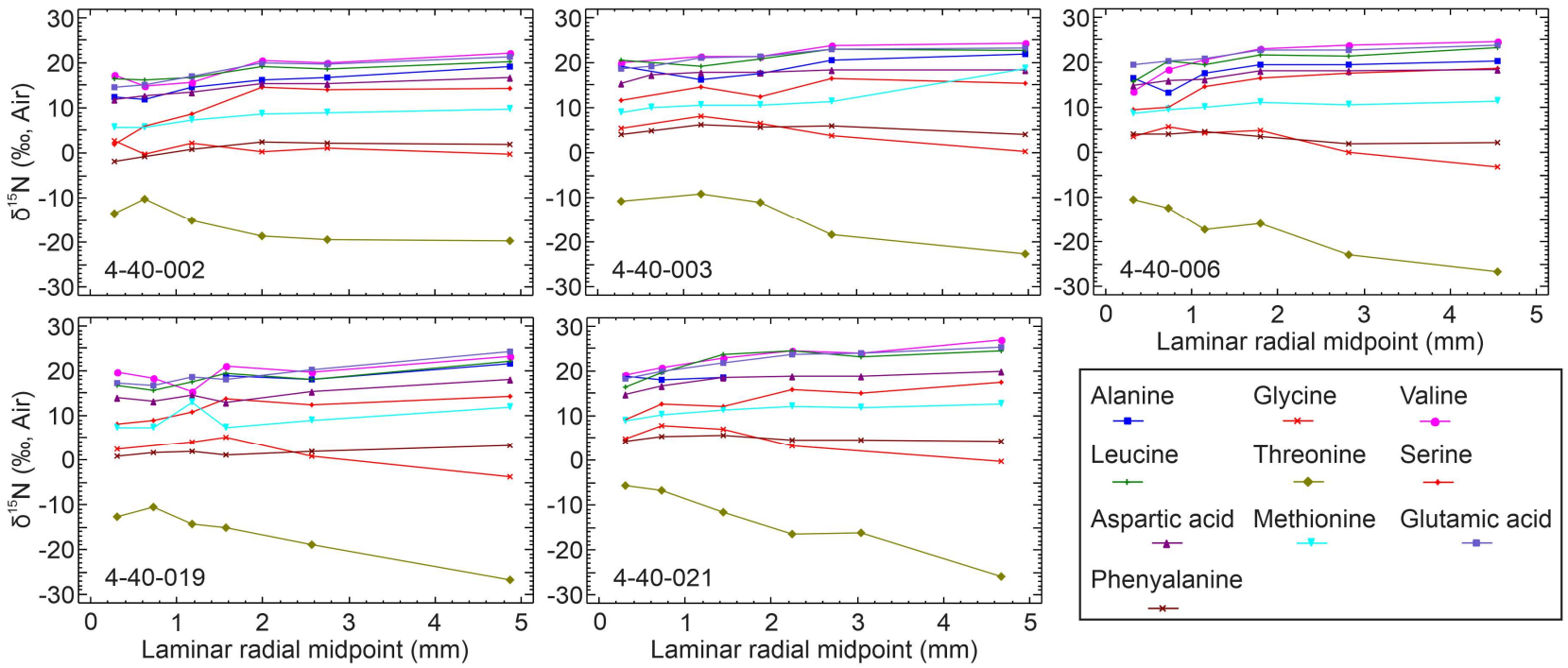

Figure 3.3a Amino acid $\delta^{15}N$ measurements by fish at 4-40. Each line represents an amino acid plotted by laminar radial midpoint. Each group is an individual with a sample number in the lower left corner. Six laminae were measured for each fish. Laminar radial midpoints close to zero are when the fish is young. The higher the number, the larger and older the fish.

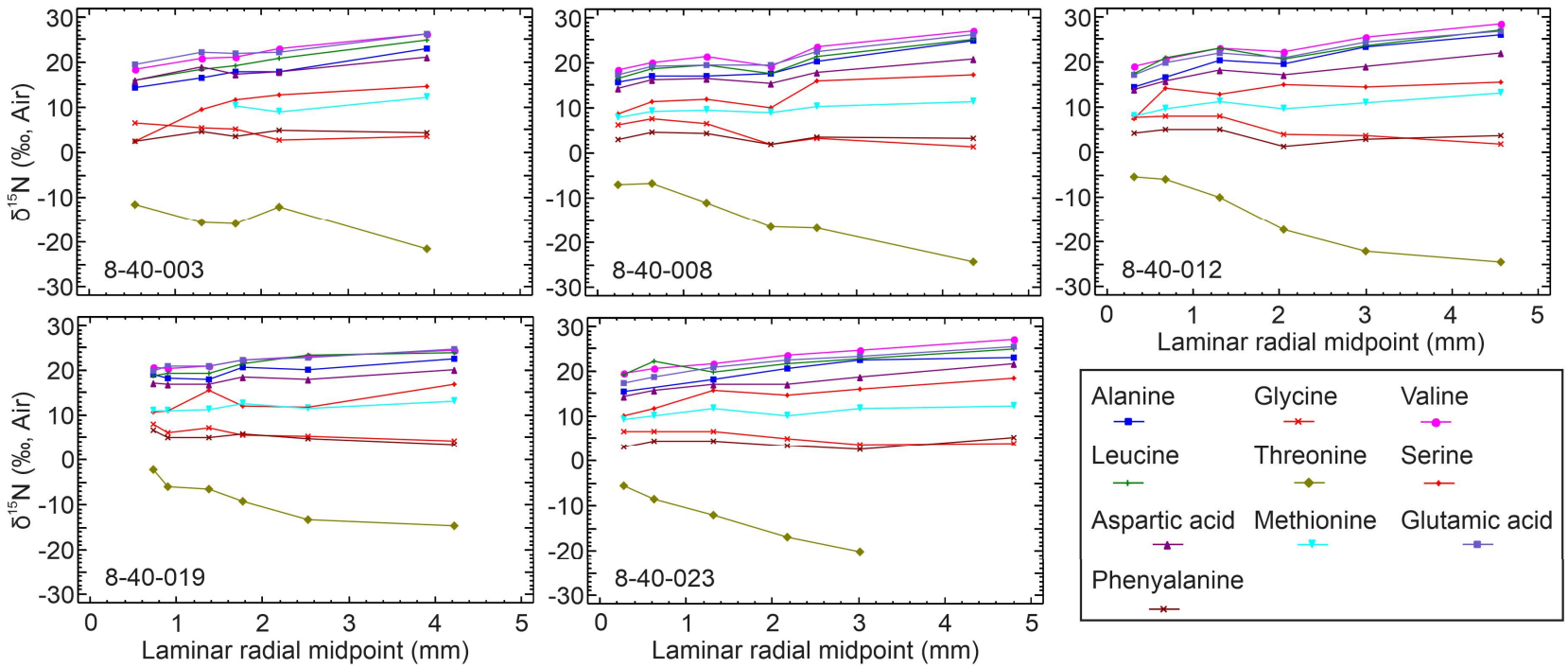

Figure 3.3b Amino acid $\delta^{15}N$ measurements by fish at 8-40. Each line represents an amino acid plotted by laminar radial midpoint. Each group is an individual with a sample number in the lower left corner. Six laminae were measured for each fish. Laminar radial midpoints close to zero are when the fish is young. The higher the number, the larger and older the fish.

Chapter 4. Comparison of fish species using life-histories reconstructed from eye-lens amino acids

4.1 Introduction

Analysis of bulk-tissue stable isotopes (bulk analysis) is often used to study energy transfer through food webs (DeNiro and Epstein 1981; Peterson and Fry 1997;Post 2002). Isotopic gradients identified from around the world have led to the development of isotopic maps, or isoscapes, which can then be used to track animal migrations (Hobson 1999; Phillips et al. 2009; Wassenaar et al., 2009; Bowen 2010; Newsome et al. 2015). The introduction of compound-specific isotope analysis (CSIA) has led to amino-acid isotope analysis (CSIA-AA), which has, in turn, has allowed more accurate estimates of trophic positions (TP) for individual animals (Popp et al. 2007; Chikaraishi et al. 2009). There are two types of amino acids used in trophic-position estimations. The first type is trophic amino acids. Trophic amino acids undergo multiple transamination and deamination reactions during protein synthesis (Braun 2014). Each reaction is an opening for potential isotopic fractionation of nitrogen to occur. Trophic amino acids fractionate greatly compared to source amino acids, which are the second type of amino acids used in trophic-position estimations. Source amino acids undergo fewer transamination and deamination reactions and, therefore, fractionate minimally if at all. Source amino acids capture the baseline $\delta^{15}N$ of the consumer's dominant basal resources (Braun et al. 2014;

McMahon and McCarthy 2016). With recent work supporting eye-lenses as conservative isotopic recorders of stable carbon and nitrogen isotopes (Wallace et al. 2014; Quaeck-Davies et al. 2018; Kurth et al. 2019), lifetime trophic geographies can now be reconstructed using CSIA-AA of eye-lens amino acids as the animals cross the isoscapes of their environment (Chapter 3).

The two amino acids used in the present research are glutamic acid and phenylalanine. There are two variables required for CSIA-AA trophic-position estimation. The first is the trophic discrimination factor, which is the change in $\delta^{15}N$ with each increase in trophic level. The second is β, which is defined as the $\Delta\delta^{15}N$ between the two analytical amino acids at the primary producer level (Bradley et al. 2015). Glutamic acid fractionates greatly at approximately 5.7‰ per trophic level increase (Bradley et al. 2015). Phenylalanine does not fractionate (0‰ per trophic level; Bradley et al. 2015) and is thus an ideal source amino acid for this type of analysis. These two amino acids are heavily studied and are the most reliably resolved using current gas chromatography-combustion-isotope ratio mass spectrometry (GC-C-IRMS) methods. Bradley et al. (2015) conducted a meta-analysis of 224 samples of 47 species that spanned a broad range of trophic positions and marine ecosystem types. The trophic discrimination factors and β values used in this chapter are specific to glutamic acid and phenylalanine in marine teleosts. If the representative trophic and source amino acids change, then the trophic discrimination factors and β values will change accordingly (Bradley et al. 2015). Trophic discrimination factors and β will also change with increases in the number of amino acids used in analysis, as in a multi-amino acid approach.

The purpose of this chapter is to assess two types of fish, a reef fish (Red Snapper, *Lutjanus campechanus*) and a highly migratory fish (King Mackerel, *Scomberomorus cavalla*), using CSIA of eye-lens amino acids to see if we can distinguish different patterns of migratory behavior with this technique. Here, "model species" is used to describe a well-studied species that can be used as a representative for a group. For example, Red Snapper was chosen as the model reef-fish species in part because the species is abundant and also because this species is thought to have high site fidelity in the Gulf of Mexico (Strelcheck et al 2007). Adult Red Snapper are opportunistic feeders that prey on a wide variety of taxa such as fishes, squids, crustaceans, and larger zooplankton (McCawley and Cowan 2007, Bruger et al. 2017). Genetic studies have identified a single Red Snapper population in the northern Gulf of Mexico (Gold et al, 1997). In contrast, King Mackerel are a model of a highly migratory species. King Mackerel undergo long seasonal migrations between the southern and northern Gulf of Mexico, generally following seasonal shifts at the 20°C isotherm at depths that are generally shallower than 70m (Manooch 1978). King Mackerel are managed as two stocks, one in the Gulf of Mexico and the other in the Atlantic Ocean, and the two stocks are only thought to intermix during winter at the southern end of the Florida peninsula (Sheppard et al. 2010; Addis et al. 2018). Adult King Mackerel feed primarily on small, schooling coastal-pelagic fishes, groundfishes, and squids (Manooch 1978). The concept of model species is important to exploratory studies such as the present one. Establishing isotopic patterns for well-studied species will help identify anomalies in species that are less understood.

There are two objectives to the present study. The first is to identify trophic growth and any isotopic patterns that may distinguish high-site fidelity reef-fish from highly migratory fish.

The second objective is to use the lifetime isotope profiles from these two model species to investigate the migratory behavior of a third, relatively unstudied species, Greater Amberjack (*Seriola dumerili*). The majority of work published on Greater Amberjack has concentrated on age, length, and growth because of this species' value to recreational and commercial fisheries and also due to the need for basic information required by stock assessments (Cummings and McClellan 1996). The Greater Amberjack is primarily pelagic and sometimes epibenthic, and is associated with hard structures such as reefs, rock outcrops, and wrecks (Harris et al. 2007). However, Greater Amberjack can reach up to 200 cm in length, which is a size that enables fast swimming speeds and high mobility (Murie and Parkyn 2010). As with King Mackerel, there are currently two managed populations, one in the Gulf of Mexico and one in the Atlantic Ocean. Based on 35 years of tagging data, the populations are also thought to minimally intermix in Southern Florida (Cummings and McClellan 1996). It has been suggested that the Dry Tortugas and Florida Keys act as a geographical barrier to mixing by the two stocks (Cummings and McClellan 1996).

4.2 Methods

4.2.1 Sample collection

Two Greater Amberjack were collected during August 2013 and ten Red Snapper were collected during August 2014 on the R/V *Weatherbird II* using long-line fishing techniques (Murawski et al. 2018). At each station (Figure 4.1), 8 km of 544 kg test monofilament mainline was deployed with approximately 500 baited hooks via gangions. Each gangion consisted of 3.7 m of 91 kg test monofilament line with #13 circle hooks that were alternately baited with

Atlantic Mackerel (*Scomber scombrus*) and squids of various species. Four King Mackerel were collected from the Tampa Bay location (Figure 4.1) by recreational fishermen during two different periods, December 2015 and April 2016, using hook-and-line gear. All King Mackerel were caught using local live bait harvested in the same area on the same-day as sample collection. Whole King Mackerel eyes were collected using a knife in the field and were kept frozen between -20° and -40°C until time of lens delamination. Lenses were delaminated using forceps and a dissecting scope according to the technique described by Wallace et al. (2014) and Chapter 3.

4.2.2 Fish Length Estimation at Laminar Radial Midpoint

Eye lenses grow at a rate proportional to fish length (Lima et al. 2012, de Busserolles et al. 2013). Therefore, standard length (SL) was estimated at each laminar radial midpoint (LRM) using the following equation

$$SL_{LRM} = SL_{Max}(LRM/Lens_{MaxRad}),$$

where SL_{Max} is the standard fish length at collection and $Lens_{MaxRad}$ is the radius of the intact lens.

4.2.3 Bulk isotope analysis

A total of 260 laminae from three species were analyzed for bulk $\delta^{15}N$. Between 300 and 600 µg of dry lamina was placed in tin capsules, combusted, and analyzed for nitrogen isotopes. All $^{15}N/^{14}N$ was measured in duplicate using a Carlo-Erba NA2500 Series II elemental analyzer coupled with a continuous-flow ThermoFinnegan Delta+ XL isotope ratio mass

spectrometer. The lower limit of quantification was 12 µg of nitrogen. Calibration standards were NIST 8573 and NIST 8574 L-glutamic acid standard reference materials. Analytical precision (±0.16 ‰ for $\delta^{15}N$ and ±0.09 ‰ for $\delta^{13}C$) was obtained by replicate measurements of NIST 1577b bovine liver. Results are presented in standard notation (δ, in ‰) relative to air.

4.2.4 Compound-specific isotope analysis

A total of 186 laminae were analyzed for $\delta^{15}N$ of glutamic acid (trophic AA, $\delta^{15}N_{Glu}$) and phenylalanine (source AA, $\delta^{15}N_{Phe}$). Samples were derivatized using methods outlined by Ellis (2012) and Chapter 3. In short, eye lens laminae were hydrolyzed using 6N HCl and amino acids were extracted from non-amino-acid components using an ion-exchange resin column. Amino acids were then esterified with acidic isopropanol and acylated with acetic anhydride. Ideally, more than 1 mg of lamina would be hydrolyzed; however, some laminae had low mass, limiting samples to as little as 426 µg.

All Red Snapper, King Mackerel, and one Greater Amberjack amino acid $^{15}N/^{14}N$ were measured in replicate using an Agilent 6890 gas chromatograph coupled to a continuous-flow ThermoFinnegan Delta+ XL isotope ratio mass spectrometer with a GCC II/III interface. Amino acids were separated chromatographically using a 60 m x 0.25 mm x 0.5 µm OV-1701 column. Amino-acid 15N/14N from the second Greater Amberjack specimen was measured in replicate using a ThermoFinnegan Trace 1310 gas chromatograph coupled to a continuous-flow Delta V Plus isotope ratio mass spectrometer with a GC IsoLink II interface. Amino acids were separated chromatographically using a 60 m x 0.25 mm x 0.5 µm OV-1701 column for chromatographic separation.

4.2.5 Trophic position calculation

Trophic position was calculated using the following equation from Bradley et al. (2015)

$$TP_{CSIA} = \frac{\left(\delta^{15}N_{trp} - \delta^{15}N_{trp} - \beta\right)}{TDF_{AA}} + 1$$

where TP_{CSIA} is the trophic position calculated from amino-acid isotope ratios, *trp* and *src* is are trophic and source amino acids respectively, β is the difference between trophic and source amino acids at the primary producer level, and TDF_{AA} (trophic discrimination factor) is the difference between $\delta^{15}N_{trp}$ and $\delta^{15}N_{src}$ with each increasing trophic level. The addition of 1 at the end of the equation corrects the result to the convention of referring to primary producers as trophic level 1, rather than 0. As mentioned above, the amino acids used in this study were glutamic acid (trophic) and phenylalanine (source). Thus, according to Bradley et al. (2015), β = 3.6‰ and TDF_{AA} = 5.7‰. These values were specifically calculated for marine teleosts, and this value for β is very similar to the values calculated for primary producers in early studies such as Chikaraishi et al. (2009) and McClelland and Montoya (2002). Although there is advocacy for using multiple trophic and source amino acids, glutamic acid and phenylalanine were used because of they are well documented and are the most reliably resolved.

4.2.6 Geographic variation and isoscape comparison

Empirical and modeled isoscapes currently exist for the entire Gulf of Mexico and, more specifically, the West Florida Shelf (Radabaugh et al. 2013; Radabaugh and Peebles 2014;

Peebles and Hollander 2020). These isoscapes have been created using fish muscle, particulate organic matter from surface water, and benthic algae harvested from sea urchin stomachs.

Bulk $\delta^{15}N$ is assumed to be a combination of trophic $\delta^{15}N$ variation and geographic $\delta^{15}N$ variation. To plot individual fish movement, the trophic $\delta^{15}N$ signal must be removed from the bulk $\delta^{15}N$. To achieve this, first trophic positions calculated from CSIA (TP_{CSIA}) must be reverted to an isotopic equivalent to bulk $\delta^{15}N$ by multiplying it by the bulk trophic discrimination factor. TPCSIA was translated to an isotopic equivalent using the following equation

$$GV_{CSIA} = \delta^{15}N_{Bulk} - \left(3.4 \times (TP_{CSIA} - 1)\right)$$

where GV_{CSIA} is geographic variation, $\delta^{15}N_{Bulk}$ is the laminar bulk $\delta^{15}N$, TP_{CSIA} is the trophic position calculated using glutamic acid and phenylalanine $\delta^{15}N$, and 3.4 is the bulk $\delta^{15}N$ TDF for marine teleosts (Post et al. 2002). All King Mackerel and Greater Amberjack laminae were analyzed using CSIA-AA; thus, no data interpolation was necessary. Red Snapper have been previously identified as being high-site-fidelity reef fish and only six laminae were analyzed using CSIA-AA for each individual (Strelcheck et al; Watterson et al). Accordingly, the core and its adjacent lamina were processed for CSIA to gather early-life $\delta^{15}N$ and the remaining laminae were selected for CSIA-AA by skipping over a fixed number of laminae. For example, 18 laminae were isolated from Red Snapper specimen 4-40-002. Laminae 1 (the core, LRM = 0.28 mm), 2 (LRM = 0.63 mm), 6 (LRM = 1.18 mm), 10 (LRM = 2.00 mm), 14 (LRM = 2.75), and 18 (LRM = 4.88 mm) were analyzed using CSIA-AA (i.e., after the core and adjacent lamina, every fourth lamina was analyzed in this specimen). These laminar radial midpoint measurements are not

the same for every fish eye lens as the lens radius, number of laminae, and laminar thickness varied among individuals. After calculating trophic position for the six points, trophic position data for each laminar radial midpoint were interpolated using a best fitting regression model, thus producing trophic growth curves. Trophic growth is defined as change in trophic position during the life of the individual (Wallace et al. 2014, Bradley et al. 2015). The best-fitting regressions for each individual, as determined by the Comparison of Alternative Models routine in Statgraphics Centurion (v. 18, Statpoint Technologies, Inc., Warrenton, VA) are listed in Table 1.

In an effort to compare reconstructed geographic histories to isoscapes, isotopic geographic variation was normalized to the sample collection point. It had to be assumed that the fish had been in the area long enough to fully assimilate local isotopic baselines into the lamina at the maximum laminar radial midpoint; this assumption places the collection site at zero in certain figures (see Figures 4.5, 4.8, and 4.11). When the normalized geographic variation is compared to published isoscapes, zero values are equivalent to $\delta^{15}N$ at the point of capture, positive values represent locations to the north and west (i.e., the north-central Gulf of Mexico) and negative indicate locations to the south and east (i.e., toward Florida Bay and southern tip of the Florida peninsula).

4.2.7 Ethics statement

King Mackerel, Red Snapper, and Greater Amberjack are not protected except by recreational and commercial harvest regulations. Red Snapper and Greater Amberjack were obtained from surveys conducted by the University of South Florida (USF) according to protocol

IS00000515 approved by the USF Institutional Animal Care and Use Committee (IACUC; Murawski et al. 2018). King Mackerel samples were taken from recreational fishermen's catches. No fish were collected or killed specifically for this study. All tissues used in this study were collected post-mortem according to USF IACUC protocol IS00000504.

4.3 Results

4.3.1 Isotopic assessment of reef species: Red Snapper

A total of 60 laminae were analyzed via CSIA-AA for Red Snapper (n = 10 individuals). Glutamic acid varied from 14.7 to 27.1‰ and phenylalanine varied from -1.8 to 6.6‰. Nine Red Snapper had six TP_{CSIA} estimates and one Red Snapper had five TP_{CSIA} estimates (Figure 4.2). Glutamic acid and phenylalanine were not resolved for one lamina in Red Snapper specimen 8-40-003. TP_{CSIA} for the Red Snapper varied from 2.6 to 4.6‰.

Individual trophic growth regressions (Figure 4.3, Table 4.1) for Red Snapper had $R^2 \geq 0.89$, but the best-fitting model for all Red Snapper individuals combined did not fit as well ($R^2 = 0.77$). Individual trophic growth regressions were used to interpolate trophic position for each laminar radial midpoint not empirically measured; the resulting curves represent the trophic growth of individual Red Snapper.

Bulk $\delta^{15}N$ was measured in each lamina, totaling 142 Red Snapper laminae. Bulk $\delta^{15}N$ varied among and within individuals (Figure 4.4). TP_{CSIA} was converted to an isotopic equivalent and then subtracted from each bulk $\delta^{15}N$ at a given laminar radial midpoint. The remaining isotopic variation was attributed to geographic changes in isotopic space or, in other

words, a change in baseline $\delta^{15}N$. Geographic variation for these specific Red Snapper varied from 0.3 to 7.8‰. Red Snapper individuals collected at site 4-40 had a larger range (7.8–0.3 = 7.5‰) than those collected at 8-40 (6.8–2.0 = 4.8‰). Figure 4.5 depicts geographic variation normalized to $\delta^{15}N$ at the collection point. All increasing and positive values indicate locations that are more northern and western, whereas decreasing and negative values represent locations that are more southern and eastern. Therefore, fish traveling from higher $\delta^{15}N$ areas to lower $\delta^{15}N$ areas are traveling in a southerly and easterly direction. Red Snapper had approximately 2-3‰ variation in their carbon isotopes (Figures 4.12 and 4.13).

4.3.2 Isotopic assessment of highly migratory species: King Mackerel

A total of 78 King Mackerel laminae were analyzed using CSIA-AA (n = 4 individuals). Because King Mackerel are known to be highly migratory, all laminae were analyzed using CSIA-AA. Glutamic acid varied from 14.3 to 26.6‰ and phenylalanine varied from -0.9 to 7.7‰ (Figure 4.6). There was a clear cyclical pattern present in both the glutamic acid and the phenylalanine, although the oscillations were more pronounced in the phenylalanine (Figure 4.6). TP_{CSIA} is plotted against both laminar radial midpoint and estimated standard length in Figure 4.7. TP_{CSIA} varied from 2.8 to 4.8. Geographic variability was calculated and is plotted in Figure 4.8, normalized to collection point. The cyclical pattern present in geographic variation varied from -0.4 to 8.5‰.

4.3.3 Isotopic assessment of unknown teleost: Greater Amberjack

Relatively little is known about the Greater Amberjack's life history. Thus, all laminae (48 in total, n = 2 individuals) were analyzed for $\delta^{13}C$ and $\delta^{15}N$ of laminar bulk and $\delta^{15}N$ CSIA-AA.

The two Greater Amberjack exhibited the same cyclical pattern as the King Mackerel, with glutamic acid varying from 15.3 to 27.2‰ and phenylalanine varying from -3.2 to 7.6‰ (Figure 4.9). As in King Mackerel, TP_{CSIA} was determined for each Greater Amberjack (Figure 4.10), and geographic isotopic variability was normalized to collection point and plotted (Figure 4.11). TP_{CSIA} varied from 3.3 to 4.9 and isotopic geography varied from -0.1 to 6.5‰.

4.4 Discussion

4.4.1 Trophic growth comparison of reef and migratory species

Because the Red Snapper is considered a species with high site fidelity, six laminae were analyzed from each fish, revealing trophic positions associated with varying LRM. The outcome of combining all Red Snapper trophic position estimates produced a generalized trophic growth curve (Figure 4.3) that is similar to a von Bertalanffy growth curve. Upon also determining trophic growth curves for individual Red Snapper, it became apparent that individuals may take different paths to reach their maximum trophic position (Figure 4.3). Some Red Snapper exhibited linear growth, whereas others experienced square-root growth (Table 4.1). While the fit of the generalized Red Snapper trophic-growth curve is lower than those for individual fish (R^2 = 0.77 vs. mean $R^2 \geq 0.89$), it is still a reasonable approximation of the individual curves and could be used as a substitute for these if they are unknown. Because only ten Red Snapper were used to create the generalized model, increasing sample size may statistically improve it. Also, by choosing only six laminae for individual model construction, there is a chance the data were aliased (i.e., the six data points failed to capture shorter-term trends and may not have even produced the correct slopes). The decision to only take six

measurements was based on published findings regarding diet and site fidelity, but in hindsight, each Red Snapper lamina should have been analyzed using CSIA-AA to confirm that no cyclical patterns were present (as was done for King Mackerel and Greater Amberjack).

King Mackerel are highly migratory fish that undergo long-distance (>300 km) seasonal migrations (Briggs, 1958; Sutherland and Fable, 1980). To capture these seasonal migrations, all laminae were analyzed. It was not possible to use regressions to model trophic growth in King Mackerel because the TP_{CSIA} was continually changing. All King Mackerel (KM 2, KM 3, KM 4, KM 6) underwent lifetime TP_{CSIA} fluctuations (Figure 4.7). Traditionally, trophic growth is presented as increasing throughout life, but the present data suggests otherwise for King Mackerel. The changing trophic position can be explained by prey switching. Prey switching is when the predator feeds on the most abundant or available prey and switches to different prey as prey abundances and availabilities change (Murdoch 1969). In this case, the long seasonal migrations to new waters mean there is a new “most-abundant” prey. When the King Mackerel are off the coast of the Florida peninsula in the Gulf of Mexico, the dominant prey is schooling coastal pelagics such as clupeids and carangids, which are zooplanktivores (Beaumariage 1973; Pierce and Mahmoudi 2001; Addis et al. 2018). However, when King Mackerel are in the northern Gulf of Mexico, they feed primarily on larger sizes of menhaden (Brevoortia spp.), which are primarily phytoplanktivores. As herbivores, this places the menhaden at a relatively low trophic position near 2.0 and their predators near trophic position 3.0. This geographical prey switching by King Mackerel is likely driving some of the trophic position fluctuation evident in Figure 4.7.

The King Mackerel sampled for this study were caught at sizes equivalent to age 2+ fish. However, many of the isotopic measurements are from when the King Mackerel are less than 42.5 cm fork length, which is during the young-of-the-year life stage (Manooch et al. 1987). Young-of-the-year (YOY) are fish in their first year of life, which are also referred to as "Age-0" fish. Relatively little is known about YOY King Mackerel ecology. During delamination, 19 laminae were separated for CSIA-AA. King Mackerel 2 exhibited considerable trophic position fluctuation (Figure 4.7). There were at least five discernable cycles of moving from a low TP_{CSIA} (in some cases as low as 2.8) to a higher TP_{CSIA} of approximately 4.0 before returning to the lower TP_{CSIA}. However, it seems very unlikely that all King Mackerel were making migrations equivalent to the north-south distance of the Gulf of Mexico multiple times in their first year of life. Manooch et al. (1987) reported a mean back-calculated FL = 42.5 cm for Age-1 fish and FL = 63.5 mm for Age-2 fish. Older ages at these particular fork lengths would support multiple trophic position changes during possible seasonal migrations. Assuming isometric growth between eye lens radius and fish length (de Busserolles et al. 2013, Lima et al. 2012), many of the CSIA-AA measurements obtained during this study relate to the YOY time period; note that the retrospective approach used here allows YOY information to be obtained from specimens that are older than YOY. KM 6 was the largest King Mackerel sampled and had a FL = 88.9 cm. Of the data presented for KM 6, the majority of measurements corresponded to estimated standard lengths <40 cm.

4.4.2 Comparison of isotopic geography between reef and migratory species

Isoscapes for the West Florida Shelf and, even more recently, the entire Gulf of Mexico, have shown isotopic trends with higher values $\delta^{15}N$ to the north and lower $\delta^{15}N$ to the

south (Radabaugh et al. 2013, Radabaugh and Peebles 2014, Peebles and Hollander 2020). On the West Florida Shelf, gradients are created due to riverine inputs to the north (higher $\delta^{15}N$) and oligotrophic waters to the south that are dominated by nitrogen fixation (lower $\delta^{15}N$). This persistent gradient allows CSIA-AA $\delta^{15}N$ to be interpreted geographically. There is also an inshore-offshore $\delta^{13}C$ gradient that has been documented on the West Florida Shelf (Radabaugh et al. 2013; Radabaugh and Peebles 2014; Harper et al.2017). The gradient explains the basal-resource shift from more enriched benthic algae onshore to a more phytoplankton-dominant contribution to the base of the food web offshore.

CSIA-AA is usually employed to investigate trophic position using a tissue such as muscle. Wallace et al. (2014, Chapter 3) demonstrated that fish eye lenses are useful as an isotopic recorder. As demonstrated above, trophic histories of individuals can be reconstructed using CSIA-AA and taken one step further to reconstruct geographic histories by removing trophic growth from bulk $\delta^{15}N$ and $\delta^{13}C$. Both bulk and CSIA-AA $\delta^{15}N$ analysis must be conducted on the same samples unless trophic growth can be modeled, as in the case of Red Snapper.

When geographic paths are reconstructed using CSIA-AA of Red Snapper eye-lenses, it is apparent that Red Snapper may not have the long-term high site fidelity that has typically been associated with the species. For example, of the ten Red Snapper analyzed here, six exhibited a lifetime migration from areas of much higher isotopic values from where they were collected (Figure 4.5). Six Red Snapper had isotopic values consistent with an individual showing periods of high site fidelity but later making a lifetime-scale migration from higher isotopic areas (north

and west) to those of lower isotopic value (south and east). Fish 4-40-019 had very little geographic variability, yet fish 4-40-003 showed a large isotopic change from early to late life (≈6.5‰). Considering it took fish 4-40-003 its entire life to make it to the point of capture, there still appear to be periods in its life where it exhibited high site fidelity. Lifetime west-to-east migrations in Red Snapper have been documented by Patterson et al. (2001), Addis et al. (2013), and Dance and Rooker (2019). It is possible that nursery grounds to the north are important for Red Snapper recruitment to the West Florida Shelf (Dance and Rooker 2019).

Analyses were strengthened by adding geographic $\delta^{13}C$ to the geographic $\delta^{15}N$ data (Figures 4.12-4.14). Red Snapper are known to switch habitats during early life (Wells et al. 2008), but also appear to move substantial distances as adults (Figures 4.12 and 4.13). While there are large changes in geographic $\delta^{15}N$ showing migration from the northern Gulf of Mexico, there also seems to be an inshore-offshore movement indicated by increasing and decreasing $\delta^{13}C$.

King Mackerel geographic profiles were different from those of Red Snapper (Figures 4.12-4.14). While Red Snapper seem to undergo lifetime migrations, the King Mackerel (Figure 4.14) complete many trips between more positive and more negative $\delta^{15}N$ isotopic geographies, which is consistent with the known seasonal migrations that this species undergoes each year by following the 20°C isotherm (Manooch 1978; Addis et al. 2018). However, the estimated age at standard length for a majority of the King Mackerel data is between age 0 and age 1, or young-of-the-year (YOY). Little is known about YOY King Mackerel, but a scenario where YOY make two or three isotopically similar migrations (complete cycles to

and from) in one year when larger King Mackerel only make one migration does not seem likely. Using the length at age calculations provided by Manooch et al. (1987), King Mackerel 2 would be approximately Age 2 at collection, which would support the geographic variation indicative of seasonal migration. However, there is still much fluctuation at sizes smaller than FL = 42.5 cm which do not support seasonal migration. If YOY King Mackerel are in local areas with steep isotopic gradients (e.g., in offshore Louisiana waters, where river discharges dynamically intersperse with ocean water), it is possible that isotopic fluctuations occur as they travel locally. Another explanation is that there could be an ontogenetic diet shift causing this variation. YOY King Mackerel are a documented bycatch of the shrimping industry in the northern Gulf of Mexico, but little else is known about them (Ortiz and Andrew, 2008; Bruger et al., 2017). There is not enough published information to definitively explain the isotopic variation in young King Mackerel; however, the present research provides a new approach for doing this.

In contrast to Red Snapper, King Mackerel seem to show very little inshore-offshore movement (Figure 4.14). KM 2, KM 3, and KM 6 varied in carbon by approximately 1‰ throughout their life. KM 4 was an exception and had a 3‰ increase with age, suggesting KM 4 moved more inshore as it got older.

In total, three types of movement patterns are evident: (1) resident (e.g., Red Snapper 4-40-19, Figure 4.5), (2) life-time migrator with intermittent site-fidelity (e.g., Red Snapper 4-40-003, Figure 4.5), and (3) periodic migrator (e.g., KM 6, Figure 4.8). These patterns can be compared with those of under-studied species.

4.4.3 Analysis of unknown: Greater Amberjack

The final step of this study was examining a fish with a relatively unknown life history and applying CSIA-AA to eye lenses to create profiles for this species. Greater Amberjack specimens GAJ 1 and GAJ 2 were sampled for a total of 48 laminae (Figure 4.4). Their bulk $\delta^{15}N$ increased sharply and then fluctuated, and TP_{CSIA} variation of 3.3-4.9 does not seem unreasonable for a large predatory fish. In the Mediterranean Sea, adult Greater Amberjack diets consist of small, schooling pelagics (i.e., scads, sardines) and squid, whereas juveniles feed on decapods and invertebrates (Andaloro and Pipitone, 1997; Addis et al., 2018). The shift from juvenile to adult diet occurs around 15-20 cm (Andaloro and Pipitone, 1997). It is only when considering the $\delta^{15}N_{Glu}$ and $\delta^{15}N_{Phe}$ that the migratory pattern becomes apparent (Figure 4.15). The baseline nitrogen (phenylalanine, Figure 4.11) oscillates much like the King Mackerel baseline, thus driving the same TPCSIA fluctuations. GAJ 1 exhibited at least five peaks and GAJ 2 may exhibited as much as seven. Based on size at capture, GAJ 1 and GAJ 2 are approximately 5-7 years of age (Manooch and Potts 1997b), and so it is possible that the observed peaks are related to annual movements of either predator (Greater Amberjack) or their prey. This suggestion of migratory behavior in Greater Amberjack is in direct contrast to the findings of the McClellan and Cummings (1997) capture-recapture study. With the help of multiple agencies across four regions of the Gulf of Mexico, 4,345 fish were tagged and 569 were recaptured (approximately 13%). Of the recaptured fish, 90% did not move more than 25 miles from where they were tagged and released. Of the fish that did move, 90% did not move more than 100 miles from where they were tagged and released. The Atlantic stock was only slightly more mobile. However, that does not mean that Greater Amberjack will not move. Nine fish

tagged in Gulf of Mexico were recaptured in the Atlantic Ocean and 11 from the Atlantic were recaptured in the Gulf of Mexico. The low rate of cross-population, though, has led to two separately managed stocks, Gulf of Mexico and Atlantic.

Most of the travel by GAJ 1 and GAJ 2 was to-and-from locations to the south and east of the collection point. Considering these fish were collected in the northern Gulf of Mexico (site 9-80), they were already located in one of the highest $\delta^{15}N$ areas in the Gulf of Mexico (Brianna Michaud, USF, unpublished; Peebles and Hollander 2020). A majority of the movement would thus have to be to lower $\delta^{15}N$ areas in the Gulf of Mexico. Greater Amberjack are considered to be mostly pelagic/partly epibenthic and have a very strong association with structure (i.e., reefs, rock outcrops, wrecks; Harris 2007). It is understood that Greater Amberjack feed on migratory, coastal pelagics as adults, and therefore the migratory pattern observed in GAJ 1 and GAJ 2 could be geographic variation originating from the prey rather than the predator. Given these considerations, the interpretation of geographic variation for Greater Amberjack is quite different from that of King Mackerel. In the Greater Amberjack, it seems more likely that it is the prey, rather than the predator, that is moving seasonally driving $\delta^{15}N$ changes in the consumer's tissues. This conclusion is not definitive, however.

4.4.5 Areas for future study

Isotopic analysis of eye-lens amino acids is a novel approach to recreating trophic and geographic histories in fish. Although this record is proving valuable, it is not without areas for improvement. First, as stated above, it is still not possible to differentiate between geographic variation contributed by predator versus prey; geographic variation can be attributed to a

migratory predator feeding on local prey or a local predator feeding on migratory prey. The geographic $\delta^{15}N$ variation propagates similarly through the food web, regardless of which scenario is occurring.

An area requiring the greatest amount of future research is that of trophic discrimination factors. Trophic discrimination factors drive interpretation of $\delta^{15}N$ data, both bulk and CSIA-AA alike. Currently, additive models assume a fixed trophic discrimination factors for each increasing trophic level. Marine teleosts have an accepted trophic discrimination factor of ≈3.4‰, but there is much debate around the value because of the observed variability associated with it among different studies (DeNiro and Epstein 1981; Peterson and Fry 1987; Post 2002; Caut et al. 2009). Hussey et al. (2014) proposed a scaled approach to modeling, allowing trophic discrimination factors to decrease with increasing trophic position. Essentially, lower trophic levels should have a trophic discrimination factor greater than 3.4‰. As the trophic position increases, the trophic discrimination factor decreases. Hussey et al. (2014) successfully demonstrated that a scaled model for trophic position estimation more accurately identified trophic position in both South Africa and the Canadian Arctic, whereas the additive approach (constant TDF) underestimated lower trophic positions while overestimating higher trophic positions.

The data presented here for Red Snapper and King Mackerel support further investigation into a scaled trophic discrimination factor approach. Trophic positions calculated for both Red Snapper and King Mackerel fell below the assumed minimum trophic position of 3.0, which would require herbivory that is not believed to exist at any stage during the lives of

these species. Applying a scaled approach to CSIA-AA analysis would increase lower trophic positions estimates and decrease upper trophic positions. Furthermore, adjusting the trophic discrimination factors and trophic positions will also affect the geographic variation calculated from CSIA-AA. The changing geographic variation $\delta^{15}N$ value will not be uniform as it depends on further study and implementation of trophic discrimination factors for both bulk $\delta^{15}N$ and CSIA-AA $\delta^{15}N$. Bulk trophic discrimination factors are derived from CSIA-AA trophic discrimination factors.

Table 4.1 Red Snapper regression equations for the models presented in Figure 3. Each regression uses six laminae CSIA-AA measurements except 8-40-003. Glutamic acid and phenylalanine were resolved for five laminae.

Fish ID	Regression	R^2	p-value
All Red Snappers	$TP_{CSIA}=(1.58716+0.928147*sqrt(LRM))^2$	0.77	0.000
4-40-002	$TP_{CSIA}=sqrt(9.68102+0.928147*LRM)$	0.89	0.004
4-40-003	$TP_{CSIA}=2.81634+0.181456*LRM$	0.98	0.000
4-40-006	$TP_{CSIA}=sqrt(5.72935+5.66284*sqrt(LRM))$	0.94	0.002
4-40-019	$TP_{CSIA}=sqrt(9.06041+1.4742*LRM)$	0.93	0.002
4-40-021	$TP_{CSIA}=sqrt(4.25502+5.75193*sqrt(LRM))$	0.95	0.001
8-40-003*	$TP_{CSIA}=sqrt(10.9947+0.415781*(LRM)^2)$	0.96	0.009
8-40-008	$TP_{CSIA}=(1.64425+0.102286*LRM)^2$	0.97	0.000
8-40-012	$TP_{CSIA}=1/(0.311087-0.0610164*ln(LRM))$	0.99	0.000
8-40-019	$TP_{CSIA}=sqrt(6.62762+2.4871*LRM)$	0.98	0.001
8-40-023	$TP_{CSIA}=1/(0.308392-0.0402982*ln(LRM))$	0.90	0.004

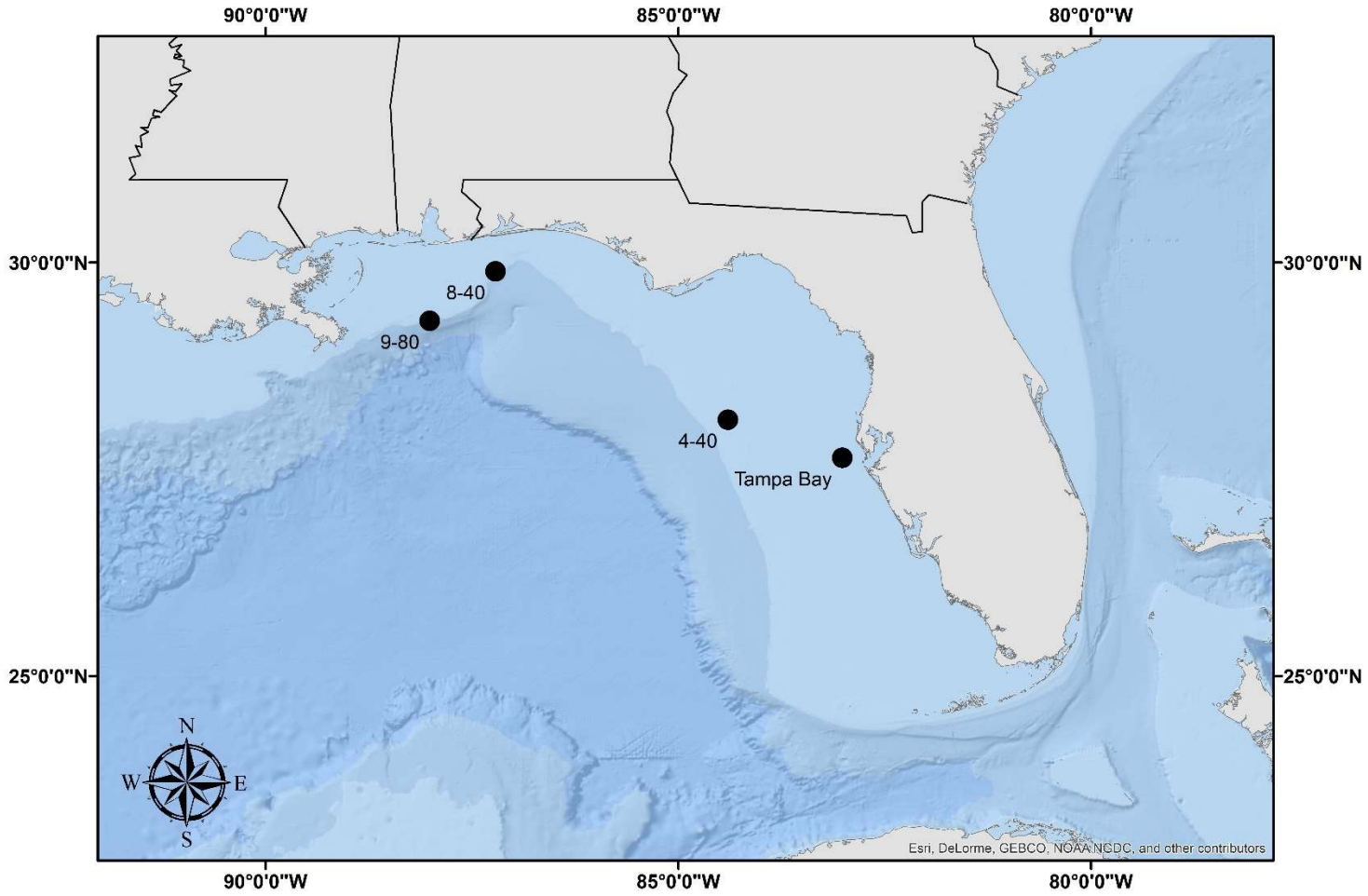

Figure 4.1 Sample collection points. Red Snapper were collected from 4-40 and 8-40. King Mackerel were collected at Tampa Bay. Greater Amberjack were collected at 9-80.

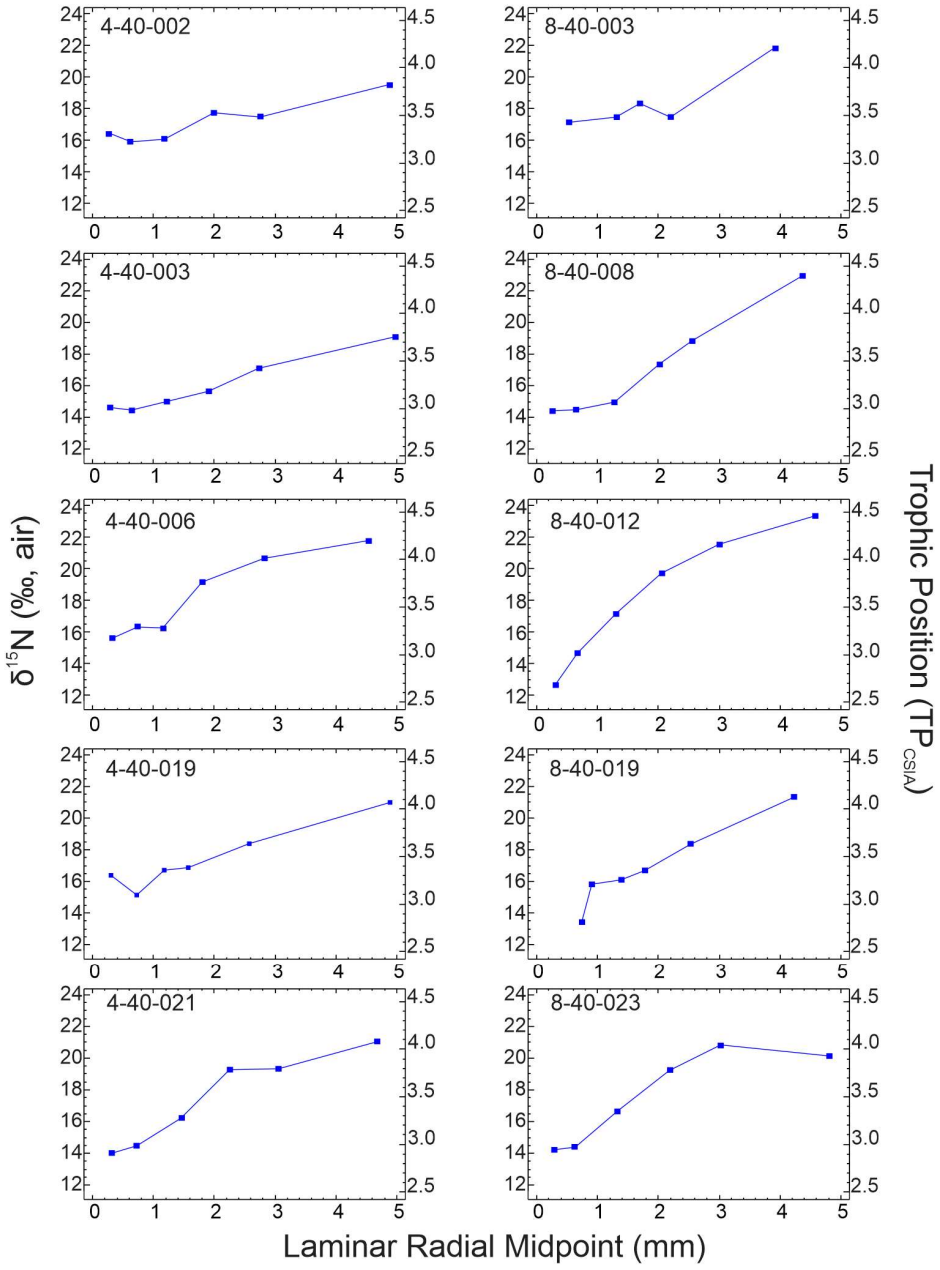

Figure 4.2 Red Snapper $\delta^{15}N_{Glu\text{-}Phe}$ and corresponding trophic position. Trophic position is calculated from the difference between the isotopic ratios of glutamic acid and phenylalanine using an equation and trophic discrimination factors defined by Bradley et al. (2015).

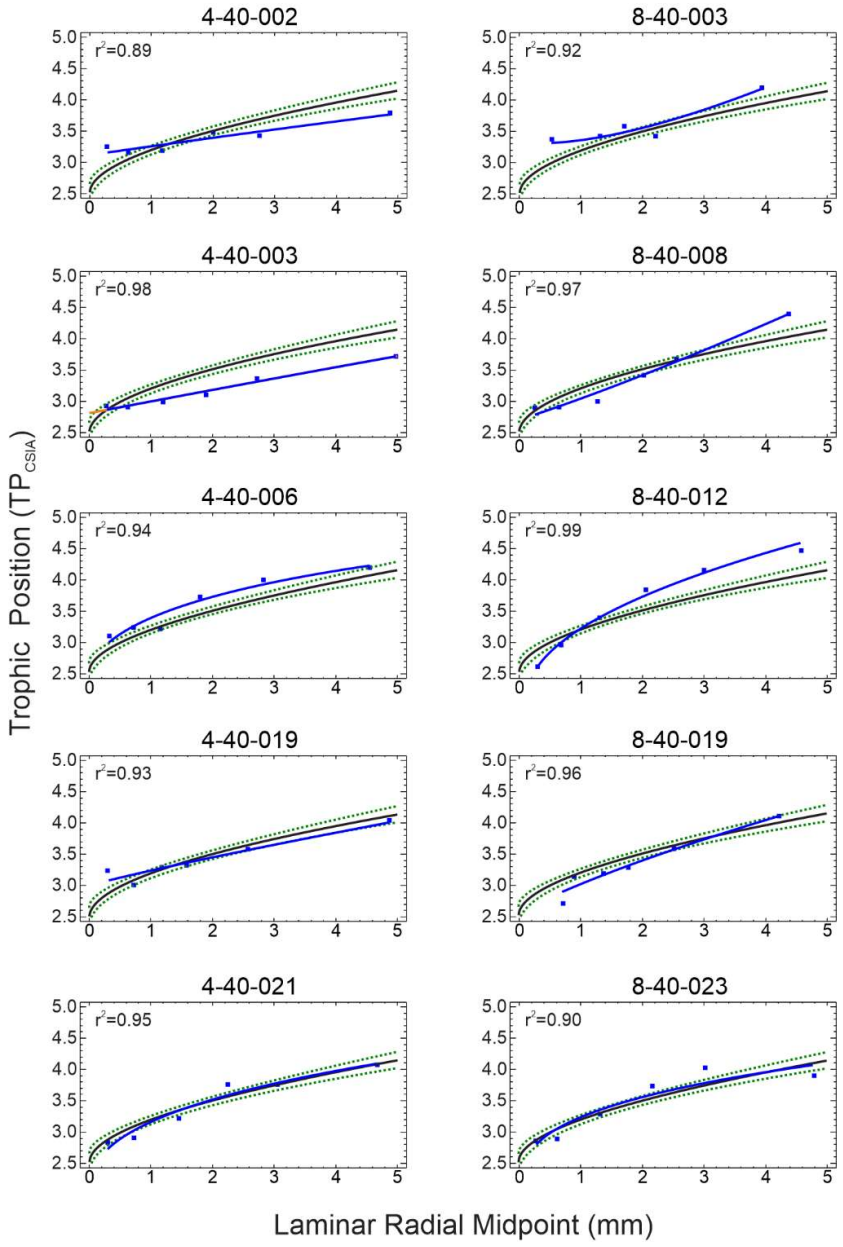

Figure 4.3 Trophic growth models calculated by using best fit regression for the Red Snapper species compared to individuals. Blue squares are the TP_{CSIA} for individual laminae, blue solid line is the model for the specific fish, black solid line is the Red Snapper species model calculated using all TP_{CSIA} values measured for each lamina, and green dotted lines are the 95% confidence interval for the Red Snapper species model.

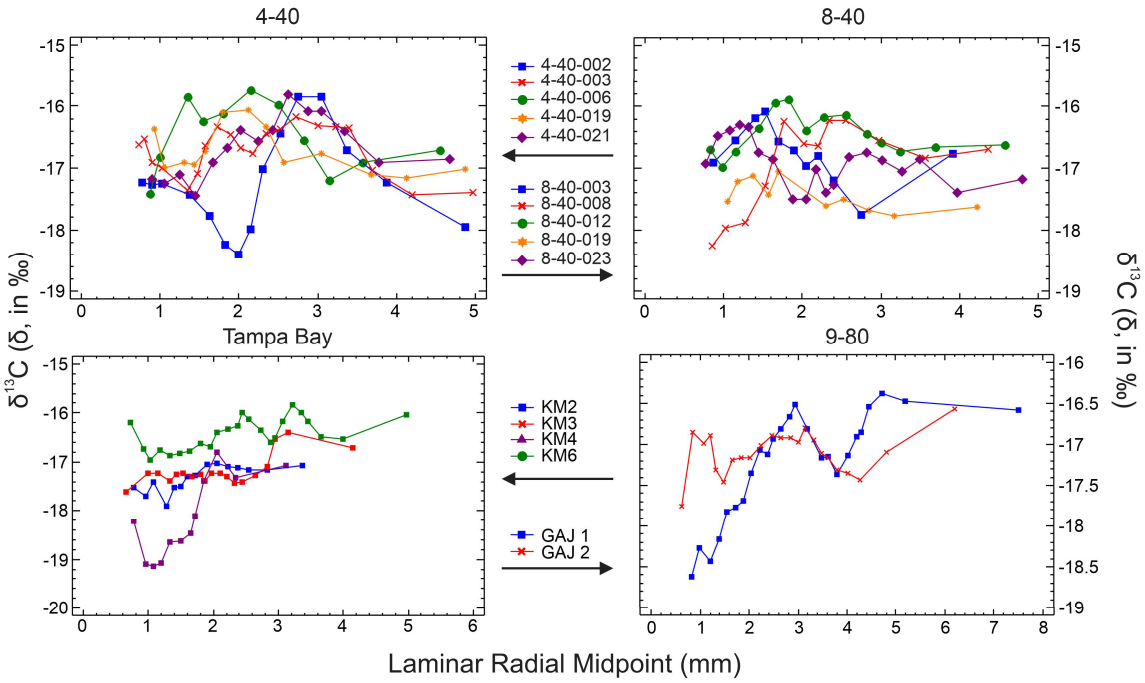

Figure 4.4 Bulk $\delta^{15}N$ for each individual, plotted against laminar radial midpoint (LRM). As LRM increases, the age and size of the individual increases. 4-40: 5 Red Snapper, 8-40: 5 Red Snapper, Tampa Bay: 4 King Mackerel, 9-80: 2 Greater Amberjack

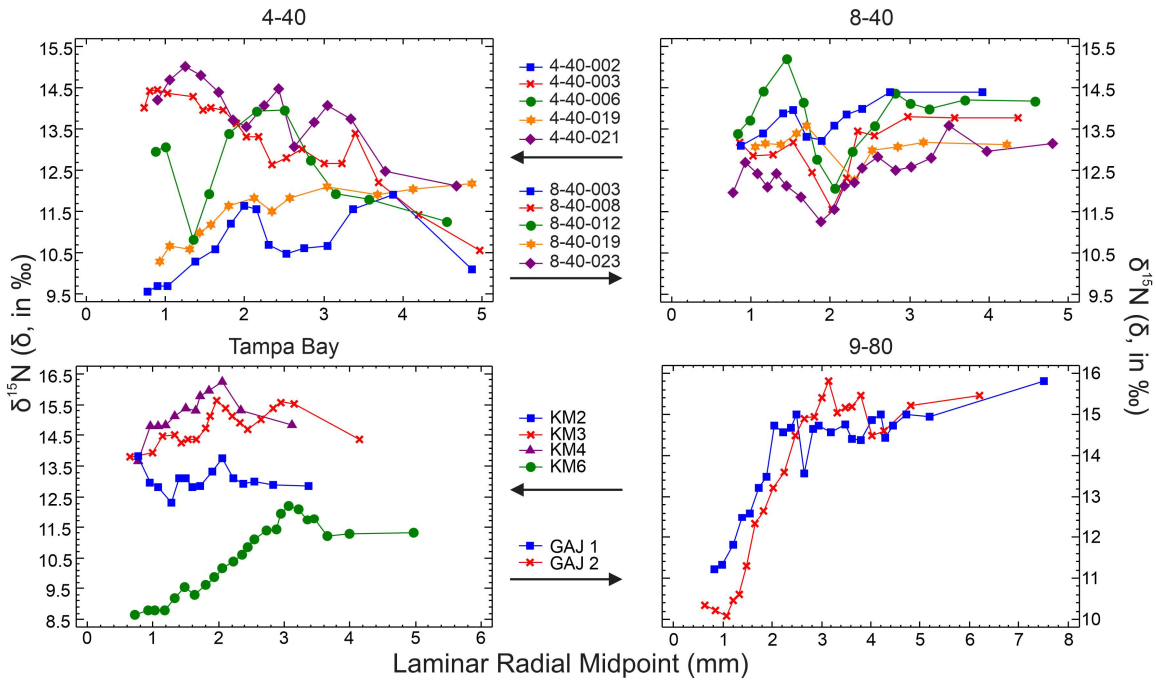

Figure 4.5 Bulk $\delta^{13}C$ for each individual, plotted against laminar radial midpoint (LRM). As LRM increases, the age and size of the individual increases. 4-40: 5 Red Snapper, 8-40: 5 Red Snapper, Tampa Bay: 4 King Mackerel, 9-80: 2 Greater Amberjack

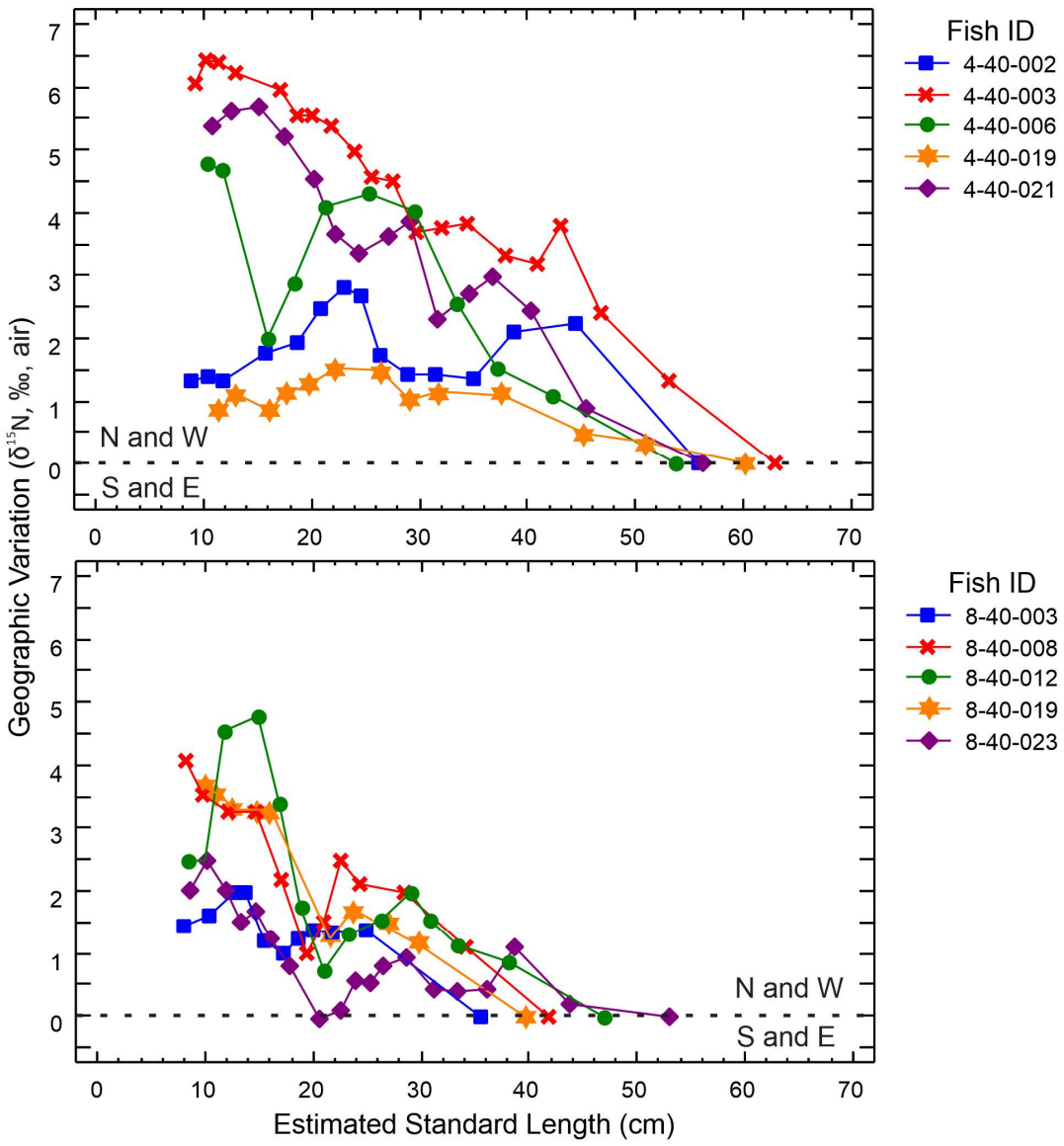

Figure 4.6 Red Snapper movements in isotopic space. Geographic variation was calculated by removing the trophic isotopic signature from the bulk $\delta^{15}N$. It was then plotted normalized to point of collection (dashed line) under the assumption that the individual was in the capture location long enough to assimilate isotopically. There are two collection points, 4-40 and 8-40. Each line represents an individual. Positive values indicate locations north and west of the point of capture. Negative values indicate locations south and east.

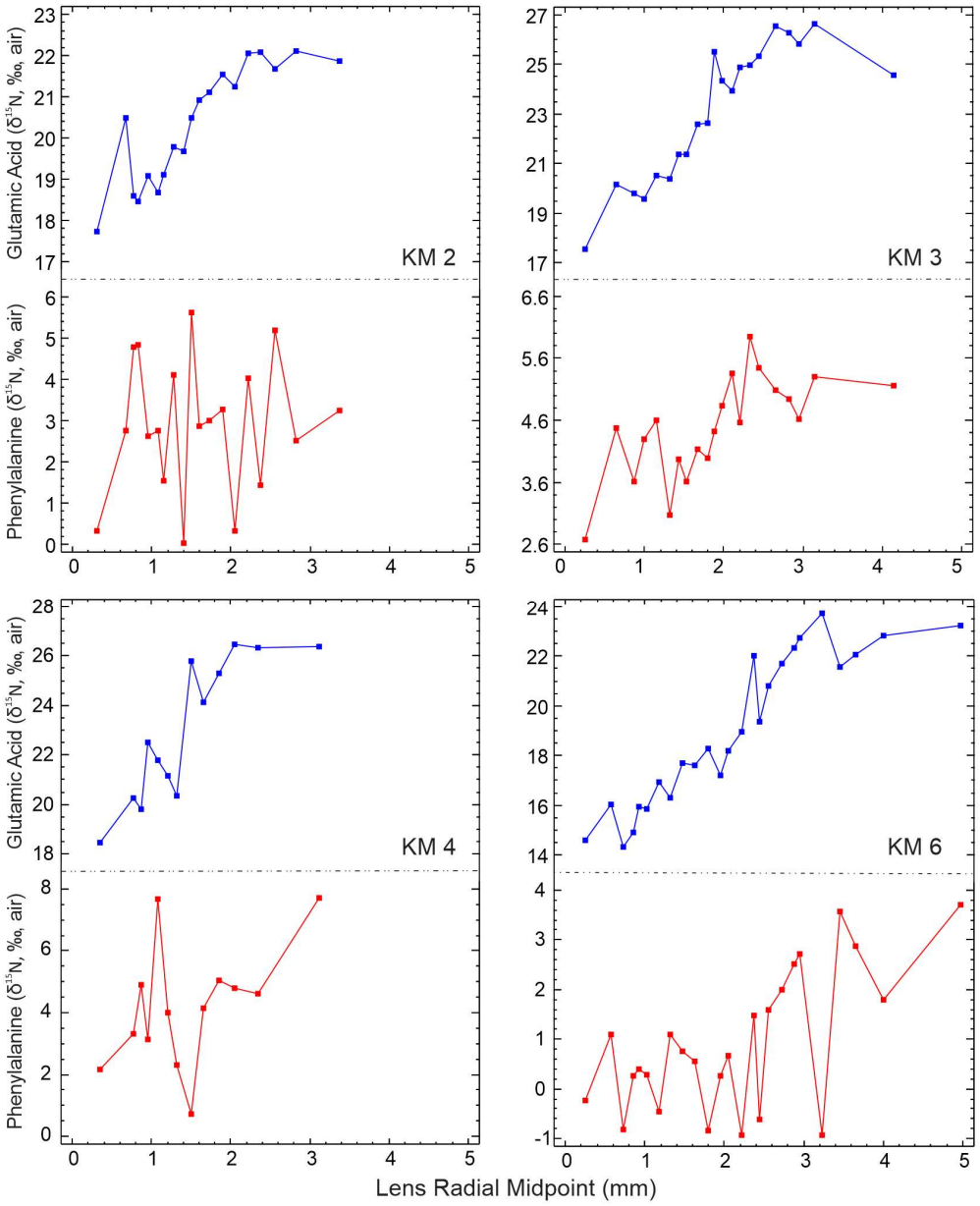

Figure 4.7 Individual King Mackerel $\delta^{15}N_{Glu}$ and $\delta^{15}N_{Phe}$. Each point was measured using CSIA-AA and associated with laminar radial midpoint measurement. Blue lines are glutamic acid and red lines are phenylalanine.

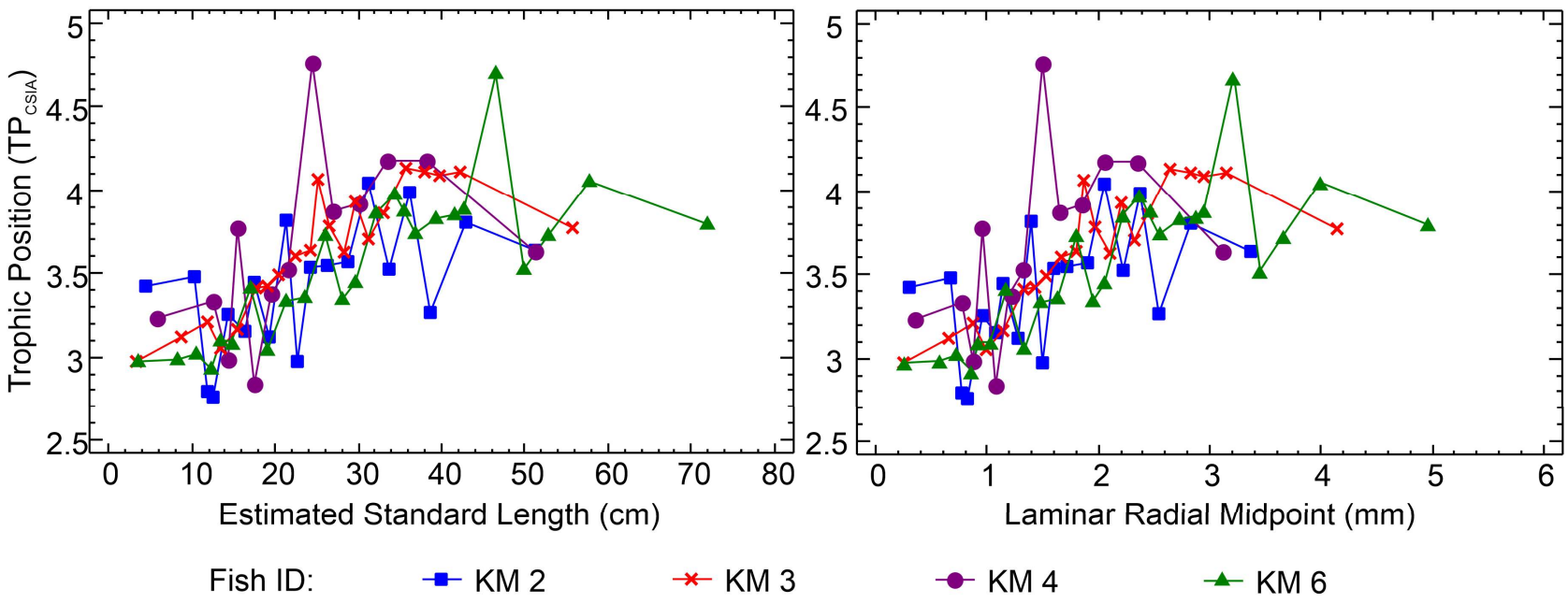

Figure 4.8 Trophic position at estimated standard length and laminar radial midpoint (LRM) for King Mackerel. Trophic position calculated using empirical data for glutamic acid and phenylalanine generated using CSIA-AA. Standard length calculated for each LRM assuming isometric growth after post-larval phase. Each line is an individual King Mackerel.

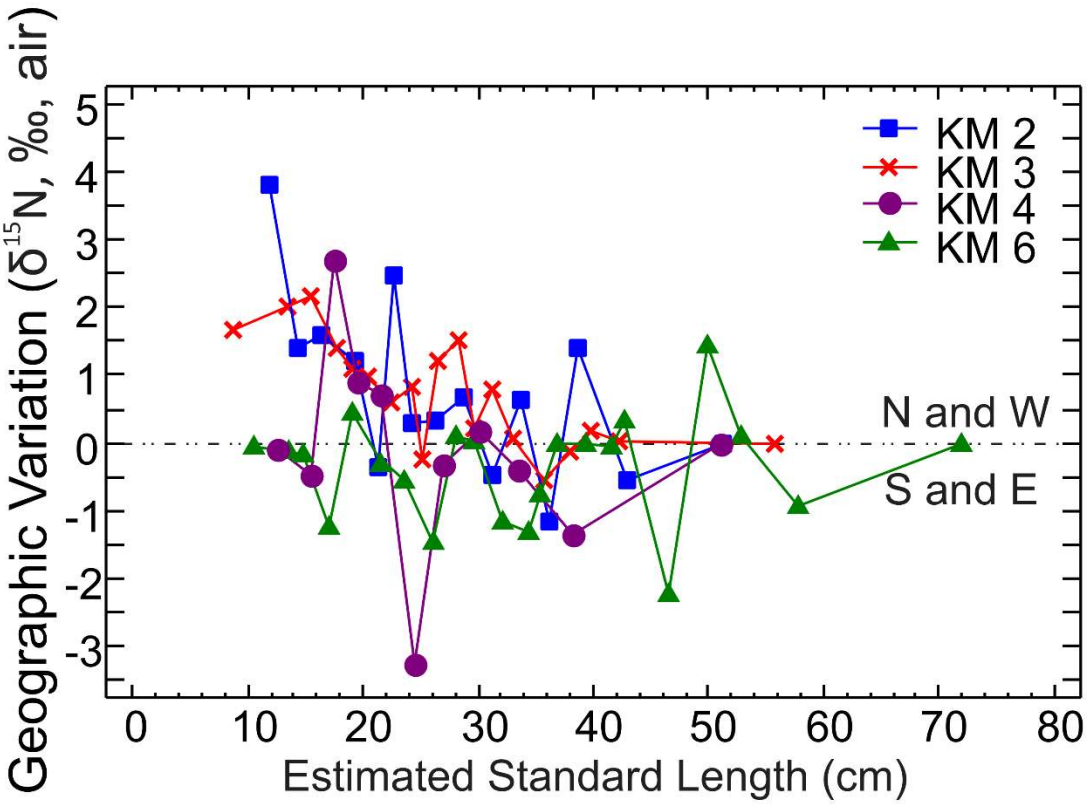

Figure 4.9 King Mackerel movements in isotopic space. Geographic variation was calculated by removing the trophic isotopic signature from the bulk δ^{15}N. It was then plotted normalized to point of collection (dashed line) under the assumption that the individual was in the capture location long enough to assimilate isotopically. Each line represents an individual. Positive values indicate locations north and west of the point of capture. Negative values indicate locations south and east.

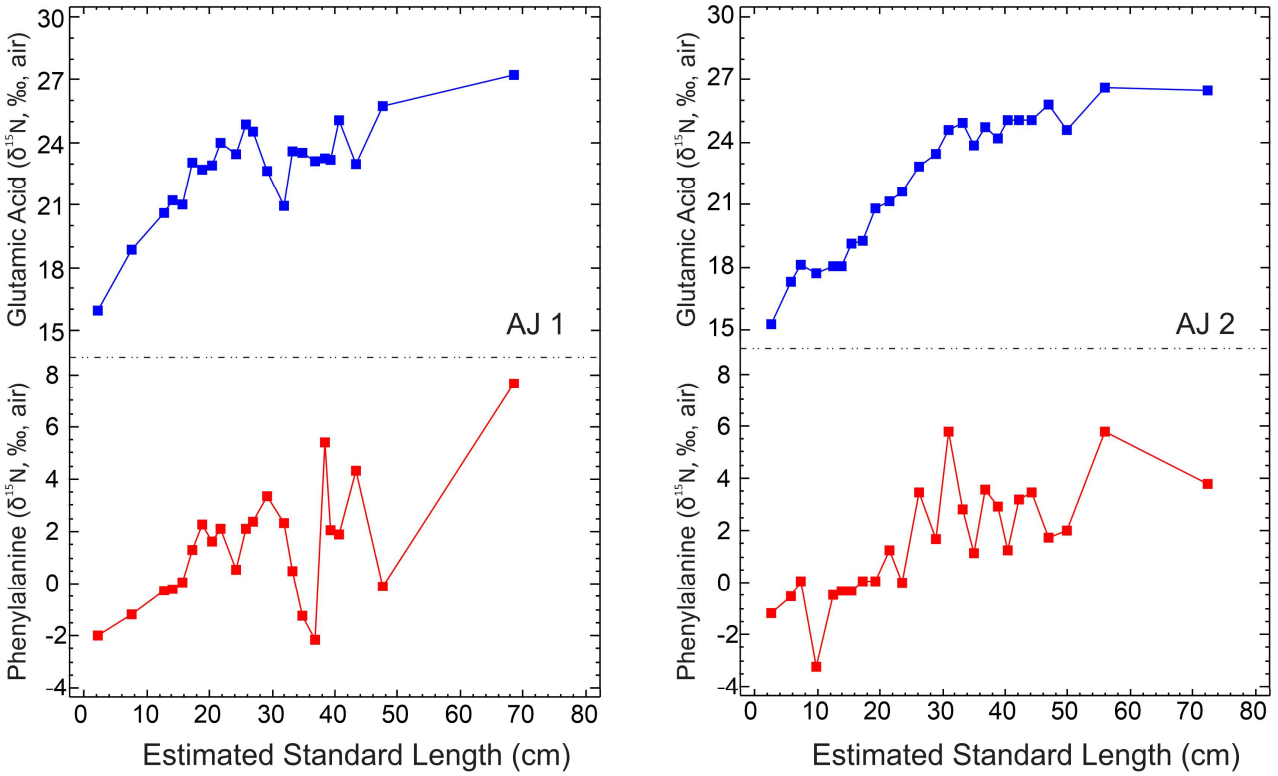

Figure 4.10 Individual Greater Amberjack $\delta^{15}N_{Glu}$ and $\delta^{15}N_{Phe}$. Each point was measured using CSIA-AA and associated with laminar radial midpoint measurement. Blue lines are glutamic acid and red lines are phenylalanine.

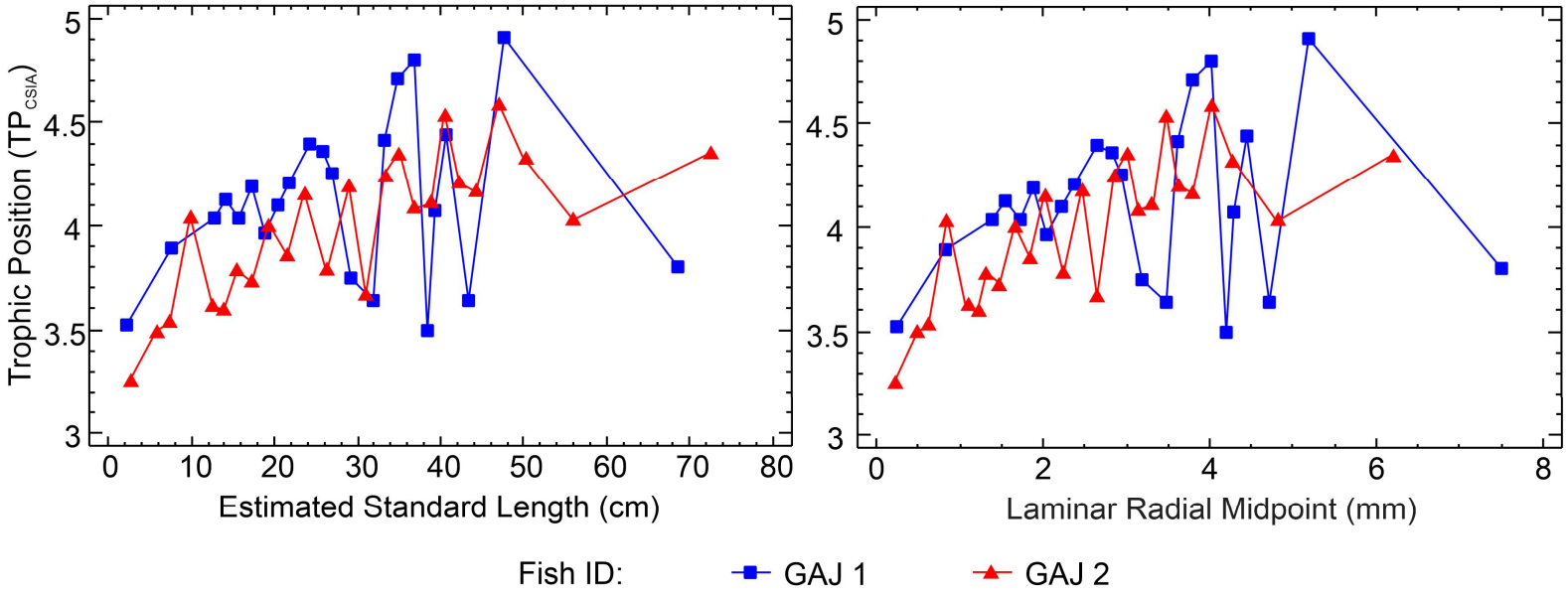

Figure 4.11 Trophic position at estimated standard length and laminar radial midpoint (LRM) for Greater Amberjack. Trophic position calculated using empirical data for glutamic acid and phenylalanine generated using CSIA-AA. Standard length calculated for each LRM assuming isometric growth after post-larval phase. Each line is an individual Greater Amberjack.

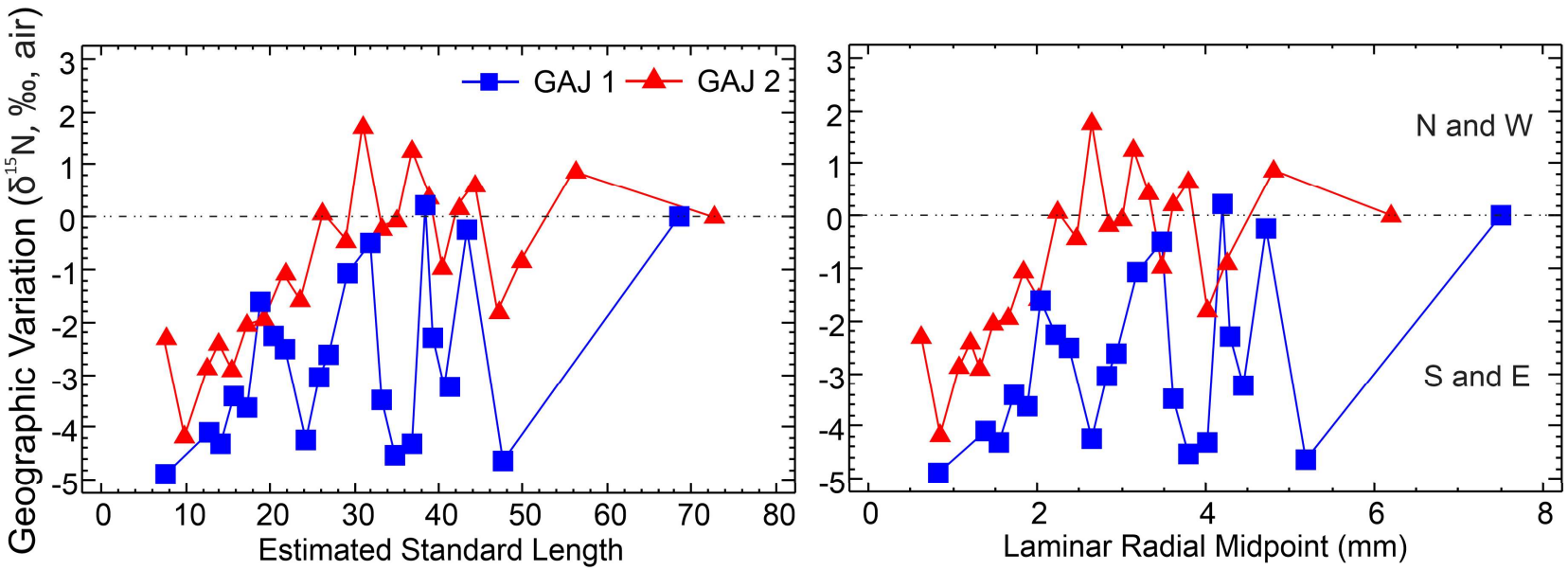

Figure 4.12 Greater Amberjack movements in isotopic space. Geographic variation was calculated by removing the trophic isotopic signature from the bulk δ^{15}N. It was then plotted normalized to point of collection (dashed line) under the assumption that the individual was in the capture location long enough to assimilate isotopically. Each line represents an individual. Positive values indicate locations north and west of the point of capture. Negative values indicate locations south and east.

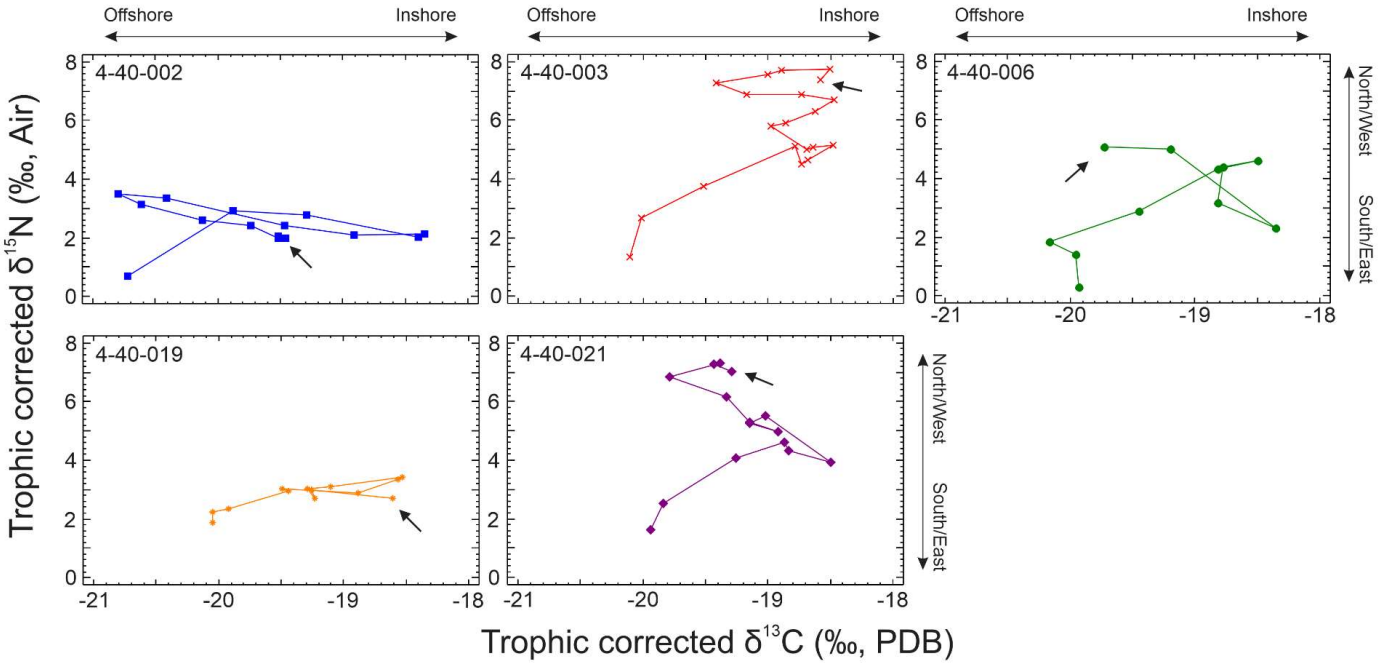

Figure 4.13 Geographic variation using trophic corrected $\delta^{13}C$ and trophic corrected $\delta^{15}N$ for Red Snapper from 4-40. Trophic positions were calculated from CSIA and then translated to a bulk equivalent using the respective trophic discrimination factor ($\delta^{13}C$ = 1‰; $\delta^{15}N$ = 3.4‰). $\delta^{13}C$ and $\delta^{15}N$ were plotted on axes that represent the gradients' orthogonal pattern to one another. $\delta^{13}C$ becomes enriched while moving inshore and $\delta^{15}N$ becomes enriched toward the northern Gulf of Mexico. By plotting $\delta^{13}C$ and $\delta^{15}N$ together, individual fish movements can be inferred. The arrow points to the beginning of the time series.

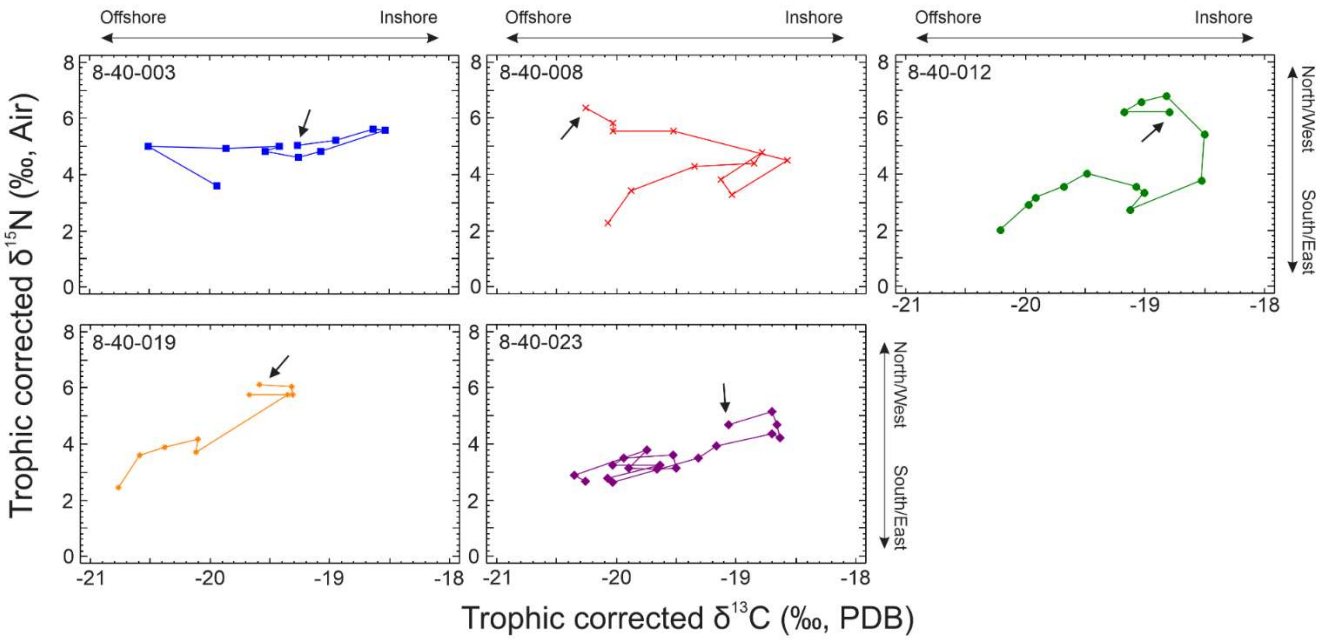

Figure 4.14 Geographic variation using trophic corrected $\delta^{13}C$ and trophic corrected $\delta^{15}N$ for Red Snapper from 8-40. Trophic positions were calculated from CSIA and then translated to a bulk equivalent using the respective trophic discrimination factor ($\delta^{13}C$ = 1‰; $\delta^{15}N$ = 3.4‰). $\delta^{13}C$ and $\delta^{15}N$ were plotted on axes that represent the gradients' orthogonal pattern to one another. $\delta^{13}C$ becomes enriched while moving inshore and $\delta^{15}N$ becomes enriched toward the northern Gulf of Mexico. By plotting $\delta^{13}C$ and $\delta^{15}N$ together, individual fish movements can be inferred. The arrow points to the beginning of the time series.

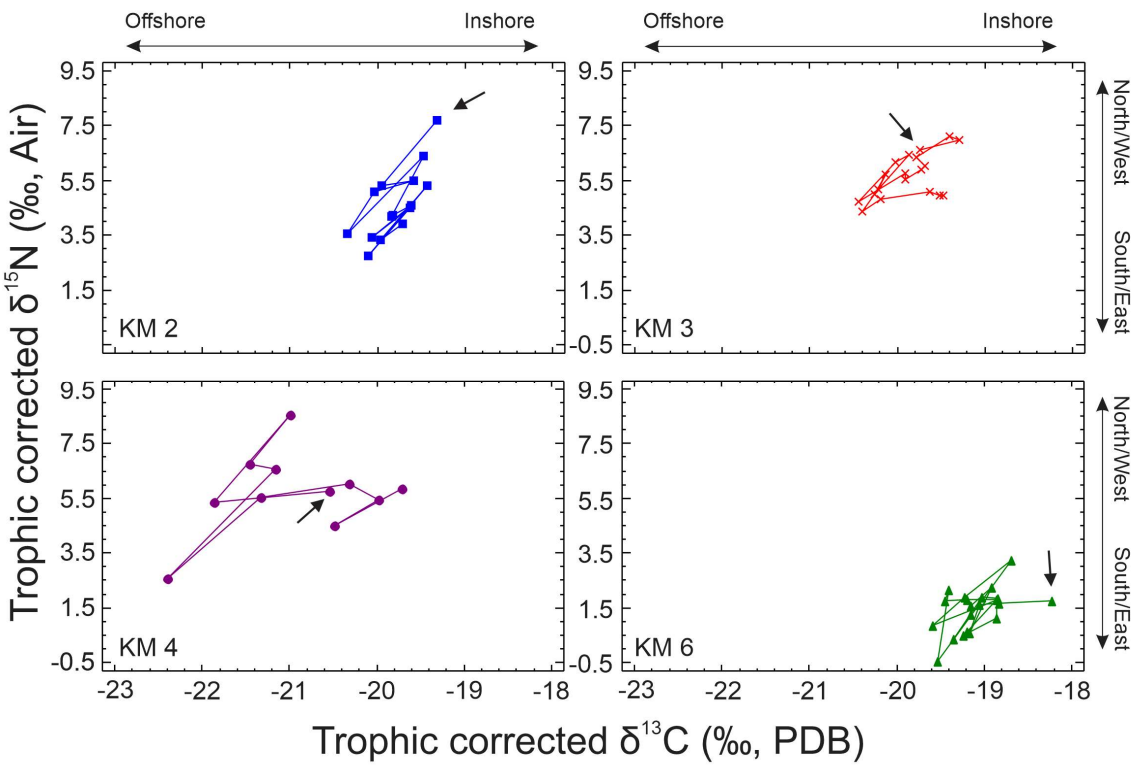

Figure 4.15 Geographic variation using trophic corrected $\delta^{13}C$ and trophic corrected $\delta^{15}N$ for King Mackerel from Tampa Bay. Trophic positions were calculated from CSIA and then translated to a bulk equivalent using the respective trophic discrimination factor ($\delta^{13}C$ = 1‰; $\delta^{15}N$ = 3.4‰). $\delta^{13}C$ and $\delta^{15}N$ were plotted on axes that represent the gradients' orthogonal pattern to one another. $\delta^{13}C$ becomes enriched while moving inshore and $\delta^{15}N$ becomes enriched toward the northern Gulf of Mexico. By plotting $\delta^{13}C$ and $\delta^{15}N$ together, individual fish movements can be inferred. The arrows point to the beginning of the time series.

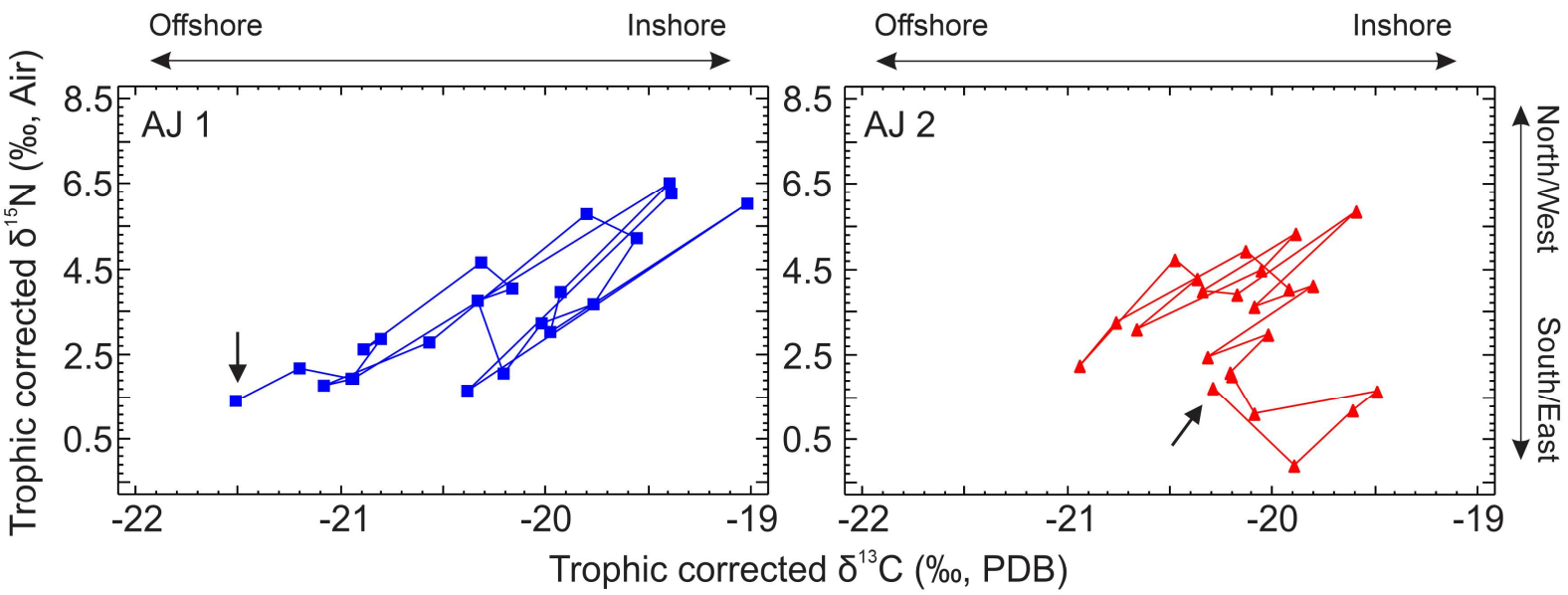

Figure 4.16 Geographic variation using trophic corrected $\delta^{13}C$ and trophic corrected $\delta^{15}N$ for Greater Amberjack from 9-80. Trophic positions were calculated from CSIA and then translated to a bulk equivalent using the respective trophic discrimination factor ($\delta^{13}C$ = 1‰; $\delta^{15}N$ = 3.4‰). $\delta^{13}C$ and $\delta^{15}N$ were plotted on axes that represent the gradients' orthogonal pattern to one another. $\delta^{13}C$ becomes enriched while moving inshore and $\delta^{15}N$ becomes enriched toward the northern Gulf of Mexico. By plotting $\delta^{13}C$ and $\delta^{15}N$ together, individual fish movements can be inferred. The arrow points to the beginning of the time series.

Chapter 5. Conclusions

5.1 Conclusions

The research in this dissertation successfully identified and examined a new natural, stable-isotopic record in the form of fish eye lenses. In contrast to a coarse-scale temporal analysis that can mask patterns, the fine-scale temporal resolution of stable isotope history in eye lenses lends itself to fish research as a tool for exploring relatively unstudied periods during fish life histories, including seasonal-scale periods. My research highlights the utility of this record on an exploratory scale, but can be applied to much larger sample sizes. Although the present study focuses solely on marine fish, it is possible to extend it to other vertebrate species.

In Chapter 2, I found that lifetime records in bulk $\delta^{13}C$ and $\delta^{15}N$ appear to exist within fish eye lenses. Because eye lenses are protein-rich and form in successive layers, $\delta^{13}C$ and $\delta^{15}N$ are abundant for analyses, unlike otoliths which currently provide the only other complete life-history record in bony fish, but have very low nitrogen content. Eye-lenses lend themselves to temporally fine data resolution that is currently unmatched; for example, in a King Mackerel approximately two years old (standard length = 63.5 cm), I was able to measure bulk $\delta^{13}C$ and $\delta^{15}N$ within 19 laminae, indicating temporal resolution can be sub-seasonal. In this method, temporal resolution is limited by the research technician's manual dexterity and not the amount of tissue required for isotopic analysis. In general, isotopic trends within and among

species were in agreement with lifetime trends documented in the literature, which is encouraging.

In chapter 3, I found that compound-specific stable isotope analysis on eye-lens amino acids is not only possible but can be practical. Using well established derivatization methods, I was able to reliably resolve 10 amino acids for subsequent stable-isotope analysis. With additional methods development and amino-acid targeting, it should be possible to resolve isotopic trends within at least 13 amino acids. While two amino acids (glutamic acid and phenylalanine) were highlighted in my dissertation research, it is becoming a more common practice to use multiple amino acids to isolate geographic trends from changes in trophic position.

In chapter 4, I applied bulk and compound-specific analysis of $\delta^{13}C$ and $\delta^{15}N$ to successfully reconstruct the first individual trophic histories of wild-caught fish. Red Snapper and King Mackerel were chosen because of their well-studied, contrasting life-histories. Red Snapper are structure-oriented reef fish with documented high site-fidelity and King Mackerel are a highly migratory fish that travel the entire north-south distance of the Gulf of Mexico. Based on existing information, these two species were hypothesized to be isotopically, trophically, and geographically different. After isolating and analyzing glutamic acid (trophic amino acid) and phenylalanine (source amino acid), I reconstructed the individual trophic histories of ten Red Snapper and four King Mackerel. Red Snapper produced smooth trophic growth curves that reflected increasing trophic position as the first got larger. King Mackerel produced irregular trophic growth patterns, having both increasing and decreasing trophic positions with changes in size.

In chapter 4, I also reconstructed migration patterns by backing the trophic $\delta^{13}C$ and $\delta^{15}N$ out of the bulk $\delta^{13}C$ and $\delta^{15}N$ measurements. Bulk isotopes combine variation caused by trophic position changes with baseline variation that is associated with changes in geographic location. Subtracting trophic position from the bulk trends in bulk $\delta^{13}C$ and $\delta^{15}N$ isolated the geographic components of the record, resulting in the first complete geographic histories of fish based on stable-isotope analysis. One interesting finding was that some Red Snapper underwent a one-way lifetime migration from locations to the north and west (north-central Gulf of Mexico) to the West Florida Shelf while experiencing shorter periods of high site fidelity. This is a trend that has been suggested through tagging data but has only recently been documented by Dance and Rooker (2019). There were also two Red Snapper that did not appear to move much, except for some movement back and forth in the inshore-offshore direction. I was also able to confirm cyclic isotopic changes in the migratory King Mackerel. While this cyclic behavior was initially suspected to be a result of migration, the cycles were observed in Age-0 King Mackerel, and the pattern is now suspected of being related to local noise caused by physical interactions between oligotrophic water masses and more eutrophic, river-influenced water masses on the continental shelf of the north-central Gulf of Mexico. The various observed migration trends (i.e., one-way migration, resident, and local noise) were compared to two specimens of an understudied species, Greater Amberjack (aged 6-7 years). The two Greater Amberjack had trophic and geographic patterns that were similar to those of the King Mackerel, suggesting that either the Greater Amberjack or its primary prey are highly migratory.

5.2 Implications and future work

The present research is part of a programmatic approach to improve the utility of stable isotopes in studies of fish ecology, including studies that are relevant to fisheries management. The program has included fundamental investigations of differences in the photosynthetic fractionation of different types of microalgae (benthic algae vs. phytoplankton; Radabaugh et al. 2014). That effort focused on understanding the processes that cause different basal resources to be isotopically distinguishable in consumers that are at higher positions in the food web. These two basal-resource types have very different $\delta^{13}C$, in particular, and the difference can be attributed to many factors, with the light environment being notably important. Another step in the program involved building and modeling isoscapes. Robust isotopic gradients were identified using phytoplankton (as POM), benthic algae (from sea urchin stomachs), and demersal fish muscle (Radabaugh et al. 2013; Radabaugh and Peebles 2014; Huelster 2015). While these efforts were underway, techniques for compound-specific stable-isotope analysis were being refined for individual amino acids from marine fishes and gastropods (Ellis 2012). Soon after fish eye lenses were discovered to contain lifetime stable-isotope records (Chapter 2; Wallace et al. 2014), Granneman (2018) conducted a diet-switch experiment with Red Drum (*Sciaenops ocellatus*) that confirmed that dietary isotopes are incorporated into the outer eye lens layers after an average lag of 16 days. The research presented here adds to this programmatic approach.

Eye lenses offer an important and emerging stable-isotope record. Reconstructing trophic and geographic histories will fill data gaps in fish ecology caused by sampling bias, migrations, or by simply not being able to locate particular life stages for study. Using stable-

isotope records, ontogenetic shifts and other important life-cycle events can be investigated, even if the fish captured for study are much older than the period of interest. Such older fish are inherently survivors and comparing isotopic histories of older survivors with those of younger fish is a promising approach that may identify which life-history or habitat trends are the most successful.

There are also a few broad-scale areas for new research. We can likely expand both the utility and the interpretive power of this general approach by adding additional isotopes to the study (e.g., ^{18}O, ^{34}S, ^{2}H). Sulfur would be an easy one to start with, as it is already studied in other isotope research that is based on muscle tissue (i.e., protein). There are multiple amino acids that contain sulfur (the one that was present and measurable in the present study is methionine).

Another area for future improvement involves the trophic discrimination factor. Trophic discrimination factors are the mathematical basis for trophic and geographic isotope studies. Current methods, this study included, have used an additive approach (i.e., the trophic discrimination factor was treated as a constant for all life periods). However, other studies have identified a wide range of trophic discrimination factors based on study tissue, species, location, and the trophic position of the study species. It has been suggested that there is not simply one trophic discrimination factor, but trophic discrimination factors that respond in a more complex manner to other factors. Additional experiments with trophic discrimination factors are warranted and will likely improve the accuracy of estimates associated with trophic geography. Eye-lenses offer an opportunity to study trophic discrimination across the lifetime of an individual, which is something that has been impossible until now.

Another way to improve methodology is to refine gas-chromatography techniques in order to target specific amino acids. Current methods described in the present research attempted to maximize the number of amino acids that were isolated in order to capture the most information possible. However, moving forward, it could be beneficial to target specific amino acids. Chromatography (peak size and shape) could be optimized for the most useful amino acids, resulting in reductions in the time required for analysis.

The final area for future work involves investigation of the assumptions associated with stable-isotope ecological research. In addition to uncertainties in the trophic discrimination factor, another assumption in isotope research is that bulk isotope ratios are a combination of variation caused by trophic position and baseline values (i.e., location), which is simply not the case. Studies have documented isotopic variation based on diet quality, excretion types, and gut microbiomes, but how these variations affect trophic discrimination is not well understood.

This is not a comprehensive account of future research directions. These eye-lens-based methods are new, and because of this, there are other topics that are promising candidates for future study. We have only begun to examine the utility of these new methods.

Chapter 6. References

Adams RF (1974) Determination of amino acid profiles in biological samples by gas chromatography. Journal of Chromatography 95:189-212

Addis DT, Patterson III WF, Dance MA, Ingram Jr GW (2013) Implications of reef fish movement from unreported artificial reef sites in the norther Gulf of Mexico. Fisheries Research 147:349-358. doi:10.1016/j.fishres.2013.07.011

Addis D, Allen S, Mahmoudi B, Muller RG, Munyandorero J, O'Hop J, Smith EH, Swanson C (2018) Florida's inshore and nearshore species: 2018 status and trends report. Florida Fish and Wildlife Conservation Commission, Fish Wildlife Research Institute, St. Petersburg, FL, USA. December. 323 p

Alt-Epping U, Mil-Homens M, Hebbeln D, Abrantes F, Schneider RR (2007) Provenance of organic matter and nutrient conditions on a river and upwelling influenced shelf: a case study from the Portuguese Margin. Marine Geology 243: 169–179.

Al-Hassan LAJ, Al-Sayab AA (1994) Eye lens diameter as an age indicator in the catfish, *Silurus triostegus*. Pakistan Journal of Zoology 26(1): 81-82.

Al-Mamry J, Jawad L, Al-Busaidi J, Al-Mamari A, Al-Mamry S, Al-Owisi K, Al-Rubiey M, Al-Hasani L (2012) The use of eye lens diameter and weight in age determination in *Siganus canaliculatus* (Park, 1797) (Perciformes, Siganidae) collected from the Arabian Sea coasts of Oman. Natura Montenegrina 11(1): 73-78

Andalaro F, Pipitone C (2007) Food and feeding habits of the amberjack, Seriola dumerili, in the Central Mediterranean Sea during the spawning season. Cahiers de Biologie Marine 38:91-96.

Bagenal TB, Mackereth FJH, Heron J (1973) The distinction between brown trout and sea trout by strontium content of their scales. Journal of Fish Biology 5: 555-557.

Barnes C, Jennings S, Barry JT (2009) Environmental correlates of large-scale spatial variation in the $\delta^{13}C$ of marine animals. Estuarine, Coastal and Shelf Science 81:368-374. doi:10.1016/j.ecss.2008.11.011

Bastos RF, Corrêa F, Winemiller KO, Carcia AM (2017) Are you what you eat? Effects of trophic discrimination factors on estimates of food assimilation and trophic position with a new estimation method. Ecological indicators 75:234-241. doi:10.1016/j.ecolind.2016.12.007

Beamish RJ, Chilton D (1977) Age Determination of Lingcod (*Ophiodon elongatus*) using dorsal fin rays and scales. Journal of the Fisheries Research Board of Canada 34: 1305-1313.

Bearhop S, Adams CE, Waldron S, Fuller RA, MacLeod H (2004) Determining trophic niche width: a novel approach using stable isotope analysis. Journal of Animal Ecology 73:1007-1012.

Beaumariage DS (1973) Age, growth, and reproduction of King Mackerel, *Scomberomorus cavalla,* in Florida. Florida Marine Research Publications 1:45 p

Berman ER (1991) Biochemistry of the eye. Plenum Press. pp. 476. doi:10.1111/j.1095-8649.1988.tb05496.x

Block BA, Jonsen ID, Jorgensen SJ, Winship AJ, Shaffer SA, Bograd SJ, Hazen EL, Foley DG, Breed GA, Harrison AL, Ganong JE, Swithenbank A, Castleton M, Dewar H, Mate BR, Shillinger GL, Schaefer KM, Benson SR, Wise MJ, Henry RW, Costa DP (2011) Tracking apex marine predator movements in a dynamic ocean. Nature 475:86-90. doi:10.1038/nature10082

Bloemendal H (1982) Lens proteins. CRC Critical Reviews in Biochemistry 12(1): 1-38.

Boecklen WJ, Yarnes CT, Cook BA, James AC (2011) On the use of stable isotopes in trophic ecology. Annual Review of Ecology, Evolution, and Systematics 42:411-440. doi:10.1146/annurev-ecolsys-102209-144726

Bowen GJ (2010) Isoscapes: Spatial pattern in isotopic biogeochemistry. Annual Review of Earth and Planetary Sciences 38:161-187. doi:10.1146/annurev-earth-040809-152429

Bradley CJ, Wallsgrove NJ, Choy A, Drazen JC, Hetherington ED, Hoen DK, Popp BN (2015) Trophic position estimates of marine teleosts using amino acid compound specific isotopic analysis. Limnology and Oceanography: Methods 13: 476-493. doi:10.1002/lom3.10041

Bradley CJ, Longenecker K, Pyle RL, Popp BN (2016) Compound-specific isotopic analysis of amino acids reveals dietary changes in mesophotic coral-reef fish. Marine Ecology Progress Series 558: 65-79. doi:10.3354/meps11872

Braun A, Vikari A, Windisch W, Auerswald K (2014) Transamination governs nitrogen isotope heterogeneity of amino acids in rats. Journal of Agricultural and Food Chemistry 62: 8008-8013. doi:10.1021/jf502295f

Briggs JC (1958) A list of Florida fishes and their distribution. Bulletin of Florida State Museum 2(8):287

Bruger J, Chen Y, Hawkins WE, Holzwart KR, Keithly Jr WR, Overstreet RM, Roberts KJ, Valverde RA, Würsig B (2017) Habitats and biota of the Gulf of Mexico: Before the Deepwater Horizon oil spill. Volume 2. Ward CH, editor. New York, Springer:869-1757

Brunnschweiler JM, Andrews PLR, Southall EJ, Pickering M, Sims DW (2005) Rapid voluntary stomach eversion in a free-living shark. Journal of the Marine Biological Association of the United Kingdom 85:1141-1144. doi:10.1017/S0025315405012208

Burkett RD, Jackson WB (1971) The eye lens as an age indicator in freshwater drum. The American Midland Naturalist 85(1): 222-225.

Campana SE (1999) Chemistry and composition of fish otoliths: pathways, mechanisms and applications. Marine Ecology Progress Series 188:263–297.

Caut S, Angulo E, Courchamp F (2009) Variation in discrimination factors ($\Delta^{15}N$ and $\Delta^{13}C$): the effect of diet isotopic values and applications for diet reconstruction. Journal of Applied Ecology 46:443-453.

Chikaraishi Y, Kashiyama Y, Ogawa NO, Kitazato H, Ohkouchi N (2007) Metabolic control of nitrogen isotope composition of amino acids in macroalgae and gastropods: implications for aquatic food web studies. Marine Ecology Progress Series 342:85-90.

Chikaraishi Y, Ogawa NO, Kashiyama Y, Takano Y, Suga H, et al. (2009) Determination of aquatic food-web structure based on compound-specific nitrogen isotopic composition of amino acids. Limnology and Oceanography: Methods 7:740-750.

Chikaraishi Y, Ogawa NO, Ohkouchi N (2010) Further evaluation of the trophic level estimation based on nitrogen isotopic composition of amino acids. In Earth, Life and Isotopes: Kyoto University Press: Kyoto, Japan 415: 37-51.

Chikaraishi Y, Steffan SA, Takano Y, Ohkouchi N (2015) Diet quality influences isotopic discrimination among amino acids in an aquatic vertebrate. Ecology and Evolution 5(10):2048-2059. doi:10.1002/ece3.1491

Clements KD, Raubenheimer D, Choat JH (2009) Nutritional ecology of marine herbivorous fishes: ten years on. Functional Ecology 23:79-92. doi: 10.1111/j.1365-2435.2008.01524.x

Corr LT, Berstan R, Evershed RP (2007) Optimisation of derivatization procedures for the determination of $\delta^{13}C$ values of amino acids by gas chromatography/combustion/isotope ratio mass spectrometry. Rapid Communications in Mass Spectrometry 21:3759-3771.

Cummings NJ, McClellan DB (1996) Movement patterns and stock interchange of Greater Amberjack, Seriola dumerili in the southeastern U.S. Miami, Florida: National Marine Fisheries Service

Curtis JSC (2016) Resource use overlap in native grouper and invasive lionfish. Masters thesis, University of South Florida, Tampa, FL.

Dahm R (1999) Lens fibre cell differentiation—a link with apoptosis? Ophthalmic Res 31(3): 163-183.

Dahm R, Schonthaler HB, Soehn AS, van Marle J, Vrensen GFJM (2007) Development and adult morphology of the eye lens in the zebrafish. Experimental Eye Research 85(1): 74–89.

Dale JJ, Wallsgrove NJ, Popp BN, Holland KN (2011) Nursery habitat use and foraging ecology of the brown stingray *Dasyatis lata* determined from stomach contents, bulk and amino acid stable isotopes. Marine Ecology Progress Series 433: 221-236. doi:10.3354/meps09171

Dalerum F, Angerbjörn A (2005) Resolving temporal variation in vertebrate diets using naturally occurring stable isotopes. Oecologia 144:647-658.

Dance MA, Rooker JR (2019) Cross-shelf habitat shifts by red snapper (Lutjanus campechanus) in the Gulf of Mexico. PLoS ONE 14(3):e0213506. doi:10.1371/jounal.pone.0213506

de Busserolles F, Fitzpatrick JL, Paxton JR, Marshall NJ, Collin SP (2013) Eye-Size Variability in Deep-Sea Lanternfishes (*Myctophidae*): An Ecological and Phylogenetic Study. PLoS ONE 8(3): e58519. doi:10.1371/journal.pone.0058519

Deb D (1997) Uncertainty vs parsimony in food web research. Oikos 78(1):191-194.

Deegan LA (1993) Nutrient and energy transport between estuaries and coastal marine ecosystems by fish migration. Canadian Journal of Fisheries and Aquatic Sciences 50:74-79.

Del Castillo CE, Coble PG, Conmy RN, Muller-Karger FE, Vanderbloemen L, Vargo GA (2001) Multipectral in situ measurements of organic matter and chlorophyll fluorescence in seawater: Documenting the intrusion of the Mississippi River plume in the West Florida Shelf. Limnology and Oceanography 46(7): 1836-1843.

DeNiro M, Epstein S (1978) Influence of diet on the distribution of carbon isotopes in animals. Geochimica et Cosmochimica Acta 42:495-506

DeNiro M, Epstein S (1981) Influence of diet on the distribution of nitrogen isotopes in animals. Geochimica et Cosmochimica Acta 45:341-351

Dingle H, Drake VA (2007) What is migration? BioScience 57(2):113-121. doi:10.1641/B570206

Drew K, Die DJ, Arocha F (2006) Understanding vascularization in fin spines of White Marlin (*Tetrapturus albidus*). Bulletin of Marine Science 79: 847-852. doi:10.1007/s002270050258

Ellis G (2012) Compound-specific stable isotopic analysis of protein amino acids: Ecological applications in modern and ancient systems. Doctoral dissertation, University of South Florida, Tampa, FL.

Elsdon TS, Ayvazian S, McMahon KW, Thorrold SR (2010) Experimental evaluation of stable isotope fractionation in fish muscle and otoliths. Marine Ecology Progress Series 408:195-205. doi:10.3354/meps08518

Estep MLF, Vigg S (1985) Stable carbon and nitrogen isotope tracers of trophic dynamics in natural-populations and fisheries of the Lahontan lake system, Nevada. Canadian Journal of Fisheries and Aquatic Science 42: 1712-1719. doi:10.1139/f85-215

Estrada JA, Rice AN, Natanson LJ, Skomal GB (2006) Use of isotopic analysis of vertebrae in reconstructing ontogenetic feeding ecology in white sharks. Ecology 87(4): 829-834.

Ethier DM, Kyle CJ, Kyser TK, Nocera JJ (2010) Variability in the growth patterns of the cornified claw sheath among vertebrates: implications for using biogeochemistry to study animal movement. Canadian Journal of Zoology 88:1043-1051.

Fable Jr WA, Trent L, Bane GW, Ellsworth SW (1989) Movements of King Mackerel, Scomberomorus cavalla, tagged in southeast Louisiana, 1983-85. Marine Fisheries Review 49(2):98-101

Fallows C, Gallagher AJ, Hammerschlag N (2013) White Sharks (Carcharodon Carcharias) scavenging on whales and its potential role in further shaping the ecology of an apex predator. PLoS ONE 8(4):e.60797. doi:10.1371/journal.pone.0060797

Fantle MS, Dittel AI, Schwalm SM, Epifanio CE, Fogel ML (1999) A food web analysis of the juvenile blue crab, *Callinectes sapidus*, using stable isotopes in whole animals and individual amino acids. Oecologia 120, 416-426.

Finlay JC and Kendall C (2007) Stable tracing of temporal and spatial variability in organic matter sources to freshwater ecosystems. In: Michener R and Lajtha K, editors. Stable isotopes in ecology and environmental science. Blackwell: Oxford. pp. 283-324.

Fisher JP, Pearcy WG (1990) Spacing of scale circuli versus growth rate in young coho salmon. Fisheries Bulletin 88: 637-643. doi:10.1023/A:1007372832213

Fisk AT, Hobson KA, Norstrom RJ (2001) Influence of chemical and biological factors on trophic transfer of persistent organic pollutants in the Northwater Polynya marine food web. Environmental Science and Technology 35:732-738.

Fitzhugh GR, Koenig CC, Coleman FC, Grimes, CB, Sturges W (2005) Spatial and temporal patterns in fertilization and settlement of young gag (Mycteroperca microlepis) along the West Florida Shelf. Bulletin of Marine Science 77(3): 377-396.

Fouda MM (1979) Studies on scale structure in the Common goby, *Pomatoschistus microps* (Pisces). Journal of Zoology 189: 503-522.

Fry B (1988) Food web structure on Georges Bank from stable C, N, and S isotopic compositions. Limnology and Oceanography 33(5):1182-1190.

Fry B, Arnold C (1982) Rapid C-13/C-12 turnover during growth of brown shrimp (*Penaeus aztecus*). Oecologia 54(2): 200-204.

Fry B, Sherr EB (1984) $\delta^{13}C$ measurements as indicators of carbon flow in marine and freshwater ecosystems. Contributions in Marine Science 27:13-48.

Germain LR, Koch PL, Harvey J, McCarthy MD (2013) Nitrogen isotope fractionation in amino acids from harbor seals: implications for compound-specific trophic position calculations. Marine Ecology Progress Series 482: 265-277. doi:10.3354/meps10257

Gillanders BM, Kingsford MJ (2000) Elemental fingerprints of otoliths of fish may distinguish estuarine 'nursery' habitats. Marine Ecology Progress Series 201: 273-286. doi:10.3354/meps201273

Gold JR, Sun F, Richardson LR (1997) Population structure of Red Snapper from the Gulf of Mexico as inferred from analysis of mitochondrial DNA. Transactions of the American Fisheries Society 126:386-396.

Graham BS, Koch PL, Newsome SD, McMahon WK, Aurioles D (2010) Using isoscapes to trace the movements and foraging behavior of top predators in oceanic ecosystems. In: West JB, Bowen GJ, Dawson TE, Tu KP, editors. Isoscapes: Understanding movement, pattern, and process on Earth through isotope mapping. New York: Springer. pp.299-318.

Granneman, J.E. (2018) Evaluation of trace-metal and isotopic records as techniques for tracking lifetime movement patterns in fishes. Doctoral dissertation, University of South Florida, Tampa, FL.

Haché S, Hobson KA, Bayne EM, Van Wilgenburg SL, Villard MA (2014) Tracking natal dispersal in a coastal population of a migratory songbird using feather stable isotope ($\delta^{2}H$, $\delta^{34}S$) tracers. PLoS ONE. doi: 10.1371/journal.pone.0094437

Haines EB, Montague CL (1979) Food sources of estuarine invertebrates analyzed using 13C/12C ratios. Ecology 60(1): 48-56.

Hairston Jr NG, Hairston Sr NG (1993) Cause-effect relationships in energy flow, trophic structure, and interspecific interactions. The American Naturalist 142(3):379-411.

Harper A, Landing W, Chanton JP (2018) Controls on the variation of methylmercury concentration in seagrass bed consumer organisms of the Big Bend, Florida, USA. Estuaries and Coasts. doi:10.1007/s12237-017-0355-6

Harris PJ, Wyanski DM, White DB, Mikell PP (2007) Age, growth, and reproduction of Greater Amberjack off the southeastern U.S. Atlantic coast. Transactions of the American Fisheries Society 136:1534-1545. doi:10.1577/T06-113.1

Huelster, S.A. (2015) Comparison of isotope-based biomass pathways with groundfish community structure in the eastern Gulf of Mexico. Master's thesis, University of South Florida, Tampa, FL.

Hill KT, Cailliet GM, Radtke RL (1989) A comparative analysis of growth zones in four calcified structures of Pacific Blue Marline, Makaira nigricans. Fisheries Bulletin 87:829-843. doi:10.1007/s12237-009-9134-3

Hobson KA (1999a) Tracing origins and migration of wildlife using stable isotopes: a review. Oecologia 120:314-326.

Hobson KA (1999b) Stable-carbon and nitrogen isotope ratios of songbird feathers grown in two terrestrial biomes: Implications for evaluating trophic relationships and breeding origins. Condor 101(4):799-805.

Hobson KA (2008) Applying isotopic methods to tracking animal movements. In: Hobson KA and Wassenaar LI, editors. Tracking Animal Migration with Stable Isotopes. Elsevier. pp 45-78.

Hobson KA, Barnett-Johnson R, Cerling T (2010) Using isoscapes to track animal migration. In: West JB, Bowen GJ, Dawson TE, Tu KP, editors. Isoscapes: Understanding movement, pattern, and process on Earth through isotope mapping. New York: Springer. pp. 273-298.

Hobson KA, Clark RG (1992a) Assessing avian diets using stable isotopes I: Turnover of 13C in tissues. Condor 94(1): 181-188.

Hobson KA, Clark RG (1992b) Assessing avian diets using stable isotopes II: Factors influencing diet-tissue fractionation. Condor 94(1): 189-197.

Hobson KA and Norris DR (2008) Animal migration: A context for using new techniques and approaches. In: Hobson KA and Wassenaar LI, editors. Tracking Animal Migration with Stable Isotopes. Elsevier. pp 1-19.

Hobson KA, Piatt JF, Pitocchelli J (1994) Using stable isotopes to determine seabird trophic relationships. Journal of Animal Ecology 63(4):786-798.

Horwitz J (2003) Alpha-crystallin. Experimental Eye Research 76(2): 145-153.

Hunsicker ME, Essington TE, Aydin KY, Ishida B (2010) Predatory role of the commander squid *Berryteuthis magister* in the eastern Bering Sea: Insights from stable isotopes and food habits. Marine Ecology Progress Series 415: 91-108.

Hussey NE, MacNeil MA, McMeans BC, Olin JA, Dudley SFJ, Cliff G, Winter SP, Fennessy ST, Fisk AT (2014) Rescaling the trophic structure of marine food webs. Ecology Letters 17: 239-250. doi:10.1111/ele.12226

Hutchinson JJ, Trueman CN (2006) Stable isotope analyses of collagen in fish scales: limitations set by scale architecture. Journal of Fish Biology 69:1874–1880.

Hyslop EJ (1980) Stomach contents analysis-a review of methods and their application. Journal of Fish Biology 17: 411-429.

Jones CM (1986) Determining age of larval fish with the otolith increment technique. Fisheries Bulletin 84:91-103.

Kaiser FE, Gehrke GW, Zumwalt RQ, Kuo KC (1974) Amino acid analysis: Hydrolysis, ion-exchange cleanup, derivatization, and quantitation by gas-liquid chromatography. Journal of Chromatography A 94: 113-133.

Karpouzi VS, Stergiou KI (2003) The relationships between mouth size and shape and body length for 18 species of marine fishes and their trophic implications. Journal of Fish Biology 62:1353-1365.

Kerr LA, Andrews AH, Cailliet GM, Brown TA, Coale KH (2006) Investigations of $\Delta^{14}C$, $\delta^{13}C$, and $\delta^{15}N$ in vertebrae of white shark (*Carcharodon carcharias*) from the eastern North Pacific Ocean. Environ Biol Fishes 77(3-4): 337-353.

Kurth BN, Peebles EB, Stallings CD (2019) Atlantic Tarpon (*Megalops atlanticus*) exhibit upper estuarine habitat dependence followed by foraging system fidelity after ontogenetic habitat shifts. Estuarine, Coastal, and Shelf Science 225. doi:10.1016/j.ecss.2019.106248

Lima ARA, Barletta M, Dantas DV, Possato RE, Ramos JAA, Costa MF (2012) Early development and allometric shifts during the ontogeny of a marine catfish (*Cathorops spixii-Ariidae*). Journal of Applied Ichthyology 28: 217-225. doi:10.1111/j.1439-0426.01903.x

Manooch III CS (1979) Recreational and commercial fisheries for king mackerel *Scombermorus cavalla*, in the south Atlantic Bight and Gulf of Mexico, USA. Proceedings of the Mackerel Colloquium. pp. 33-41

Manooch III CS, Naughton SP, Grimes CB, Trent L (1987) Age and growth of King Mackerel, Scombermorus cavalla, from the U.S. Gulf of Mexico. Marine Fisheries Review 49(2):102-108.

Manooch III CS, Potts JC (1997) Age, growth, and mortality of Great Amberjack, Seriola Dumerili, from the U.S. Gulf of Mexico headboat fishery. Bulletin of Marine Science 61(3):671-683.

Martinez del Rio C, Wolf N, Carleton SA, Gannes LZ (2009) Isotopic ecology ten years after a call for more laboratory experiments. Biological Review 84:91-111.

Martinez del Rio C, Carleton SA (2012) How fast and how faithful: the dynamics of isotopic incorporation into animal tissues. Journal of Mammalogy 93(2):353-359.

McCawley JR, Cowan Jr JH (2007) Seasonal and size specific diet and prey demand of Res Snapper on Alabama artificial reefs. American Fisheries Society Symposium 60:77-104.

McClellan DB, Cummings NJ (1997) Preliminary analysis of tag and recapture data of the Greater Amberjack, Seriola dumerili, in the southeastern United States. Proceedings of the 49th Gulf and Caribbean Fisheries Institute. 25-45 p.

McClelland JW, Montoya JP (2002) Trophic relationships and the nitrogen isotopic composition of amino acids in plankton. Ecology 83:2173

McCutchan JH, Lewis WM, Kendall C, McGrath CC (2003) Variation in trophic shift for stable isotope ratios of carbon, nitrogen, and sulfur. Oikos 102:378-390.

McMahon KW, Hamady LL, Thorrold SR (2013) Ocean ecogeochemistry: a review. Oceanography and Marine Biology: An Annual Review 51:327-373.

McMahon KW and McCarthy MD (2016) Embracing variability in amino acid d15N fractionation: mechanisms, implications, and applications for trophic ecology. Ecosphere 7(12): e01511. doi:10.1002/ecs2.1511

McMahon KW, Thorrold SR, Elsdon TS, McCarthy MD (2015) Trophic discrimination of nitrogen stable isotopes in amino acids varies with diet quality in marine fish. Limnology and Oceanography 60:1076-1087.

Michener R and Lajtha J (2007) Stable isotopes in ecology and environmental science. Blackwell: Oxford. pp. 566.

Minagawa M, Wada E (1984) Stepwise enrichment of 15N along food chains: Further evidence and the relation between $\delta^{15}N$ and animal age. Geochimica et Cosmochimica Acta 48:1135-1140.

Mulholland MR, Bernhardt PW, Heil CA, Bronk DA, O'Neil JM (2006) Nitrogen fixation and release of fixed nitrogen by *Trichodesmium* spp. In the Gulf of Mexico. Limnology and Oceanography 51:1762–1776.

Murawski SA, Peebles EB, Garcia A, Tunnell, Jr. JW and Armenteros M. (2018). Comparative abundance, species composition, and demographics of continental shelf fish assemblages throughout the Gulf of Mexico. Marine and Coastal Fisheries 10:325-346.

Murdoch WW (1969) Switching in general predators: Experiments on predator specific and stability of prey populations. Ecological Monographs 39(4): 335-354.

Murie DJ, Parkyn DC (2008) Age, growth, and sex maturity of Greater Amberjack (Seriola dumerili) in the Gulf of Mexico. SEDAR33-RD13. SEDAR, North Charleston, SC. 41 pp.

Nelson TC, Doukakis P, Lindley ST, Schreier AD, Hightower JE, Hildebrand LR, Whitlock RE, Webb MAH (2013) Research tools to investigate movements, migrations, and life history of sturgeons (*Acipenseridae*), with an emphasis on marine-oriented populations. PLoS ONE 8(8): e71552. doi:10.1371/journal.pone.0071552

Nerot C, Lorrain A, Grall J, Gillikin DP, Munaron JM, Le Bris H, Paulet YM (2012) Stable isotope variations in benthic filter feeders across a large depth gradient on the continental shelf. Estuarine, Coastal and Shelf Science 96: 228-235.

Newsome SD, Martinez del Rio C, Bearhop S, Phillips DL (2007) A niche for isotopic ecology. Frontiers in Ecology and the Environment 5(8): 429-436. doi:10.1890/060150.01

Newsome et al. (2015) Multi-tissue δ^2H analysis reveals altitudinal migration and tissue-specific discrimination patterns in *Cinclodes*. Ecosphere 6(11):213. doi:10.1890/ES15-00086.1

Nicol JAC (1989) The eyes of fishes. Oxford: Oxford University Press. 308p.

Nielsen JM, Clare EL, Hayden B, Brett MT, Kratina P (2015) Diet tracing in ecology: Method comparison and selection. Methods in Ecology and Evolution 9: 278-291. doi:10.1111/2041-210X.12869

O'Brien DM, Fogel ML, Boggs CL (2002) Renewable and non-renewable resources: amino acid turnover and allocation to reproduction in Lepidoptera. Proceedings of the National Academy of Sciences of the United States of America 99:4413-4418.

Olson RJ, Popp BN, Graham BS, Lapez-Ibarra GA, Galvan-Maga F, Lennert-Cody CE, Bocanegra-Castillo N, Wallsgrove NJ, Gier E, Ramirez VA, Balance LT, Fry B (2010) Food-web inferences of stable isotope spatial patterns in copepods and yellowfin tuna in the pelagic eastern Pacific Ocean. Progress in Oceanography 86(1):124-138

Ortiz M, Andrew KI (2008) Updated estimates of Gulf King Mackerel bycatch from the U.S. Gulf of Mexico shrimp trawl fishery. SEDAR16-AW07.

Paine RT (1988) Food webs: Road maps of interactions or grist for theoretical development? Ecology 69(6):1648-1654.

Parry MP (2003) The trophic ecology of two ommastrephid squid species, *Ommastrephes bartramii* and *Sthenoteuthis oualaniensis*, in the North Pacific sub-tropical gyre. Doctoral dissertation, University of Hawaii at Manoa.

Patterson III WF, Cowan Jr JH, Wilson CA, Shipp RL (2001) Age and growth of red snapper, Lutjanus campechanus, from an artificial reef area off Alabama in the northern Gulf of Mexico. Fisheries Bulletin 99(4):617-627.

Peebles EB, Hollander DJ (2020) Combining isoscapes with tissue-specific isotope records to recreate the geographic histories of fish. In Murawski SA et al. (eds.) Scenarios and Responses to Future Deep Oil Spills, Springer, p. 203-218. doi:10.1007/978-3-030-12963-7_12

Peterson BJ, Fry B (1987) Stable isotopes in ecosystem studies. Annual Review of Ecology, Evolution, and Systematics 18:293-320.

Phelps QE, Whitledge GW, Tripp SJ, Smith KT, Garvey JE, Herzog DP, Ostendorf DE, Ridings JW, Crites JW, Hrabik, Doyle WJ, Hill TD (2012) Identifying river of origin for age-0 *Scaphirhynchus* sturgeons in the Missouri and Mississippi rivers using fin ray microchemistry. Canadian Journal of Fisheries and Aquatic Science 69:930-941.

Phillips RA, Bearhop S, Mcgill RAR, Dawson DA (2009) Stable isotopes reveal individual variation in migration strategies and habitat preferences in a suite of seabirds during the nonbreeding period. Oecologia 160:795-806. doi:10.1007/s00442-009-1342-9

Phillips DL, Eldridge PM (2006) Estimating the timing of diet shifts using stable isotopes. Oecologia 147(2): 195-203.

Pierce DJ, Mahmoudi B (2001) Nearshore fish assemblages along the central west coast of Florida. Bulletin of Marine Science 68(2):243-270.

Ponsard S, Averbuch P (1999) Should growing and adult animals fed on the same diet show different $\delta^{15}N$ values? Rapid Communications in Mass Spectrometry 13: 1305-1310.

Popp BN, Graham BS, Olson RJ, Hannides CCS, Lott MJ, Lopez-Ibarra GA, Galvan-Magana F, Fry B (2007) Insight into the trophic ecology of Yellowfin Tuna, *Thunnus albacares*, from compound-specific nitrogen isotope analysis of proteinaceous amino acids. Terrestrial Ecology 1: 173-190.

Post DM (2002) Using stable isotopes to estimate trophic position: Models, methods, and assumptions. Ecology 83(3): 703–718.

Post DM, Layman CA, Arrington DA, Takimoto G, Quattrochi J, Montaña CG (2007) Getting to the fat of the matter: models, methods and assumptions for dealing with lipids in stable isotope analyses. Oecologia 152:179-189.

Post DM , Pace ML, Hairston Jr NG (2000) Ecosystem size determines food-chain length in lakes. Nature 405:1047-1049.

Quaeck-Davies K, Vendall VA, MacKenzie KM, Hetherington S, Newton J, Trueman CN (2018) Teleost and elasmobranch eye lenses as a target for life-history stable isotope analyses. PeerJ: e4883. doi:10.7717/peerj.4883

Rabalais NN, Turner RE, Justice D, Dortch Q, Wiseman WJ, Sen Gupta BK (1996) Nutrient changes in the Mississippi River and system responses on the adjacent continental shelf. Estuaries 19: 386-407.

Radabaugh KR, Hollander DJ, Peebles EB (2013) Seasonal $\delta^{13}C$ and $\delta^{15}N$ isoscapes of fish populations along a continental shelf trophic gradient. Continental Shelf Research 68: 112–121.

Radabaugh KR, Malkin EM, Hollander DJ, Peebles EB (2014) Evidence for light-environment control of carbon isotope fractionation by benthic microalgal communities. Marine Ecology Progress Series 495:77-90.

Radabaugh KR, Peebles EB (2014) Multiple regression models of $\delta^{13}C$ and $\delta^{15}N$ for fish populations in the eastern Gulf of Mexico. Continental Shelf Research 84: 158–168.

Ramos R, Gonzalez-Solis J (2012) Trace me if you can: the use of intrinsic biogeochemical markers in marine top predators. Frontiers in Ecology and the Environment 10(5):258-266. doi:10.1890/110140

Rieutord (1999) Physiologie animale, vol 2. Les grandes fonctions. Masson, Paris

Rooney N, McCann K, Gellner G, Moore JC (2006) Structural asymmetry and the stability of diverse food webs. Nature 442: 265-269. doi:10.1038/nature04887

Roth JD, Hobson KA (2000) Stable carbon and nitrogen isotopic fractionation between diet and tissue of captive red fox: implications for dietary reconstruction. Canadian Journal of Zoology 78:848-852.

Rounick JS, Winterbourn MJ (1986) Stable carbon isotopes and carbon flow in ecosystems. BioScience 36:171-177.

Schofield G, Hobson VJ, Fossette S, Lilley MKS, Katselidis KA, Hays GC (2010) Fidelity to foraging sites, consistency of migration routes and habitat modulation of home range by sea turtles. Diversity and Distributions 16:840-853.

Seminoff JA, Benson SR, Arthur KE, Eguchi T, Dutton PH, Tapilatu RF, Popp BN (2012) Stable isotope tracking of endangered sea turtles: Validation with satellite telemetry and $\delta^{15}N$ analysis of amino acids. PLoS ONE 7(5): e37403. doi:10.1371/journal.pone.0037403

Sharma KK, Santhoshkumar P (2009) Lens aging: Effects of crystallins. Biochimica et Biophysica Acta 1790(10):1095-1108.

Sharp Z (2007) Principles of Stable Isotope Geochemistry. Pearson Prentice Hall, Upper Saddle River, NJ. p.344.

Sheppard KE, Patterson III WF, DeVries DA, Ortiz M (2010) Contemporary versus historical estimates of King Mackerel (*Scomberomorus cavalla*) age and growth in the U.S. Atlantic Ocean and Gulf of Mexico. Bulletin of Marine Science 86(3):515-532.

Schoeninger MJ, DeNiro MJ, Tauber H (1983) Stable nitrogen isotope ratios of bone collagen reflect marine and terrestrial components of prehistoric human diet. Science 220(4606):1381-1383.

Siezen RJ (1989) Eye lens aging in the spiny dogfish (*Squalus acanthias*): 1. Age-determination from lens weight. Current Eye Research 8(7):707-712.

Silfer JA, Engel MH, Macko SA, Jumeau EJ (1991) Stable carbon isotope analysis of amino acid enantiomers by conventional isotope ratio mass spectrometry and combined gas chromatography/isotope ratio mass spectrometry. Analytical Chemistry 63(4):370-274.

Simpson SJ, Sims DW, Trueman CN (2019) Ontogenetic trends in resource partitioning and trophic geography of sympatric skates (*Rajidae*) inferred from stable isotope composition across eye lenses. Marine Ecology Progress Series 624:103-116. doi:10.3354/meps13030

Sims DW, Andrews PLR, Young JZ (2000) Stomach rinsing in rays. Nature 404:566

Smith KT (2010) Evaluation of fin ray and fin spine chemistry as indicators of environmental history for five fish species. Maters thesis. Southern Illinois University Carbondale. doi:10.1387/ijdb.15272389

Sobolevsky TG, Revelsky AI, Miller B, Oriedo V, Chernetsova ES, Revelsky IA (2003) Comparison of silylation and esterification/acylation procedures in GC-MS analysis of amino acids. Journal of Separation Science 26:1474-1478.

Strelcheck AJ, Cowan Jr JH, Patterson WF (2007) Site fidelity, movement, and growth of Red Snapper: Implications for artificial reef management. American Fisheries Society Symposium 60:147-162.

Stoner AW, Zimmerman RJ (1988) Food pathways associated with penaeid shrimps in a mangrove-fringed estuary. Fishery Bulletin 86(3):543-551.

Suresh Babu VV, Vasanthakumar GR, Tantry SJ (2005) N-silylation of amines and amino acid esters under neutral conditions employing TMS-Cl in the presence of zinc dust. Tetrahedron Letters 46:4099-4102.

Sutherland DF, Fable WA (1980) Results of a King Mackerel (*Scomberomorus cavalla*) and Atlantic Spanish Mackerel (*Scombermorus maculatus*) migration study, 1975-79. NOAA Technical Memorandum NMFS-SEFC-12.

Szedlmayer ST, Shipp RL (1994) Movement and growth of Red Snapper, Lutjanus campechanus, from and artificial reef area in the northeastern Gulf of Mexico. Bulletin of Marine Science 55:887-896.

Thompson RC, Ballou JE (1956) Studies of metabolic turnover with tritium as a tracer: V. The predominantly non-dynamic state of body constituents in the rat. J Biol Chem 223(2): 795-809.

Thorrold SR, Campana SE, Jones CM, Swart PK (1997) Factors determining $\delta^{13}C$ and $\delta^{18}O$ fractionation in aragonitic otoliths of marine fish. Geochimica et Cosmochimica Acta 61(14):2909-2919.

Tieszen LL, Boutton TW, Tesdahl KG, Slade NA (1983) Fractionation and turnover of stable carbon isotopes in animal tissues: implications for $\delta^{13}C$ analysis of diet. Oecologia 57(1-2): 32-37.

Trueman CN, Moore A (2007) Use of the stable isotope composition of fish scales for monitoring aquatic ecosystems. In: Dawson TE, Siegwolf RTW, (eds.) Terrestrial Ecology Volume1.

Tzadik OE, Goddard EA, Hollander DJ, Koenig CC, Stallings CD (2015) Non-lethal approach identified variability of $\delta^{15}N$ values in the fin rays of Atlantic Goliath Grouper, *Epinephelus itajara*. PeerJ 3:e1010. doi:10.7717/peerj.1010

Tzadik OE, Curtis JS, Granneman JE, Kurth BN, Pusack TJ, Wallace AA, Hollander DJ, Peebles EB, Stallings CD (2017) Chemical archives in fishes beyond otoliths: A review on the use of other body parts as chronological recorders of microchemical constituents for expanding interpretations of environmental, ecological, and life-history changes. Limnology and Oceanography: Methods 15:238-263. doi:10.1038/nature04887

Vander Zanden MJ, Rasmussen JB (1999) Primary consumer $\Delta^{13}C$ and $\Delta^{15}N$ and the trophic position of aquatic consumers. Ecology 80:1395-1404.

Vanderklift MA, Ponsard S (2003) Sources of variation in consumer-diet d15N enrichment: a meta-analysis. Oecologia 136:169-182. doi:10.1007/s00442-1270-z

Vihtelic TS (2008) Teleost lens development and degeneration. Int Rev Cell Mol Biol 269: 341-373.

Wainwright SC, Fogarty MJ, Greenfield RC, Fry B (1993) Long-term changes in the Georges Bank food web: Trends in stable isotopic compositions of fish scales. Marine Biology 115:481-493

Walker JL, Macko SA (1999) Dietary studies of marine mammals using stable carbon and nitrogen isotopic ratios of teeth. Marine Mammal Science 15(2): 314-334.

Wallace AA, Hollander DJ, Peebles EB (2014) Stable Isotopes in fish eye lenses as potential recorders of trophic and geographic history. PLoS ONE 9(10): e108935. doi:10.1371/journal.pone.0108935

Walsh RG, Shaoneng H, Yarnes CT (2014) Compound-specific $\delta^{13}C$ and $\delta^{15}N$ analysis of amino acids: a rapid, chloroformate-based method for ecological studies. Rapid Communication in Mass Spectrometry 28: 96-108.

Wassenaar LI, Van Wilgenburg SL, Larson K, Hobson KA (2009) A groundwater isoscape (δD, $\delta^{18}O$) for Mexico. Journal of Geochemical Exploration 102: 123-136.

Watterson JC, Patterson III WF, Shipp RL, Cowan JH (1998) Movement of Red Snapper, Lutjanus campechanus, in the north central Gulf of Mexico: Potential effects of hurricanes. Gulf of Mexico Science 16:92-104. doi:10.18785/goms.1601.13

Wells RJ, Cowan Jr JH, Fry B (2008) Feeding ecology of red snapper Lutjanus campechanus in the northern Gulf of Mexico. Marine Ecology Progress Series 361: 213-225.

Werry JM, Lee SY, Otway NM, Hu Y, Sumpton W (2011) A multi-faceted approach for quantifying the estuarine-nearshore transition in the life cycle of the bull shark, Carcharhinus leucas. Marine and Freshwater Research 62(12): 1421-1431.

West JB, Bowen GJ, Dawson TE (2010) Preface: Context and background for the topic and book. In: West JB, Bowen GJ, Dawson TE, Tu KP, editors. Isoscapes: Understanding movement, pattern, and process on Earth through isotope mapping. New York: Springer. pp. v-xi.

Whitfield AK (1990) Life-history styles of fishes in South African estuaries. Environmental Biology of Fishes 28:295-308.

Whiteman JP, Elliott Smith EA, Besser AC, Newsome SD (2019) A guide to using compound-specific stable isotope analysis to study the fates of molecules in organisms and ecosystems. Diversity 11(8). doi:10.3390/d11010008

Woodcock SH, Walther BD (2014) Trace elements and stable isotopes in Atlantic tarpon scales reveal movements across estuarine gradients. Fisheries Research 153:9–17.

Wride MA (2011) Lens fibre cell differentiation and organelle loss: many paths lead to clarity. Philosophical Transactions of the Royal Society of London B: Biological Sciences 366:1219-1233. doi:10.1098/rstb.2010.0324

Appendix A-Data analyzed

Table A.1 Catch data and metadata for Tables A.2, A.3, and A.4.

Fish ID	Capture Date	Sex	Standard Length (cm)	Fork Legth (cm)	Total Length (cm)
4-40-002	14 Aug 2014	M	55	—	63
4-40-003	14 Aug 2014	F	59	—	69
4-40-006	14 Aug 2014	M	54	—	62
4-40-019	14 Aug 2014	M	59	—	68
4-40-021	14 Aug 2014	M	56	—	65
8-40-003	16 Aug 2014	M	38	—	44
8-40-008	16 Aug 2014	F	41	—	47
8-40-012	16 Aug 2014	M	47	—	53
8-40-019	16 Aug 2014	F	42	—	49
8-40-023	16 Aug 2014	M	51	—	58
KM 2	13 Apr 2016	F	57.7	63.5	78.1
KM 3	01 Dec 2015	M	67.9	73.7	82.9
KM 4	01 Dec 2015	F	60.3	65.4	73.7
KM 6	22 Apr 2016	F	83.1	88.9	104.1
AJ 1	20 Aug 2013	M	87	91	—
AJ 2	20 Aug 2013	F	84	89	—

TP_{CSIA}	Trophic position calculated using Bradley et al. (2015) equation.TL=[(Glu-Phe-β)/TDF]+1. TDF=5.7; β=3.6
Bulk $\delta^{15}N$	Bulk stable isotope measurements. Blank values did not have enough material for analysis after AA-CSIA
Bulk $\delta^{13}C$	Bulk stable isotope measurements. Blank values did not have enough material for analysis after AA-CSIA
Trophic Growth (Generic)	Trophic positions interpolated by the species regression in Table 4.1.
Trophic Growth (Specific)	Trophic positions interpolated by the individual specific regressions in Table 4.1.
GV Nitrogen	Trophic positions calculated by CSIA multiplied by bulk TDF for nitrogen and subtracted from Bulk $\delta^{15}N$; Bulk^{15}N-(3.4*(TL-1))
Nitrogen GV normalized	Nitrogen GV normalized to the sample collection point
GV Carbon	Trophic positions calculated by CSIA multiplied by bulk TDF for nitrogen and subtracted from Bulk $\delta^{13}C$; Bulkδ^{13}C-(1*(TL-1))
Carbon GV normalized	Carbon GV normalized to the sample collection point

Table A.2 Red Snapper

Sample ID	Lens Radial Midpoint (mm)	Estimated Standard Length	Alanine	Glycine	Valine	Leucine	Isoleucine	Threonine	Proline	Serine	Aspartic Acid	Methionine	Glutamic Acid	Phenylalanine	TP_{CSIA}	Bulk $\delta^{15}N$	Bulk $\delta^{13}C$	Trophic Growth Regression (Generic)	Trophic Growth Regression (Specific)	GV_{CSIA} Nitrogen	Nitrogen IM	Trophic Corrected Carbon	Carbon IM
SL4-40-002 AA1	0.275	3.2	12.37	2.62	17.17	16.48	13.76	-13.50	10.45	2.03	11.83	5.65	14.65	-1.80	3.25			2.87	3.15				
SL4-40-002 AA2	0.625	7.2	11.80	-0.14	14.93	16.10	15.30	-10.30	10.08	5.90	12.75	5.80	15.04	-0.85	3.16			3.05	3.20				
SL4-40-002 AA3	0.775	8.9														9.57	-17.23	3.11	3.22	2.00	1.33	-19.46	1.27
SL4-40-002 AA4	0.900	10.3														9.70	-17.27	3.16	3.24	2.07	1.40	-19.51	1.21
SL4-40-002 AA5	1.025	11.7														9.68	-17.25	3.21	3.26	1.99	1.32	-19.51	1.21
SL4-40-002 AA6	1.175	13.5	14.63	2.25	15.73	16.66	12.84	-15.10	13.30	8.51	13.54	7.22	16.98	0.92	3.19			3.26	3.28				
SL4-40-002 AA7	1.375	15.8														10.29	-17.43	3.32	3.31	2.43	1.76	-19.74	0.99
SL4-40-002 AA8	1.625	18.6														10.58	-17.78	3.40	3.35	2.61	1.94	-20.13	0.60
SL4-40-002 AA9	1.825	20.9														11.21	-18.24	3.46	3.37	3.14	2.47	-20.62	0.11
SL4-40-002 AA10	2.000	22.9	16.29	0.17	20.46	19.05	16.90	-18.75	16.70	14.66	15.37	8.70	20.10	2.37	3.48	11.64	-18.40	3.50	3.40	3.49	2.81	-20.80	-0.07
SL4-40-002 AA11	2.150	24.6														11.55	-17.99	3.54	3.42	3.33	2.66	-20.41	0.32
SL4-40-002 AA12	2.300	26.3														10.70	-17.03	3.58	3.44	2.41	1.74	-19.46	1.26
SL4-40-002 AA13	2.525	28.9														10.49	-16.45	3.64	3.47	2.10	1.42	-18.91	1.81
SL4-40-002 AA14	2.750	31.5	16.66	0.95	19.99	18.51	21.70	-19.33	15.26	13.92	15.42	9.03	19.71	2.26	3.43	10.61	-15.85	3.69	3.50	2.12	1.44	-18.35	2.38
SL4-40-002 AA15	3.050	34.9														10.65	-15.86	3.76	3.54	2.03	1.35	-18.39	2.33
SL4-40-002 AA16	3.375	38.7														11.54	-16.71	3.83	3.58	2.77	2.10	-19.29	1.44
SL4-40-002 AA17	3.875	44.4														11.90	-17.24	3.93	3.64	2.91	2.23	-19.88	0.85
SL4-40-002 AA18	4.875	55.8	19.21	-0.36	22.07	20.32	14.98	-19.82	13.05	14.42	16.83	9.79	21.45	1.93	3.79	10.09	-17.96	4.13	3.77	0.67	0.00	-20.73	0.00
SL4-40-003 AA1	0.275	3.5	19.30	5.29	19.97	20.48	18.94	-10.80	14.14	11.70	15.50	8.85	18.69	4.09	2.93			2.87	2.87				
SL4-40-003 AA2	0.625	7.9									17.30	10.00	19.20	4.74	2.91			3.05	2.93				
SL4-40-003 AA3	0.725	9.2														14.01	-16.63	3.09	2.95	7.38	6.06	-18.58	1.53
SL4-40-003 AA4	0.800	10.1														14.43	-16.54	3.12	2.96	7.76	6.44	-18.50	1.61
SL4-40-003 AA5	0.900	11.4														14.44	-16.91	3.16	2.98	7.71	6.39	-18.89	1.22
SL4-40-003 AA6	1.025	13.0														14.36	-17.00	3.21	3.00	7.55	6.23	-19.00	1.11
SL4-40-003 AA7	1.200	15.2	16.25	8.16	21.21	19.30	17.09	-9.10	16.85	14.45	17.76	10.53	21.18	6.22	2.99			3.27	3.03				
SL4-40-003 AA8	1.350	17.1														14.29	-17.35	3.32	3.06	7.28	5.96	-19.41	0.70
SL4-40-003 AA9	1.475	18.7														13.96	-17.09	3.35	3.08	6.87	5.55	-19.18	0.94
SL4-40-003 AA10	1.575	19.9														14.01	-16.63	3.38	3.10	6.87	5.54	-18.73	1.38
SL4-40-003 AA11	1.725	21.8														13.95	-16.34	3.43	3.13	6.71	5.39	-18.47	1.64
SL4-40-003 AA12	1.900	24.1	17.44	6.45	21.37	20.82	16.86	-11.00	18.10	12.53	17.91	10.67	21.33	5.71	3.11	13.64	-16.46	3.48	3.16	6.29	4.97	-18.63	1.49
SL4-40-003 AA13	2.025	25.6														13.32	-16.68	3.51	3.18	5.89	4.57	-18.86	1.25
SL4-40-003 AA14	2.175	27.5														13.32	-16.77	3.55	3.21	5.80	4.48	-18.98	1.13
SL4-40-003 AA15	2.350	29.8														12.64	-16.45	3.59	3.24	5.02	3.70	-18.69	1.42
SL4-40-003 AA16	2.525	32.0														12.80	-16.36	3.64	3.27	5.07	3.75	-18.64	1.47
SL4-40-003 AA17	2.725	34.5	20.43	3.83	23.79	23.09	26.65	-18.39	18.09	16.36	18.39	11.21	23.02	5.94	3.37	13.01	-16.17	3.68	3.31	5.15	3.83	-18.48	1.63
SL4-40-003 AA18	3.000	38.0														12.66	-16.32	3.75	3.36	4.63	3.31	-18.68	1.43
SL4-40-003 AA19	3.225	40.8														12.66	-16.33	3.80	3.40	4.49	3.17	-18.73	1.38
SL4-40-003 AA20	3.400	43.0														13.40	-16.35	3.83	3.43	5.13	3.80	-18.79	1.32
SL4-40-003 AA21	3.700	46.8														12.20	-17.03	3.90	3.49	3.74	2.42	-19.52	0.60
SL4-40-003 AA22	4.200	53.2														11.42	-17.44	4.00	3.58	2.66	1.33	-20.02	0.09
SL4-40-003 AA23	4.975	63.0	21.84	0.33	24.17	22.70	23.44	-22.80	7.71	15.26	18.34	18.68	23.24	4.15	3.72	10.57	-17.39	4.15	3.72	1.32	0.00	-20.11	0.00

Table A.2 continued

Sample ID	Lens Radial Midpoint (mm)	Estimated Standard Length	Alanine	Glycine	Valine	Leucine	Isoleucine	Threonine	Proline	Serine	Aspartic Acid	Methionine	Glutamic Acid	Phenylalanine	TPcsia	Bulk d15N	Bulk d13C	Trophic Growth Regression (Generic)	Trophic Growth Regression (Specific)	GVcsia Nitrogen	Nitrogen IM	Trophic Corrected Carbon	Carbon IM
SL4-40-006 AA2	0.325	3.8	16.47	3.43	13.54	15.62	8.32	-10.60	14.20	9.35	14.95	8.55	19.58	4.02	3.10			2.90	2.99				
SL4-40-006 AA3	0.725	8.6	13.13	5.68	18.49	20.24	14.89	-12.30	15.40	10.11	16.00	9.42	20.33	4.03	3.23			3.09	3.25				
SL4-40-006 AA4	0.875	10.3														12.96	-17.41	3.15	3.32	5.07	4.76	-19.73	0.20
SL4-40-006 AA5	1.000	11.8														13.07	-16.82	3.20	3.38	4.99	4.68	-19.20	0.73
SL4-40-006 AA6	1.150	13.6	17.44	4.25	20.44	19.32	17.62	-17.33	16.44	14.61	16.29	10.02	20.79	4.57	3.21			3.25	3.44				
SL4-40-006 AA7	1.350	15.9														10.84	-15.85	3.32	3.51	2.31	2.00	-18.35	1.58
SL4-40-006 AA8	1.550	18.3														11.93	-16.24	3.38	3.57	3.17	2.86	-18.81	1.12
SL4-40-006 AA9	1.800	21.3	19.41	4.75	22.84	21.63	17.89	-15.80	18.18	16.53	17.98	10.99	22.75	3.62	3.72	13.40	-16.12	3.45	3.65	4.39	4.08	-18.77	1.16
SL4-40-006 AA10	2.150	25.4														13.94	-15.75	3.54	3.75	4.60	4.29	-18.49	1.44
SL4-40-006 AA11	2.500	29.5														13.95	-15.98	3.63	3.83	4.32	4.01	-18.81	1.12
SL4-40-006 AA12	2.825	33.4	19.53	0.11	23.85	21.37	24.39	-23.00	18.90	17.60	18.15	10.40	22.69	2.02	3.99	12.76	-16.55	3.71	3.90	2.88	2.58	-19.45	0.48
SL4-40-006 AA13	3.150	37.2														11.93	-17.19	3.78	3.97	1.83	1.52	-20.16	-0.23
SL4-40-006 AA14	3.575	42.2														11.80	-16.90	3.87	4.05	1.42	1.11	-19.96	-0.03
SL4-40-006 AA15	4.550	53.7	20.31	-3.17	24.53	23.22	16.73	-26.70	15.40	18.50	18.40	11.40	23.80	2.03	4.19	11.26	-16.71	4.07	4.22	0.31	0.00	-19.93	0.00
SL4-40-019 AA1	0.300	3.7		2.57	19.83	16.79	13.72	-12.65	12.08	7.98	13.94	7.25	17.34	0.94	3.25			2.88	3.08				
SL4-40-019 AA2	0.725	9.0			18.34	15.67	12.14	-10.64	12.60	8.92	13.17	7.21	16.70	1.57	3.02			3.09	3.18				
SL4-40-019 AA3	0.925	11.4														10.29	-16.38	3.17	3.23	2.71	0.84	-18.61	1.44
SL4-40-019 AA4	1.050	13.0														10.67	-17.00	3.22	3.26	2.99	1.13	-19.25	0.79
SL4-40-019 AA5	1.175	14.5		4.01	15.37	17.55	16.26	-14.20	15.25	10.85	14.68	13.07	18.50	1.80	3.30			3.26	3.29				
SL4-40-019 AA6	1.300	16.1														10.57	-16.92	3.30	3.31	2.71	0.84	-19.23	0.82
SL4-40-019 AA7	1.425	17.6														10.98	-16.94	3.34	3.34	3.02	1.15	-19.29	0.76
SL4-40-019 AA8	1.575	19.5	18.95	5.19	20.96	19.37	21.14	-15.00	16.54	13.86	12.83	7.18	18.07	1.20	3.33	11.17	-16.73	3.38	3.37	3.09	1.23	-19.11	0.94
SL4-40-019 AA9	1.800	22.3														11.65	-16.10	3.45	3.42	3.41	1.54	-18.53	1.52
SL4-40-019 AA10	2.125	26.3														11.82	-16.07	3.54	3.49	3.35	1.48	-18.56	1.48
SL4-40-019 AA11	2.350	29.1														11.51	-16.34	3.59	3.54	2.88	1.01	-18.88	1.16
SL4-40-019 AA12	2.575	31.8	18.07	0.85	19.81	18.18	15.25	-18.90	17.02	12.49	15.51	8.82	20.25	1.89	3.59	11.82	-16.91	3.65	3.59	3.03	1.16	-19.49	0.55
SL4-40-019 AA13	3.050	37.7														12.08	-16.76	3.76	3.68	2.97	1.10	-19.44	0.60
SL4-40-019 AA14	3.675	45.4														11.90	-17.12	3.89	3.81	2.36	0.49	-19.92	0.12
SL4-40-019 AA15	4.125	51.0														12.05	-17.15	3.98	3.89	2.22	0.35	-20.05	0.00
SL4-40-019 AA16	4.875	60.3	21.50	-3.90	23.20	22.11	25.37	-26.62	8.81	14.38	18.06	11.79	24.23	3.25	4.05	12.17	-17.02	4.13	4.03	1.87	0.00	-20.05	0.00

Table A.2 continued

Sample ID	Lens Radial Midpoint (mm)	Estimated Standard Length	Alanine	Glycine	Valine	Leucine	Isoleucine	Threonine	Proline	Serine	Aspartic Acid	Methionine	Glutamic Acid	Phenylalanine	TPcsia	Bulk d15N	Bulk d13C	Trophic Growth Regression (Generic)	Trophic Growth Regression (Specific)	GVcsia Nitrogen	Nitrogen IM	Trophic Corrected Carbon	Carbon IM
SL4-40-021 AA1	0.300	3.6	19.03	4.85	19.18	16.59	13.10	-5.70	13.35	9.27	14.75	8.80	18.42	4.39	2.83			2.88	2.72				
SL4-40-021 AA2	0.725	8.7	18.03	7.80	20.89	19.81	17.06	-6.70	17.55	12.80	16.67	10.20	19.89	5.41	2.91			3.09	3.03				
SL4-40-021 AA3	0.900	10.8														14.21	-17.18	3.16	3.12	7.01	5.38	-19.29	0.65
SL4-40-021 AA4	1.050	12.6														14.69	-17.25	3.22	3.19	7.26	5.63	-19.43	0.51
SL4-40-021 AA5	1.250	15.0														15.02	-17.11	3.28	3.27	7.30	5.67	-19.38	0.56
SL4-40-021 AA6	1.450	17.5	18.74	6.93	23.03	23.81	18.27	-11.70	19.60	12.15	18.65	11.35	21.88	5.66	3.21	14.80	-17.44	3.35	3.34	6.83	5.19	-19.79	0.15
SL4-40-021 AA7	1.675	20.2														14.39	-16.91	3.41	3.42	6.16	4.53	-19.33	0.61
SL4-40-021 AA8	1.850	22.3														13.71	-16.67	3.46	3.48	5.30	3.66	-19.14	0.80
SL4-40-021 AA9	2.025	24.4														13.56	-16.39	3.51	3.53	4.97	3.34	-18.92	1.03
SL4-40-021 AA10	2.250	27.1		3.34	24.47	24.56	26.67	-16.41	19.23	15.98	18.95	12.04	23.80	4.50	3.76	14.06	-16.56	3.57	3.59	5.25	3.62	-19.15	0.79
SL4-40-021 AA11	2.425	29.2														14.46	-16.39	3.61	3.63	5.50	3.87	-19.02	0.92
SL4-40-021 AA12	2.625	31.6														13.06	-15.81	3.66	3.68	3.93	2.30	-18.50	1.44
SL4-40-021 AA13	2.875	34.6														13.67	-16.09	3.72	3.74	4.34	2.71	-18.83	1.11
SL4-40-021 AA14	3.050	36.7			24.06	23.30	20.10	-16.30	20.75	15.04	18.81	11.75	23.92	4.57	3.76	14.07	-16.08	3.76	3.78	4.61	2.98	-18.86	1.08
SL4-40-021 AA15	3.350	40.3														13.74	-16.41	3.82	3.84	4.07	2.43	-19.26	0.68
SL4-40-021 AA16	3.775	45.4														12.48	-16.91	3.91	3.93	2.53	0.89	-19.84	0.10
SL4-40-021 AA17	4.675	56.3		-0.39	26.97	24.62	25.92	-26.02	16.66	17.63	19.88	12.66	25.52	4.43	4.07	12.12	-16.86	4.09	4.09	1.63	0.00	-19.94	0.00
SL8-40-003 AA2	0.525	4.8	14.22	6.46	18.38	15.98	15.57	-11.60	12.47	2.47	15.89		19.54	2.39	3.38			3.00	3.33				
SL8-40-003 AA3	0.875	7.9														13.08	-16.90	3.15	3.36	5.05	1.45	-19.27	0.67
SL8-40-003 AA4	1.150	10.4														13.38	-16.54	3.25	3.40	5.23	1.63	-18.94	1.00
SL8-40-003 AA5	1.300	11.8	16.45	5.53	20.85	18.24	16.44	-15.74	17.00	9.50	18.77		22.16	4.72	3.43			3.30	3.42				
SL8-40-003 AA6	1.400	12.7														13.89	-16.20	3.33	3.44	5.60	2.00	-18.63	1.30
SL8-40-003 AA7	1.525	13.8														13.96	-16.07	3.37	3.46	5.60	2.00	-18.53	1.41
SL8-40-003 AA8	1.700	15.4	17.78	5.14	21.10	19.29	18.25	-16.00	18.19	11.62	17.38	10.36	21.79	3.48	3.58	13.31	-16.58	3.42	3.49	4.84	1.24	-19.07	0.87
SL8-40-003 AA9	1.900	17.2														13.24	-16.72	3.48	3.53	4.62	1.02	-19.25	0.69
SL8-40-003 AA10	2.050	18.6														13.58	-16.97	3.52	3.57	4.84	1.24	-19.54	0.40
SL8-40-003 AA11	2.200	20.0	17.72	2.70	22.89	20.92	22.41	-12.04	20.20	12.68	17.84	8.79	22.23	4.78	3.43	13.86	-16.81	3.56	3.61	5.00	1.40	-19.41	0.53
SL8-40-003 AA12	2.400	21.8														13.99	-17.20	3.61	3.66	4.95	1.35	-19.86	0.08
SL8-40-003 AA13	2.750	24.9														14.39	-17.76	3.69	3.76	5.00	1.40	-20.52	-0.58
SL8-40-003 AA14	3.925	35.6	23.04	3.59	26.08	24.82	22.25	-21.60	20.46	14.62	21.15	12.21	26.25	4.39	4.20	14.38	-16.77	3.94	4.17	3.60	0.00	-19.94	0.00

Table A.2 continued

Sample ID	Lens Radial Midpoint (mm)	Estimated Standard Length	Alanine	Glycine	Valine	Leucine	Isoleucine	Threonine	Proline	Serine	Aspartic Acid	Methionine	Glutamic Acid	Phenylalanine	TPcsia	Bulk d15N	Bulk d13C	Trophic Growth Regression (Generic)	Trophic Growth Regression (Specific)	GVcsia Nitrogen	Nitrogen IM	Trophic Corrected Carbon	Carbon IM
SL8-40-019 AA2	0.725	6.8	19.30	8.07	20.72	18.90	19.64	-2.10	18.61	10.70	17.20	11.10	20.01	6.66	2.71			3.09	2.90				
SL8-40-019 AA3	0.900	8.5	18.34	6.19	20.54	19.50	20.13	-5.90	18.50	11.00	17.11	11.20	20.96	5.17	3.14			3.16	2.98				
SL8-40-019 AA4	1.050	9.9														13.05	-17.55	3.22	3.04	6.12	3.67	-19.59	1.18
SL8-40-019 AA5	1.175	11.1														13.15	-17.22	3.26	3.09	6.05	3.60	-19.31	1.45
SL8-40-019 AA6	1.375	13.0	18.02	7.41	21.05	19.52	19.98	-6.60	18.60	15.61	16.97	11.30	21.12	5.08	3.18	13.13	-17.13	3.32	3.17	5.75	3.31	-19.30	1.46
SL8-40-019 AA7	1.575	14.8														13.40	-17.42	3.38	3.25	5.76	3.31	-19.67	1.09
SL8-40-019 AA8	1.700	16.0														13.57	-17.05	3.42	3.29	5.77	3.32	-19.34	1.42
SL8-40-019 AA9	1.775	16.7	20.75	5.66	22.52	21.60	22.10	-9.10	20.32	12.20	18.60	12.60	22.44	5.81	3.29			3.44	3.32				
SL8-40-019 AA11	2.300	21.7														12.26	-17.61	3.58	3.51	3.71	1.27	-20.12	0.64
SL8-40-019 AA12	2.525	23.8	20.19	5.31	23.27	23.42	23.11	-13.30	20.57	11.95	18.02	11.50	23.08	4.78	3.58	13.00	-17.51	3.64	3.59	4.18	1.74	-20.10	0.66
SL8-40-019 AA13	2.850	26.9														13.08	-17.68	3.71	3.70	3.89	1.44	-20.38	0.38
SL8-40-019 AA14	3.175	29.9														13.17	-17.77	3.79	3.81	3.61	1.17	-20.58	0.18
SL8-40-019 AA15	4.225	39.8	22.64	4.30	24.49	24.00	23.41	-14.68	16.82	17.11	20.15	13.20	24.77	3.49	4.10	13.12	-17.62	4.00	4.14	2.45	0.00	-20.76	0.00
SL8-40-023 AA1	0.275	3.0	15.48	6.56	19.56	19.20	16.20	-5.60	15.43	10.10	14.20	9.10	17.21	2.99	2.86			2.87	2.77				
SL8-40-023 AA2	0.625	6.9		6.42	20.50	22.10	17.80	-8.60	17.44	11.60	15.70	9.90	18.59	4.21	2.89			3.05	3.05				
SL8-40-023 AA3	0.775	8.6														11.97	-16.93	3.11	3.14	4.70	2.03	-19.07	1.19
SL8-40-023 AA4	0.925	10.2														12.68	-16.49	3.17	3.21	5.17	2.49	-18.70	1.56
SL8-40-023 AA5	1.075	11.9														12.43	-16.39	3.22	3.27	4.70	2.02	-18.66	1.60
SL8-40-023 AA6	1.200	13.3														12.11	-16.31	3.27	3.32	4.21	1.54	-18.63	1.63
SL8-40-023 AA7	1.325	14.6	17.97	6.48	21.52	19.80	19.57	-12.20	19.77	15.60	17.00	11.50	20.90	4.26	3.29	12.42	-16.33	3.31	3.37	4.38	1.70	-18.70	1.56
SL8-40-023 AA8	1.450	16.0														12.12	-16.76	3.35	3.41	3.94	1.26	-19.16	1.09
SL8-40-023 AA9	1.625	18.0														11.86	-16.85	3.40	3.46	3.49	0.81	-19.31	0.95
SL8-40-023 AA10	1.875	20.7														11.26	-17.50	3.47	3.53	2.65	-0.03	-20.03	0.23
SL8-40-023 AA11	2.050	22.6														11.56	-17.50	3.52	3.58	2.79	0.12	-20.07	0.19
SL8-40-023 AA12	2.175	24.0	20.57	4.94	23.57	21.72	20.47	-16.90	20.59	14.62	16.99	10.05	22.40	3.16	3.74	12.12	-17.02	3.55	3.61	3.25	0.57	-19.63	0.63
SL8-40-023 AA13	2.300	25.4														12.20	-17.39	3.58	3.64	3.23	0.56	-20.03	0.23
SL8-40-023 AA14	2.400	26.5														12.54	-17.28	3.61	3.66	3.49	0.82	-19.94	0.32
SL8-40-023 AA15	2.600	28.7														12.81	-16.82	3.65	3.71	3.61	0.94	-19.52	0.74
SL8-40-023 AA16	2.825	31.2														12.49	-16.75	3.71	3.75	3.13	0.46	-19.50	0.76
SL8-40-023 AA17	3.025	33.4	22.35	3.60	24.65	22.75	24.11	-20.17	19.61	15.95	18.62	11.48	23.16	2.30	4.03	12.59	-16.87	3.75	3.79	3.10	0.42	-19.66	0.60
SL8-40-023 AA18	3.275	36.2														12.79	-17.06	3.81	3.84	3.14	0.46	-19.89	0.36
SL8-40-023 AA19	3.500	38.7														13.57	-16.86	3.86	3.88	3.79	1.12	-19.74	0.52
SL8-40-023 AA20	3.975	43.9														12.95	-17.40	3.95	3.96	2.90	0.22	-20.36	-0.10
SL8-40-023 AA21	4.800	53.0	23.01	3.75	27.03	24.80	23.20			18.40	21.50	12.20	25.25	5.10	3.90	13.14	-17.18	4.11	4.08	2.68	0.00	-20.26	0.00

Table A.3 King Mackerel

Sample ID	Lens Radial Midpoint (mm)	Estimated Standard Length	Glutamic Acid	Phenylalanine	TP_{CSIA}	Bulk $\delta^{15}N$	Bulk $\delta^{13}C$	GV_{CSIA} Nitrogen	Nitrogen IM	Trophic Corrected Carbon	Carbon IM
KM2-AA1	0.300	4.56	17.72	0.32	3.42						
KM2-AA2	0.675	10.25	20.48	2.75	3.48						
KM2-AA3	0.775	11.77	18.60	4.78	2.79	13.80	-17.52	7.70	3.81	-19.32	0.39
KM2-AA4	0.825	12.53	18.45	4.84	2.76						
KM2-AA5	0.950	14.43	19.07	2.62	3.25	12.95	-17.70	5.29	1.39	-19.95	-0.24
KM2-AA6	1.075	16.32	18.67	2.76	3.16	12.83	-17.42	5.49	1.59	-19.58	0.13
KM2-AA7	1.150	17.46	19.10	1.54	3.45						
KM2-AA8	1.275	19.36	19.79	4.10	3.12	12.32	-17.91	5.11	1.21	-20.03	-0.32
KM2-AA9	1.400	21.26	19.68	0.02	3.82	13.12	-17.52	3.54	-0.36	-20.34	-0.63
KM2-AA10	1.500	22.78	20.49	5.62	2.98	13.10	-17.49	6.38	2.48	-19.47	0.24
KM2-AA11	1.600	24.29	20.92	2.86	3.54	12.83	-17.31	4.20	0.30	-19.84	-0.13
KM2-AA12	1.725	26.19	21.10	3.00	3.54	12.87	-17.28	4.22	0.32	-19.82	-0.11
KM2-AA13	1.900	28.85	21.54	3.28	3.57	13.32	-17.04	4.58	0.68	-19.61	0.09
KM2-AA14	2.050	31.13	21.24	0.32	4.04	13.77	-17.02	3.44	-0.46	-20.06	-0.35
KM2-AA15	2.225	33.78	22.04	4.03	3.53	13.11	-17.10	4.52	0.62	-19.63	0.08
KM2-AA16	2.375	36.06	22.07	1.42	3.99	12.92	-17.12	2.75	-1.15	-20.11	-0.40
KM2-AA17	2.550	38.72	21.68	5.19	3.26	12.99	-17.17	5.30	1.40	-19.43	0.28
KM2-AA18	2.825	42.90	22.11	2.50	3.81	12.90	-17.16	3.35	-0.55	-19.97	-0.26
KM2-AA19	3.375	51.25	21.87	3.25	3.63	12.86	-17.07	3.90	0.00	-19.71	0.00
KM3-AA1	0.250	3.36	17.53	2.67	2.98						
KM3-AA2	0.650	8.74	20.14	4.48	3.12	13.80	-17.62	6.60	1.66	-19.73	-0.26
KM3-AA3	0.875	11.76	19.79	3.62	3.21						
KM3-AA4	1.000	13.45	19.59	4.29	3.05	13.94	-17.24	6.96	2.02	-19.29	0.18
KM3-AA5	1.150	15.46	20.53	4.60	3.16	14.48	-17.23	7.12	2.18	-19.40	0.08
KM3-AA6	1.325	17.82	20.40	3.08	3.41	14.53	-17.38	6.35	1.41	-19.79	-0.31
KM3-AA7	1.425	19.16	21.39	3.97	3.42	14.26	-17.26	6.02	1.08	-19.68	-0.21
KM3-AA8	1.525	20.50	21.38	3.61	3.49	14.36	-17.24	5.90	0.96	-19.72	-0.25
KM3-AA9	1.675	22.52	22.58	4.14	3.60	14.37	-17.30	5.52	0.58	-19.90	-0.43
KM3-AA10	1.800	24.20	22.65	3.99	3.64	14.75	-17.26	5.76	0.82	-19.90	-0.43
KM3-AA11	1.875	25.21	25.49	4.42	4.06	15.13	-17.38	4.71	-0.23	-20.45	-0.97
KM3-AA12	1.975	26.55	24.32	4.83	3.79	15.64	-17.23	6.16	1.22	-20.02	-0.54
KM3-AA13	2.100	28.24	23.94	5.36	3.63	15.37	-17.24	6.44	1.50	-19.86	-0.39
KM3-AA14	2.200	29.58	24.86	4.56	3.93	15.14	-17.29	5.17	0.23	-20.23	-0.75
KM3-AA15	2.325	31.26	24.96	5.96	3.70	14.92	-17.44	5.73	0.79	-20.14	-0.67
KM3-AA16	2.450	32.94	25.34	5.45	3.86	14.70	-17.40	4.98	0.04	-20.26	-0.79
KM3-AA17	2.650	35.63	26.54	5.08	4.13	15.03	-17.27	4.38	-0.56	-20.41	-0.93
KM3-AA18	2.825	37.98	26.26	4.94	4.11	15.38	-17.09	4.82	-0.12	-20.20	-0.72
KM3-AA19	2.950	39.66	25.83	4.61	4.09	15.61	-16.53	5.10	0.16	-19.62	-0.15
KM3-AA20	3.150	42.35	26.64	5.31	4.11	15.53	-16.40	4.96	0.02	-19.51	-0.04
KM3-AA21	4.150	55.80	24.54	5.16	3.77	14.35	-16.70	4.94	0.00	-19.47	0.00

Table A.3 continued

Sample ID	Lens Radial Midpoint (mm)	Estimated Standard Length	Glutamic Acid	Phenylalanine	TP_{CSIA}	Bulk $\delta^{15}N$	Bulk $\delta^{13}C$	GV_{CSIA} Nitrogen	Nitrogen IM	Trophic Corrected Carbon	Carbon IM
KM4-AA1	0.350	5.70	18.47	2.17	3.23						
KM4-AA2	0.775	12.63	20.25	3.33	3.34	13.70	-18.21	5.75	-0.10	-20.55	-0.83
KM4-AA3	0.875	14.26	19.80	4.91	2.98						
KM4-AA4	0.950	15.48	22.52	3.12	3.77	14.80	-19.10	5.38	-0.47	-21.87	-2.15
KM4-AA5	1.075	17.52	21.77	7.68	2.84	14.79	-19.15	8.53	2.68	-20.99	-1.28
KM4-AA6	1.200	19.56	21.17	3.99	3.38	14.84	-19.07	6.74	0.90	-21.45	-1.74
KM4-AA7	1.325	21.59	20.33	2.32	3.53	15.15	-18.64	6.55	0.70	-21.17	-1.45
KM4-AA8	1.500	24.45	25.77	0.71	4.77	15.38	-18.63	2.58	-3.27	-22.40	-2.69
KM4-AA9	1.650	26.89	24.14	4.15	3.88	15.30	-18.46	5.52	-0.32	-21.34	-1.62
KM4-AA10	1.725	28.11				15.78	-18.12				
KM4-AA11	1.850	30.15	25.29	5.06	3.92	15.95	-17.40	6.03	0.19	-20.31	-0.60
KM4-AA12	2.050	33.41	26.48	4.80	4.17	16.24	-16.81	5.45	-0.40	-19.98	-0.27
KM4-AA13	2.350	38.30	26.33	4.62	4.18	15.30	-17.31	4.50	-1.34	-20.49	-0.77
KM4-AA14	3.125	50.93	26.35	7.70	3.64	14.83	-17.07	5.85	0.00	-19.71	0.00
KM6-AA1	0.250	3.61	14.59	-0.24	2.97						
KM6-AA2	0.575	8.31	16.03	1.10	2.99						
KM6-AA3	0.725	10.48	14.31	-0.82	3.02	8.63	-16.20	1.75	-0.05	-18.22	0.61
KM6-AA4	0.850	12.28	14.89	0.27	2.93						
KM6-AA5	0.925	13.37	15.93	0.40	3.09	8.79	-16.73	1.68	-0.13	-18.82	0.01
KM6-AA6	1.025	14.81	15.86	0.29	3.10	8.77	-16.95	1.64	-0.17	-19.05	-0.22
KM6-AA7	1.175	16.98	16.92	-0.45	3.42	8.80	-16.75	0.58	-1.22	-19.17	-0.33
KM6-AA8	1.325	19.15	16.32	1.10	3.04	9.20	-16.87	2.27	0.46	-18.91	-0.08
KM6-AA9	1.475	21.32	17.68	0.76	3.34	9.53	-16.82	1.59	-0.22	-19.15	-0.32
KM6-AA10	1.625	23.48	17.60	0.55	3.36	9.29	-16.79	1.27	-0.54	-19.15	-0.31
KM6-AA11	1.800	26.01	18.28	-0.84	3.72	9.61	-16.62	0.36	-1.45	-19.34	-0.51
KM6-AA12	1.950	28.18	17.21	0.26	3.34	9.86	-16.69	1.90	0.09	-19.03	-0.19
KM6-AA13	2.050	29.63	18.21	0.66	3.45	10.16	-16.39	1.84	0.04	-18.84	0.00
KM6-AA14	2.225	32.16	18.97	-0.93	3.86	10.36	-16.33	0.64	-1.16	-19.19	-0.35
KM6-AA15	2.375	34.32	22.04	1.49	3.97	10.62	-16.26	0.51	-1.30	-19.23	-0.39
KM6-AA16	2.450	35.41	19.35	-0.61	3.87	10.86	-15.99	1.10	-0.70	-18.86	-0.02
KM6-AA17	2.550	36.85	20.78	1.60	3.73	11.08	-16.12	1.79	-0.02	-18.85	-0.02
KM6-AA18	2.725	39.38	21.70	1.99	3.83	11.39	-16.36	1.78	-0.02	-19.19	-0.35
KM6-AA19	2.875	41.55	22.35	2.51	3.85	11.43	-16.59	1.74	-0.06	-19.44	-0.60
KM6-AA20	2.950	42.63	22.76	2.72	3.88	11.95	-16.52	2.14	0.34	-19.40	-0.57
KM6-AA21	3.075	44.44				12.20	-16.17				
KM6-AA22	3.225	46.61	23.70	-0.93	4.69	12.11	-15.84	-0.44	-2.25	-19.53	-0.70
KM6-AA23	3.350	48.41				11.74	-15.98				
KM6-AA24	3.450	49.86	21.55	3.58	3.52	11.80	-16.17	3.23	1.42	-18.69	0.14
KM6-AA25	3.650	52.75	22.04	2.87	3.73	11.19	-16.49	1.90	0.10	-19.23	-0.39
KM6-AA26	4.000	57.81	22.83	1.79	4.06	11.27	-16.52	0.87	-0.94	-19.58	-0.74
KM6-AA27	4.975	71.90	23.24	3.70	3.80	11.31	-16.04	1.81	0.00	-18.84	0.00

Table A.4 Greater Amberjack

Sample ID	Lens Radial Midpoint (mm)	Estimated Standard Length	Glutamic Acid	Phenylalanine	TP_{CSIA}	Bulk $\delta^{15}N$	Bulk $\delta^{13}C$	GV_{CSIA} Nitrogen	Nitrogen IM	Trophic Corrected Carbon	Carbon IM
AJ1-AA1	0.250	2.29	15.98	-2.01	3.52						
AJ1-AA2	0.625	5.72									
AJ1-AA3	0.825	7.56	18.87	-1.20	3.89	11.22	-18.62	1.40	-4.88	-21.51	-2.12
AJ1-AA4	0.975	8.93				11.32	-18.26				
AJ1-AA5	1.200	10.99				11.80	-18.43				
AJ1-AA6	1.400	12.82	20.61	-0.27	4.03	12.49	-18.17	2.18	-4.11	-21.20	-1.81
AJ1-AA7	1.550	14.19	21.24	-0.20	4.13	12.59	-17.82	1.95	-4.33	-20.95	-1.56
AJ1-AA8	1.725	15.80	20.99	0.06	4.04	13.21	-17.77	2.88	-3.40	-20.81	-1.42
AJ1-AA9	1.875	17.17	23.05	1.27	4.19	13.49	-17.70	2.64	-3.64	-20.89	-1.50
AJ1-AA10	2.050	18.77	22.73	2.25	3.96	14.73	-17.35	4.67	-1.61	-20.32	-0.93
AJ1-AA11	2.225	20.38	22.91	1.63	4.10	14.58	-17.06	4.03	-2.25	-20.17	-0.78
AJ1-AA12	2.375	21.75	23.98	2.09	4.21	14.67	-17.12	3.76	-2.52	-20.33	-0.94
AJ1-AA13	2.500	22.89				14.99	-16.93				
AJ1-AA14	2.650	24.27	23.46	0.53	4.39	13.58	-16.81	2.04	-4.24	-20.21	-0.82
AJ1-AA15	2.825	25.87	24.85	2.10	4.36	14.63	-16.66	3.21	-3.07	-20.02	-0.63
AJ1-AA16	2.950	27.02	24.51	2.37	4.25	14.73	-16.51	3.67	-2.61	-19.76	-0.38
AJ1-AA17	3.200	29.31	22.65	3.36	3.75	14.56	-16.81	5.21	-1.07	-19.56	-0.17
AJ1-AA18	3.475	31.82	20.98	2.35	3.64	14.75	-17.16	5.78	-0.50	-19.80	-0.41
AJ1-AA19	3.625	33.20	23.57	0.51	4.41	14.41	-17.15	2.80	-3.48	-20.56	-1.18
AJ1-AA20	3.800	34.80	23.51	-1.25	4.71	14.39	-17.37	1.77	-4.51	-21.08	-1.69
AJ1-AA21	4.025	36.86	23.09	-2.17	4.80	14.87	-17.14	1.95	-4.33	-20.94	-1.55
AJ1-AA22	4.200	38.46	23.24	5.40	3.50	15.00	-16.90	6.51	0.23	-19.40	-0.01
AJ1-AA23	4.300	39.38	23.19	2.08	4.07	14.42	-16.85	3.97	-2.31	-19.92	-0.54
AJ1-AA24	4.450	40.75	25.07	1.87	4.44	14.73	-16.54	3.05	-3.24	-19.97	-0.59
AJ1-AA25	4.725	43.27	22.97	4.35	3.64	15.00	-16.38	6.04	-0.24	-19.02	0.37
AJ1-AA26	5.200	47.62	25.76	-0.12	4.91	14.94	-16.47	1.65	-4.63	-20.38	-0.99
AJ1-AA27	7.500	68.68	27.25	7.67	3.80	15.81	-16.59	6.28	0.00	-19.39	0.00
AJ2-AA1	0.225	2.63	15.29	-1.19	3.26						
AJ2-AA2	0.500	5.83	17.30	-0.52	3.49						
AJ2-AA3	0.625	7.29	18.09	0.05	3.53	10.36	-17.76	1.74	-2.31	-20.29	-0.38
AJ2-AA4	0.850	9.92	17.70	-3.23	4.04	10.23	-16.85	-0.11	-4.17	-19.89	0.02
AJ2-AA5	1.075	12.54	18.03	-0.47	3.61	10.09	-16.99	1.20	-2.86	-19.60	0.31
AJ2-AA6	1.200	14.00	18.07	-0.32	3.59	10.47	-16.89	1.64	-2.41	-19.49	0.43
AJ2-AA7	1.325	15.46	19.16	-0.31	3.78	10.60	-17.31	1.14	-2.92	-20.09	-0.17
AJ2-AA8	1.475	17.21	19.26	0.08	3.73	11.30	-17.46	2.01	-2.05	-20.20	-0.28
AJ2-AA9	1.650	19.25	20.83	0.07	4.01	12.35	-17.19	2.11	-1.95	-20.20	-0.29
AJ2-AA10	1.850	21.58	21.15	1.27	3.86	12.69	-17.16	2.97	-1.09	-20.02	-0.10
AJ2-AA11	2.025	23.63	21.60	-0.02	4.16	13.21	-17.16	2.47	-1.59	-20.32	-0.40
AJ2-AA12	2.250	26.25	22.87	3.44	3.78	13.58	-17.02	4.14	0.08	-19.80	0.12
AJ2-AA13	2.475	28.88	23.45	1.66	4.19	14.49	-16.90	3.64	-0.42	-20.09	-0.18
AJ2-AA14	2.650	30.92	24.56	5.76	3.67	14.91	-16.92	5.85	1.79	-19.59	0.32
AJ2-AA15	2.850	33.25	24.95	2.82	4.25	14.95	-16.92	3.90	-0.16	-20.17	-0.26
AJ2-AA16	3.000	35.00	23.86	1.12	4.36	15.40	-16.98	3.98	-0.07	-20.34	-0.42
AJ2-AA17	3.150	36.75	24.73	3.56	4.08	15.81	-16.80	5.34	1.28	-19.88	0.03
AJ2-AA18	3.325	38.79	24.21	2.91	4.10	15.05	-16.95	4.50	0.44	-20.06	-0.14
AJ2-AA19	3.475	40.54	25.05	1.25	4.54	15.16	-17.11	3.10	-0.95	-20.66	-0.74
AJ2-AA20	3.625	42.29	25.06	3.18	4.21	15.19	-17.16	4.28	0.22	-20.37	-0.45
AJ2-AA21	3.800	44.33	25.07	3.47	4.16	15.47	-17.31	4.73	0.67	-20.47	-0.56
AJ2-AA22	4.025	46.96	25.79	1.72	4.59	14.47	-17.35	2.26	-1.79	-20.94	-1.02
AJ2-AA23	4.275	49.88	24.58	2.01	4.33	14.59	-17.44	3.28	-0.78	-20.77	-0.85
AJ2-AA24	4.800	56.00	26.64	5.78	4.03	15.23	-17.10	4.93	0.88	-20.12	-0.21
AJ2-AA25	6.200	72.33	26.51	3.80	4.35	15.46	-16.56	4.06	0.00	-19.91	0.00